1-1-1978

Studies of the crystallization behavior of the poly(1, 4 butylene terephthalate)/poly(ethylene terephthalate) blends.

Antonio Escala Sisquellas
University of Massachusetts Amherst

STUDIES OF THE CRYSTALLIZATION BEHAVIOR OF THE POLY(1,4 BUTYLENE TEREPHTHALATE)/ POLY(ETHYLENE TEREPHTHALATE) BLENDS

A Dissertation Presented

By

Antonio Escala Sisquellas

Submitted to the Graduate School of the
University of Massachusetts
in partial fulfillment of the requirements for the degree of

DOCTOR OF PHILOSOPHY

April 1978

Major Subject: Polymer Science and Engineering

STUDIES OF THE CRYSTALLIZATION BEHAVIOR OF THE POLY(1,4 BUTYLENE TEREPHTHALATE)/ POLY(ETHYLENE TEREPHTHALATE) BLENDS

A Dissertation Presented

By

Antonio Escala Sisquellas

Approved as to style and content by:

Richard S. Stein, Chairman of Committee

Robert W. Lenz, Member

William J. MacKnight, Member

Roger S. Porter, Member

Edwin L. Thomas, Member

William J. MacKnight, Head
Polymer Science & Engineering

April 1978

DEDICATION

To my parents and to my wife, Maria Jose.
Without their unwavering support and
sacrifice, this undertaking could
not have been completed.

ACKNOWLEDGMENT

I wish to express my sincere appreciation to Professor Richard S. Stein for his guidance and his constant encouragement throughout the course of this research.

Acknowledgment and gratitude are extended to the other members of my thesis committee - Professors W. J. MacKnight, R. W. Lenz, R. S. Porter and E. L. Thomas - each of whom contributed by their knowledge and their interest in the completion of this project.

Helpful discussions with my fellow co-workers, especially Dr. E. Balizer, are gratefully acknowledged.

I also wish to thank Drs. D. Fox, D. Jaquiss and P. Borman of the General Electric Company for providing the samples for this study and for their helpful suggestions.

Thanks are also extended to Mrs. Sophia Kinney for doing an excellent job in typing this thesis.

Last, but not least, I would like to thank my wife, Maria Jose, whose help I always took for granted and who ended up drawing all the figures in this dissertation.

The present work was supported in part by grants from the General Electric Company, the Petroleum Research Fund of the American Chemical Society and the Materials Research Laboratory of the University of Massachusetts. Travel support was provided by the Commission for Cultural Exchange between Spain and the United States of America.

ABSTRACT

STUDIES OF THE CRYSTALLIZATION BEHAVIOR
OF THE POLY(1,4 BUTYLENE TEREPHTHALATE)/
POLY(ETHYLENE TEREPHTHALATE) BLENDS

May 1978

Antonio Escala Sisquellas, Industrial Engineer, Polytechnic
University of Barcelona
M.S., Ph.D., University of Massachusetts

Directed by: Professor Richard S. Stein

The main purpose of these studies has been to determine the crystallization behavior of the poly(1,4 butylene terephthalate)/ poly(ethylene terephthalate) (PBT/PET) blends.

The evidence from wide angle x-ray scattering, differential scanning calorimetry and infrared spectroscopy shows that both polymers crystallize separately in the blends, preserving their unit cell structure, showing separate melting points and their characteristic crystalline spectroscopic bands.

While this phase separation occurs in the crystalline state, only one glass transition temperature, which is intermediate between those of the pure polymers, is observed by DSC in the amorphous samples. This first evidence of compatibility of both polymers in the amorphous state will be corroborated by the crystallization behavior.

The morphology of the crystalline state in the blends was studied by light microscopy and by small angle light scattering. Samples of the pure polymers show spherulitic structure. Upon increasing the

concentration of the other component, the spherulites become coarser, disordered and strong branching occurs. Finally, in the blends of intermediate composition, the spherulitic structure is lost. Only small rod-like crystals appear.

The crystallization kinetics were first studied by depolarized light intensity, which provides information on the overall crystallization behavior but not on the crystallization kinetics of each component. This information was obtained following the crystallization of the blends by infrared spectroscopy and density which, although it only gives information on the overall crystallization behavior, allowed us, by establishing a correlation with the infrared measurements, to obtain the absolute degrees of crystallinity of each component in the blends.

The infrared studies were performed in the blends at 90°C, 110°C, 130°C, 150°C and 200°C, and the crystallization was followed by the changes in intensity of the characteristic crystalline bands of each polymer.

The crystallization kinetics of each component are strongly affected by the presence of the second one. Examining the crystallization rate vs. temperature curves for the PET component, we can observe how the maximum increases in value and shifts towards lower temperatures with increasing amounts of PBT. The PBT component shows a decrease of crystallization rate and a shift of the maximum towards higher temperatures with increasing PET concentration. These effects can be fully accounted for in terms of the change in T_g of the amorphous samples,

which is very strong evidence for the existence of compatibility between the amorphous polymers.

The results were theoretically explained taking into account the shift of the T_g in the amorphous blends and the dilution effect caused by the presence of the second component.

A comparative study was made of the effect that annealing or cooling, from the glass or the melt, has on the crystallization behavior. It was shown how polymers with "low" crystallization rates (PET) yield identical results in both cases, but how polymers with high crystallization rates yield different morphologies, crystallization rates and ultimate crystallinities, which can be explained if we consider that, in the melt crystallized samples, when going through the maximum in crystallization rate, substantial crystallization occurs and, therefore, the crystallization is not fully isothermal.

The possibility of occurrence of the trans-esterification reaction during the melting period was studied by determining its possible effect on the crystallization kinetics and intrinsic viscosities of the blends. It was observed that for up to four minutes in the melt, no significant effect appears. These results were complemented with a study of the effect that the processing conditions had on the crystallization kinetics of the blends.

TABLE OF CONTENTS

LIST OF TABLES

LIST OF FIGURES

C H A P T E R I

INTRODUCTION

After having studied in our laboratory polymer blends of amorphous polymers with poly-ε-caprolactone and poly(vinyl chloride) (1-4), blends with a crystalline component like poly(2,6 dimethyl phenylene oxide) with isotactic polystyrene (5) and atactic polystyrene with isotactic polystyrene (6) were studied. The next obvious step was to become involved in the study of a blend of two polymers which both crystallize. The system chosen was poly(1,4 butylene terephthalate)/ poly(ethylene terephthalate) (PBT/PET) because of the previous knowledge of the crystallization behavior of the pure components.

The crystallization behavior of PBT has been extensively studied in our laboratory (7-9). This polymer has a very high crystallization rate which usually leads to a skin core morphology during the processing of the polymer (10). PET is also a semicrystalline polymer which has more moderate crystallization rates (11-23). The purpose of the present study is to observe how the crystallization of each component is affected by the presence of the second one.

We have first looked at the crystal structure of the two polymers in the blends. Wide angle x-ray scattering (WAXS), differential scanning calorimetry (DSC) and infrared spectroscopy (IR) provide us information on whether each polymer crystallizes separately in the blend according to their own unit cell structure or if they co-crystallize yielding a new unit cell structure.

Small angle light scattering (SALS) and polarized light microscopy provided information on the morphology of the crystalline structures in the blends under different crystallization conditions.

In order to study the kinetics of crystallization of the blends, two different approaches have been taken. Depolarized light intensity (DLI), DSC and density provide us with information about the overall crystallization behavior of the blends, without being able to distinguish the behavior of each component separately.

To do so, IR has proved to be very effective since we have been able to isolate absorbance bands which are sensitive to the crystallization of each component, but which are unaffected by the crystallization of the second one. In this way we have been able to follow the crystallization of each component in the blends, under the different crystallization conditions. These studies have been performed mostly at temperatures below that of the maximum of crystallization rate and show the strong influence that each polymer has on the crystallization behavior of the other one. A theoretical explanation of these results is offered through the approach of Mandelkern (24) which takes into account the dilution effect caused by the presence of the second component and the change in the glass transition temperature (T_g) of the blends.

Since most of these studies have been performed at low temperatures by annealing the samples from the glass, a comparative study was made on the difference in crystallization behavior, when the crystallization is performed from the glass or the melt.

The effect of the processing conditions of the blends on the crystallization behavior was studied, paying special attention to the effect that the trans-esterification reaction might have on the crystallization.

Finally, although the study of the mechanical properties of the blends was not the main purpose of these studies, a series of dynamic-mechanical measurements was performed in order to obtain further information on the relaxation behavior.

The samples used throughout these studies were provided by the General Electric Company. The blends, which covered all the range of compositions, have been obtained by melt-extruding, in a sterling 1 3/4" extruder, 80 rpm, at 520^{o}F (271^{o}C), two samples of PBT and PET. The melt viscosity of PBT at 250^{o}C was 2740 poises and the viscosity average molecular weight 25,600. PET had a melt viscosity at 270^{o}C of 1250 poises and a viscosity average molecular weight of 36,800.

C H A P T E R I I

CRYSTAL STRUCTURE

A. Introduction

The determination of the crystal structure of the different blends was undertaken by WAXS, DSC and IR. The purpose is to determine whether both polymer blends crystallize separately in the blends or if they co-crystallize giving a new type of crystal.

The crystal structures of PBT and PET have been studied (25-27); both unit cells are triclinic. Their dimensions are:

PBT:

$a = 4.83\text{Å}^{o}$	$\alpha = 99.7^{o}$
$b = 5.96\text{Å}^{o}$	$\beta = 115.2^{o}$
$c = 11.59\text{Å}^{o}$	$\gamma = 110.8^{o}$

PET:

$a = 4.56\text{Å}^{o}$	$\alpha = 98.5^{o}$
$b = 5.94\text{Å}^{o}$	$\beta = 118^{o}$
$c = 10.75\text{Å}^{o}$	$\gamma = 112^{o}$

To complement the information on the crystalline polymers, the T_g of the blends was determined by DSC in completely amorphous samples.

B. Experimental

The samples for crystallization were molded between Teflon-coated aluminum foil, after desiccating the pellets for 24 hours in a vacuum oven at 120°C, using a Pasadena press working at 25,000 psi and 280°C. The molded samples were quenched in an ice water mixture. A 2 mil thick aluminum shim was placed between the aluminum foil obtaining, therefore, samples with a thickness gradient. The use of Teflon coated aluminum foil permits their direct separation without the need to use HCl to dissolve the aluminum foil.

A set of quenched samples was separated and these completely amorphous samples were used to determine the T_g of the blends by DSC. The second set of samples, containing the whole range of compositions, was melted at 280°C and then crystallized in a fluidized bed for 30 minutes at 200°C. A third set of samples was melted at 280°C between hot plates and then crystallized in a fluidized bed for 30 minutes at 230°C, after which the temperature was dropped to 200°C and the samples were then crystallized for 30 more minutes.

The wide angle x-ray diffraction patterns from all the samples were obtained using CuKα radiation. The photographic film was placed 8 cm from the sample, allowing a better resolution of the different diffraction lines and avoiding their overlapping.

The infrared spectra was obtained by a Perkin Elmer Infrared Spectrophotometer, Model 283, working in the absorption mode.

The calorimetry studies were done with a Perkin Elmer DSC-2, which was able to work at subambient temperatures by means of a intracooler of middle range ($-40^{o}C$).

C. Results

1. Wide Angle X-Ray Scattering Results.

The diffraction lines for the pure polymers and the blends were obtained. They show the presence of the PBT and PET diffraction lines in the blends of intermediate composition. No new lines appear. One therefore must conclude that no co-crystallization occurs but that both polymers crystallize separately in the blends. The blends very rich in one component do not show the diffraction lines of the other one, but, as it will be shown by DSC and IR, this is not due to the fact that it does not crystallize but it is because of the method, which is not sensitive enough to distinguish them.

The outer lines in the blends appear less intense and much broader, especially in those blends of intermediate composition. This reflects the presence of smaller and more disordered crystals. The different diffraction lines for the pure polymers (25-27) and the blends are recorded in Tables 1 - 8.

Table 1

Diffraction Lines for PBT

Line #	2θ	dA (o)	Relative Intensity
1	9.24	9.57	High
2	16.13	5.50	Low
3	17.5	5.07	High
4	20.7	4.29	Low
5	23.7	3.75	High
6	26.4	3.38	High

TABLE 2

Diffraction Lines for PET

Line #	2θ	dA (o)	Relative Intensity
1	16.42	5.40	High
2	17.53	5.07	High
3	21.26	4.18	Low
4	22.23	4.00	High
5	25.68	3.47	Very High

Table 3

Observed Diffraction Lines for the 90/10 and 80/20 PBT/PET Samples

Line #	2θ	dA (Å)	Relative Intensity
1	9.24	9.57	High
2	16.13	5.50	Low
3	17.5	5.07	High
4	20.7	4.29	Low
5	23.7	3.75	High
6	26.4	3.38	High

Table 4

Observed Diffraction Lines for the 70/30 Sample

Line #	2θ	dA (Å)	Relative Intensity
1	9.24	9.57	High
2	16.13	5.50	Low
3	17.5	5.07	High
4	20.7	4.29	Low
5	23.7	3.75	High Broad
6	26.4	3.38	High Broad

Table 5

Observed Diffraction Lines for the 60/40 Sample

Line #	2θ	dA (Å)	Relative Intensity
1	9.24	9.57	High
2	16.13	5.50	Low
3	17.13	5.07	High
4	20.7	4.29	Low
4	21.47	4.18	Low
5	22.57	4.00	High
5	23.7	3.75	High
6	26.4	3.38	High

Table 6

Observed Diffraction from the 50/50 Sample

Line #	2θ	dA (Å)	Relative Intensity
1	9.24	9.57	Very Low
2	16.3	5.45	High Broad
3	17.5	5.97	High Broad
4	21.26	4.18	Low
5	22.23	4.00	High Broad
6	25.68	3.47	High Broad
7	26.4	3.38	Low

Table 7

Observed Diffraction from the 40/60 Sample

Line #	2θ	dÅ	Relative Intensity
1	16.42	5.40	High
2	17.53	5.06	High
3	21.26	4.18	Low
4	22.23	4.00	High Broad
5	25.68	3.47	Very High Broad

Table 8

Observed Diffraction from the 30/70, 20/80 and 10/90 Samples

Line #	2θ	dÅ	Relative Intensity
1	16.42	5.40	High
2	17.53	5.06	High
3	21.26	4.18	Low
4	22.23	4.00	High
5	25.68	3.47	Very High

2. Infrared Spectroscopy Results.

The infrared spectra of PET and of PBT are very similar and it is hard to isolate a crystalline band which does not appear in the amorphous state and which is characteristic of one of the components.

Initially the PET crystalline component was observed through the shift of the 424 cm^{-1} band in the amorphous state which appears in the crystalline state at 434 cm^{-1}. The PBT crystalline component was observed through the splitting and broadening that the 498 cm^{-1} band undergoes. In later studies we have isolated other bands, mainly the 848 cm^{-1} band for PET and the 917 and 810 cm^{-1} bands for PBT which are very sensitive to the crystallization process.

Through these studies we have observed the presence of the PBT and PET in their crystalline state simultaneously in the blends ranging from 90/10 to 30/70 (PBT/PET). In the 20/80 and 10/90 blends, only PET appears in its crystalline state.

3. Differential Scanning Calorimetry Results.

The melting points of each component in the blends were obtained separately by DSC, where, although certain overlapping of the endotherms occurs, the melting peaks of each polymer can be separated (Figure 1). The melting of PET can be observed in all the blends while that of PBT can be seen only in the 100/0 through 30/70 blends. These results are in accordance with those obtained by IR.

Table 9

Crystalline Component Present

Blend	WAXS	DSC	IR
100 PBT	PBT	PBT	PBT
90/10	PBT	PBT/PET	PBT/PET
85/15	PBT	PBT/PET	PBT/PET
80/20	PBT	PBT/PET	PBT/PET
70/30	PBT/PET	PBT/PET	PBT/PET
60/40	PBT/PET	PBT/PET	PBT/PET
50/50	PBT/PET	PBT/PET	PBT/PET
40/60	PET	PBT/PET	PBT/PET
30/70	PET	PBT/PET	PBT/PET
20/80	PET	PET	PET
10/90	PET	PET	PET
100 PET	PET	PET	PET

The discrepancies that appear in Table 9 only reflect the low sensitivity of the WAXS method, but the results are in good agreement.

From these results we must conclude that both polymers crystallize separately in the blends showing, therefore, phase separation in their crystalline state.

It is important to determine if the same behavior is observed in the amorphous samples. If phase separation occurs to a large degree, one would expect to find two T_g's in the blends. Calorimetry was therefore

used to determine the T_g's of the blends. Only one T_g was found for each blend and its value is intermediate between those of PBT and PET, giving a first indication of their compatibility in the amorphous state (Figure 2).

The experimental values of T_g's of the blends closely resemble the theoretical values calculated according to Fox's equation (28,29):

$$\frac{1}{T_g} = \frac{1}{w_1 + Bw_2} \left(\frac{w_1}{T_{g_1}} + \frac{Bw_2}{T_{g_2}} \right) \qquad (1)$$

where w_1 and w_2 are the weight fractions of the two polymers of glass transition temperatures T_{g_1} and T_{g_2}. As can be seen in Figure 2. a very good fit is obtained for a value for B of 0.4.

C H A P T E R I I I

MORPHOLOGY

A. Introduction

To investigate the morphology of the crystallizing polymers in the different blends, a series of studies was done in samples crystallized under different conditions, both isothermal and non-isothermal. The morphology was studied by small angle light scattering (SALS) and by polarized light microscopy.

The morphology of PET has been extensively studied (21,22,30). It has been observed that the isothermal crystallization of the samples at temperatures between 220^{o}C and 110^{o}C produced the development of 0-90 spherulites, which have their extinction patterns along the directions of the Nicol prisms. The sizes of the spherulites were dependent on the crystallization temperature.

The crystallization of PBT has been recently studied (7-9) and the appearance of two types of spherulites has been observed. In isothermally crystalline samples at a temperature above 200^{o}C, regular spherulites appeared with their maltese crosses in the directions of the polaroids. When crystallization occurred below 200^{o}C, spherulites with their maltese crosses 45^{o} to the polaroids appeared.

Corresponding to these morphologies the H_V light scattering patterns for the former had their lobes 45^o to the polars and when crystallization proceeded they became circularly symmetric due to secondary scattering. The latter show the H_V light scattering patterns with their lobes along the polars. This rotation is due to the fact that the optic axis of the crystallites in the spherulites is at 45^o to the radius.

The size of the scattering objects which was not distinguishable under the polarizing microscope can be computed from the position of the light scattering maximum intensity by using the relationship (31,32)

$$4.1 = \frac{4\pi\ Rn}{\lambda} \sin(\theta_m'/2) \qquad (2)$$

where R = spherulitic radius, λ = wavelength of source (= 0.6328 μm for red laser), n = refractive index of polymer, θ_m' = corrected scattering angle for maximum intensity and is related to the actual scattering angle (θ_m) as $\sin \theta_m' = \sin \theta_m/n$.

For small values of θ_m the above equation reduces to

$$R = \frac{4.1}{2} \frac{\lambda}{\pi\ \theta_m} = 0.413/\theta_m \qquad (3)$$

where θ_m is in radians and the value of R is in micrometers.

B. Experimental

Three sets of molded samples were made from all the blends by pressing previously desiccated pellets between sheets of Teflon-coated aluminum foil in the Pasadena press at 25,000 psi and 280°C. As there was no shim, the thickness of the films depended on the applied pressure and they were about 1 mil thick. They were then placed on a microscope slide, under a cover glass, and pressed to twice the original surface area.

The first set of samples was melted in a Mettler FP2, which has three rates of temperature change - 0.2°C/min, 2°C/min, and 10°C/min. After melting them at 280°C they were cooled to 200°C at a 2°C/min rate. The crystallization was followed through the polarizing light microscope and by light scattering.

The second set of samples was melted between two hot plates at 280°C for 1 min and crystallized in an oil bath at 130°C for 10 min, after which the samples were observed by light scattering.

The third set of samples was melted again between hot plates at 280°C for 1 min and then crystallized in the Mettler FP2 at 200°C for 10 min. The samples were examined under the polarizing microscope.

C. Morphologies

1. Samples Crystallized Non-Isothermally.

Under the polarizing microscope it was possible to detect the appearance of small crystalline entities in the 100% PET sample. These crystalline entities were volume filling and showed no superstructure. The light scattering patterns for this sample have four lobes in the directions of the polaroids (Figure 3a). This pattern has never been reported for isothermally crystallized PET, but it can be explained according to Keller's isothermal crystallization studies under the polarizing microscope (30) that show that as the crystallization temperature was increased the maltese cross in the spherulites started to show waviness and finally it was possible to observe extinction crosses at 45^{o} and 90^{o} to the polaroids. The size of the scattering entities, computed according to Equation (3), is of the order of 1.5 μm.

For the 100% PBT sample it was possible to observe the appearance of small rod-like anisotropic structures which became almost immediately volume filling. The corresponding H_V light scattering pattern, upon cooling, evolved from that of a liquid to that of a regular spherulite with a lot of background scattering and the lobes 45^{o} to the polars (Figure 3d). Finally, the pattern became circularly symmetric due to multiple scattering.

The behavior of the 20/80 sample was very similar to that of PET. Upon cooling it became immediately filled with small anisotropic entities without any visible superstructure. At the same time the H_V light scattering pattern was similar to that of slowly cooled PET, with four lobes

in the direction of the polaroids. The pattern did not change with further cooling.

The behavior of the 40/60, 50/50 and 60/40 samples was very similar in the three cases. Upon slow cooling in the Mettler under the polarizing microscope, they developed volume filling anisotropic entities which had no superstructure visible but only birefringent zones of the same retardation order. That is, upon introducing a first order red plate with its slow direction 45^{o} to the polaroid directions of the microscope, the retardation colors varied by zones in the different parts of the sample. However, they remained the same throughout wide areas of the sample. There was no systematic compensation or addition of retardation colors like would exist in a spherulitic sample. Upon further crystallization the retardation order increased similarly for the different areas. It is normal to infer from this behavior the development of rod-like structures. The H_V light scattering patterns obtained from these samples corroborated the existence of this structure (Figures 4c,d), since they showed a monotonic decrease of intensity from the center in the direction 45^{o} to the polaroids.

This rod-like structure was preserved in the three blends by slowly cooling the samples. However, if after cooling the samples to $160^{o}C$ in the Mettler, they were removed and allowed to air cool, it was possible to observe the development of spherulitic structures. In the 40/60 sample the spherulites were similar to those of PET with their maltese crosses in the directions of the polaroids. In the 60/40 sample the spherulites presented different extinction patterns resulting from highly disordered spherulites (Figure 4b).

A completely different behavior was observed with the 80/20 sample. Slow cooling of this sample produced at 218^{o} the appearance of small entities showing birefringence and different retardation order color from one to the other in an amorphous background. With further cooling at 175^{o}C it was possible to observe the appearance of small spherulites with their maltese crosses 45^{o} to the direction of the polaroids. These spherulites continued growing and their extinction crosses became multiple and in several directions. The spherulites are highly branched (Figures 5a,b) and their retardation colors under the first order red plate vary randomly throughout the spherulites, indicating a very high degree of disorder.

These spherulites are non-volume filling and their degree of disorder is such that even in samples isothermally crystallized at 175^{o}C, it is possible to observe the development of non-spherulitic superstructures, which are highly branched and resemble dendrites, in an amorphous background in which some small spherulites developed due to the inefficient quenching (Figure 5c,d). These dendritic structures can be explained as a result of the diffusion of the non-crystallizing material.

Upon reheating of these spherulites it is not possible to observe any part of their melting out first. There is a steady loss of retardation order and finally at 242^{o}C the samples were completely melted.

The examination of the H_V light scattering pattern of the above samples shows mainly the pattern belonging to regular spherulites; the lobes appear at 45^{o} to the polars.

2. Samples Isothermally Crystallized at 130°C.

The sample with 100% PET showed a light scattering pattern of typical 0-90 spherulites with the lobes 45° to the polaroid directions. The radius of the spherulite was computed through Equation (3), with its value 5.43 μm (Figure 6).

The 20/80 sample showed a scattering pattern similar to the previous one, but somewhat larger and less intense, indicating smaller and less ordered spherulites. The spherulitic radius obtained for this sample was 3.6 μm (Figure 6).

The 60/40, 50/50 and 40/60 samples did not show spherulitic light scattering patterns. Instead the patterns were characteristic of a rod-like structure (Figure 6).

The 80/20 sample showed two different types of scattering patterns, corresponding to two different kinds of spherulites. A light scattering pattern with the four lobes 45° to the polaroid directions characteristic of regular 0-90 spherulites of 2.96 μm of radius is obtained (Figure 6). In other locations in the sample it was possible to see a scattering pattern with four lobes along the directions of the polaroids, characteristic of 45° spherulites. This pattern was larger than the previous one and much less common. The spherulite radius was 1.66 μm. In other places in the sample the pattern was circularly symmetric due to the secondary scattering.

Finally the sample with 100% PBT showed light scattering patterns with the four lobes along the polaroid directions, which belongs to a spherulitic superstructure with the maltese cross 45° to the polaroid

directions. These spherulites were bigger than those of the 80/20, having their radius 2.33 μm (Figure 6).

3. Samples Isothermally Crystallized at 200°C.

The samples examined in these cases were those rich in PET. The examination was done under the polarizing microscope and it is possible to observe (Figures 7 and 8) how, as the PBT content increases, the spherulites become smaller, more branched and disorganized.

The PET sample showed extinction crosses in the directions of the polaroids, but, as the amount of PBT increased, waviness of the cross appears and finally multiple extinction crosses appear.

C H A P T E R I V

DEPOLARIZED LIGHT INTENSITY STUDIES

A. Introduction

The study of the kinetics of crystallization was initiated through the measurement of the depolarized light intensity (DLI) transmitted between crossed polaroids.

The use of DLI to follow the kinetics of crystallization has been widely used (33-38) and basically it follows the method initiated by Magill (33,34) in which a thin polymer sample is sandwiched between cover slides, melted in a thermostated chamber, and then rapidly transferred to a hot stage at the crystallization temperature. The intensity of the light transmitted between crossed polaroids in the light microscope as a function of time is then measured. The graph obtained has a sigmoidal shape. Figure 9 shows the intensity of the light transmitted between crossed polaroids as a function of time for the 50/50 blend crystallized at 200^{o}C. From these plots it is possible to obtain the crystallization half times.

Knowing the value of the intensity, I_c, when it ceases to increase and remains constant, which is assumed to represent the completion of the crystallization process, and that of the intensity at the beginning of the crystallization, I_o, it is possible to calculate the degree of crystallinity, X_c, through the empirical equation

$$1 - X_c = \frac{I_c - I_t}{I_c - I_o} \qquad (4)$$

where I_t is the intensity of the light transmitted between crossed polaroids at a time t.

The rate constants are obtained from the Avrami equation (39-43)

$$1 - X_c = e^{-kt^n} \qquad (5)$$

where k is a constant and n an integer which is characteristic of the type of nucleation and growth (39,40). Their values can be directly obtained from a plot of

$$\ln\left(-\ln\left(\frac{I_c - I_t}{I_c - I_o}\right)\right) \text{ vs } \ln t$$

These plots have been made for the different blends (Figure 10).

This method, although empirical, describes accurately the primary initial crystallization, that is, until the sample becomes volume filled with structured units. However, the intensity transmitted between crossed polaroids levels off when this occurs, and no further secondary intra-spherulitic crystallization is seen. Therefore, adequate Avrami exponents

but lower crystallization half times than those obtained by other methods like DSC or density gradient (44), are achieved. Furthermore, the turbidity of the sample changes during the course of crystallization, further changing the light transmission of the sample.

To circumvent this problem and obtain more accurate crystallization half times, it is useful to accompany the DLI measurements with the measurements of turbidity.

In the polarizing microscopies the DLI can be measured with both crossed polaroids (I_+) or with parallel polaroids ($I_{||}$). If one assumes that the light passes through a single layer of birefringent material, the transmission for crossed polaroids for the crystal of area A_c in a total area A lying in a plane perpendicular to the incident beam with its optic axis at an angle θ to the polarization direction is

$$T_+ = N(A_c/A) \sin^2\theta \cos^2\theta \sin^2 (nd\,\Delta/\lambda_o) \qquad (6)$$

where d is the sample thickness, Δ is the birefringence and λ_o is the wavelength of light in vacuum. For N such crystals having random orientation in a plane (where $\overline{\sin^2\theta \cos^2\theta} = 1/8$), the transmittance is

$$T_{+} = (1/2)\,(NA_c/A)\,\sin^2\,(nd\,\Delta/\lambda_o) \qquad (7)$$

If the medium is also scattering and has a turbidity, τ, this is modified to give

$$T_{+} = (1/2)\,(NA_c/A)\,\sin^2\,(nd\,\Delta/\lambda_o)\,e^{-\tau d} \qquad (8)$$

This equation assumes that the only effect of scattering is to reduce the intensity of the transmitted light and neglects depolarization effects.

The corresponding equation for parallel polaroids is

$$T_{\parallel} = \{(1/2)\,(NA_c/A)\,[1 + \cos^2\,(nd\,\Delta/\lambda_o)] + [1 - (NA_c/A)]\}\,e^{\tau d} \qquad (9)$$

Therefore it follows that

$$T_{\parallel} + T_{+} = e^{\tau d} \qquad (10)$$

Through the measurement of turbidity we consider not only the change of fractional area of the field occupied by crystals but also the change in birefringence of those aggregates as their crystallinity increases.

Finally the intensity of the light transmitted through crossed polaroids can also be used to detect the melting. The detection of thermal transitions through DLI has been discussed by Hobbs and Kovacs (45) and Arnei and Sauer (46). As we increase the temperature, the intensity of the light transmitted remains constant, until the melting point is approached where it increases quickly due to recrystallization occurring. At the melting point the intensity of the light transmitted decreases to zero.

B. Experimental

Four sets of molded samples are made from all the blends by pressing previously desiccated pellets between sheets of Telfon coated aluminum foil in the Pasadena press at 25,000 psi and 280^{o}C. As there was no shim, the molded films obtained were 1 mil thick. They were then placed on a microscope slide, under a cover glass, and pressed to twice the original surface area.

The first set, on which the melting studies were performed, was crystallized at 200^{o}C for 30 minutes.

The other samples were melted between hot plates at 280^{o}C and immediately transferred to the Mettler hot stage (Model FP2) where

crystallization occurred, isothermally at 200°C, 202°C and 205°C. The hot stage was placed on a Zeiss polarizing microscope, between crossed Nicol prisms, and the intensity of the light transmitted was measured as a function of time using a photocell adapted to the occular of the microscope.

C. Results

The values for the melting points determined by DLI are plotted in Figure 11. It is possible to observe the depression that melting temperatures undergo upon the addition of a small amount of the second polymer.

The melting points obtained by DLI are lower than those from DSC (Figure 1). Through DSC the melting points of PBT and PET are obtained separately in the blends, while depolarized light intensity shows the loss of anisotropy of the whole sample and is very dependent on the morphology.

From the plots of turbidity vs. time, it is possible to obtain the crystallization half times, which are plotted in Figure 12 for the different blends crystallized at 200°C, 202°C and 205°C.

These values for the crystallization half times are sensibly larger than those obtained through the measurement of the depolarized intensity alone, but they represent more accurately the crystallization process as they do not only include the initial formation of crystalline structures but also the further increase of anisotropy as the crystallization proceeded. Therefore, the crystallization half times observed

through the turbidity measurements are more in agreement with those obtained through DSC by Pratt and Hobbs for PBT and PET (44).

As we can see, the crystallization half times increase with low amounts of PET up to the 85/15 blend, and, from there, they go on decreasing with increasing amounts of PET.

The microscopic observations of the crystallizing samples show that spherulites developed for the 100, 90/10, 85/15, 80/20 and 70/30 blends. The 60/40, 50/50, 40/60 blends showed only small disordered crystalline structures. The 30/70, 20/80 and 10/90 blends showed regular PET spherulites which were very disordered as the concentration of PBT increases. The blends rich in PBT, which had the lowest crystallization rates, developed a structure containing spherulites which became disordered and smaller as the crystallization rate increased, up to a point where only small disordered crystalline structures were obtained for the samples of intermediate composition.

It is important to notice that the overall birefringence and degree of crystallinity decreased with increasing PET composition. Through DLI the crystallinity measured is its overall value. Therefore, as the partial crystallinity for PBT is much larger than that of PET, as the percentage of PET increased, the overall crystallinity decreased.

The lower crystallization half times for PET with respect to those of PBT might be misleading and they must be interpreted in terms of the crystallization temperature. Our crystallization temperatures provide a

low undercooling for PBT which explains its slow crystallization while the undercooling for PET is much larger giving a faster crystallization rate. The longest crystallization half times are obtained for those samples with the lowest degree of undercooling.

When plotting $\ln [-\ln(I_c - I_t/I_c - I_o)]$ vs. ln t, Magill recommends correcting ln t by the induction time lapsed before crystallization started occurring. In our calculations we have not done so, since, in our case, due to the large variety of blends, the induction times changed a lot from blend to blend. Furthermore, its definition is not clear and cannot equally be applied to a slowly crystallizing spherulitic blend or to a fast, low crystallinity, small structure blend. Therefore, we have decided to list the straight data from the DLI measurements. A tentative measurement of the induction times is plotted in Figure 13 and, as we can see, the induction times give also a first measurement of the crystallization rate, being in direct correspondence to the crystallization half times.

Taking induction times into account usually reduces the Avrami exponent by one integer. The Avrami exponents for the different blends are listed in Table 10.

Table 10

Uncorrected Avrami Exponents

Blend	200°C	202°C	205°C
100 PBT	3	2.8	2.6
90/10	3.5	3.5	3.5
85/15	5	5	5
80/20	5	5	5.4
70/30	5	5	5
60/40	3.3	3.3	3.3
50/50	3	3	3
40/60	2.5	3	3
30/70	3	3	3
20/80	2	2	2
10/90	2	2	2

The Avrami exponents which reach values of 5 have to be interpreted in view of the above considerations. Using the induction times plotted in Figure 13 for the 80/20 blend, the plot of $\ln [-\ln (1 - X_c)]$ vs. $\ln t$ is corrected by subtracting the induction time. The Avrami exponents then become 3.3 in contrast to the previous value of 5.5.

The DLI response may actually depend upon the size and morphology of the transformed phase as well as on its amount. It is apparent from

microscopic observations that the morphology of the crystallized blend depends upon its composition, ranging from spherulitic for high concentrations of PBT to a more random collection of crystals with increasing amounts of PET. Thus, the relationship between the amount of transformed phase and the DLI response may depend on composition of the blend and may vary during the course of crystallization. Hence the variation of the Avrami exponent with composition and the abnormally high values for the intermediate compositions may, at least in part, arise from this effect.

A further complication occurs in this case where there are two species which simultaneously crystallize. Equation (4) is valid for a situation where there is an increase in the amount of phase transformation with time where the birefringence of the developing anisotropic phase remains constant. The birefringence of a phase depends upon the local orientation of its constituent crystals. When both species are simultaneously crystallizing, the contribution to the birefringence by these components may differ. For example, for the PBT rich blends, the PBT is spherulitic with the PET presumably being located in interlamellar (or perhaps larger) regions within the spherulite. It is likely that the contribution per unit volume of PBT and PET to the birefringence will differ. Since the PBT and PET crystallize at different rates, both the amount and birefringence of the spherulites may change with time, leading to deviations from Equation (4) and to anomalous Avrami parameters.

The values of K in Avrami's equation give further information about the kinetics of crystallization. Their values are listed in Table II for the different blends at the three crystallization temperatures after obtaining them through

$$K = \frac{\ln 2}{t_{1/2}^{n}} \qquad (11)$$

Table 11

Values for the Rate Constant K (sec^{-n})

Blend	200°C	202°C	205°C
100 PBT	2.13×10^{-4}	1.03×10^{-4}	4.81×10^{-5}
90/10	1.64×10^{-6}	2.05×10^{-7}	4.48×10^{-8}
85/15	9.35×10^{-8}	4.18×10^{-8}	1.37×10^{-8}
80/20	1.54×10^{-7}	8.60×10^{-8}	4.63×10^{-9}
60/40	1.98×10^{-6}	1.31×10^{-6}	2.31×10^{-7}
50/50	9.02×10^{-6}	3.27×10^{-6}	3.50×10^{-7}
40/60	2.49×10^{-6}	5.35×10^{-6}	1.02×10^{-6}
30/70	1.93×10^{-4}	1.14×10^{-4}	4.81×10^{-5}
20/80	6.00×10^{-4}	3.93×10^{-4}	2.56×10^{-4}
10/90	6.36×10^{-4}	4.33×10^{-4}	3.21×10^{-4}
100 PET	1.20×10^{-3}	1.03×10^{-3}	5.35×10^{-4}

The information provided by DLI on the kinetics of crystallization is useful but very hard to interpret because DLI follows the overall crystallization of the sample and does not distinguish between both components, which we know crystallize separately. Similar information has been obtained by DSC on the same blends (Figure 14) by Dr. E. Balizer (47). DSC also follows the overall crystallization behavior and yields similar results to those obtained by DLI.

C H A P T E R V

DENSITY STUDIES

A. Introduction

If we consider the semicrystalline polymer as a two phase system, with sharp delineation between crystal and amorphous material, we can define an ideal degree of crystallinity. Let p^i be a particular measurable intensive property of the polymer and $\overline{p_c^i}$ and $\overline{p_a^i}$ be the "partial" properties of the crystalline and amorphous components in the same state as exists in the polymer. Then, if the ideal degree of crystallinity is X^i, one can write

$$p^i = X^i \overline{p_c^i} + (1 - X^i) \overline{p_a^i} \qquad (12)$$

This statement is rigorous by the definitions of the partial properties and must yield the same degree of crystallinity by each type of property measurement.

If we consider the solid composed of an ideal crystalline phase and an ideal liquid-like phase whose partial properties $(p_c^o)^i$ and $(p_a^o)^i$ are additive, we can obtain the degree of crystallinity X_c as

$$p^i = X_c (p_c^o)^i + (1 - X_c) (p_a^o)^i \qquad (13)$$

This degree of crystallinity for a substance composed of non-ideal phases will, in general, yield different values, depending on the property measured.

The specific volume has been widely used (48-55) as a measurement of the degree of crystallinity

$$X_c = \frac{\overline{V_a} - V}{\overline{V_a} - \overline{V_c}} \qquad (14)$$

or expressing it in terms of the densities

$$X_c = \frac{\rho_c}{\rho} \frac{\rho - \rho_a}{\rho_c - \rho_a} \qquad (15)$$

where ρ_c is the density of the crystalline material and ρ_a that of the amorphous material.

There is a dispute in the literature over the values of the crystalline density of PET. For our calculations, we have chosen the value proposed by Bunn (56) and Tadokoro (57), 1.455 g/cm^3, which has been traditionally used more often than the value of 1.515 g/cm proposed by Alter and Bonart (58) which would give lower degrees of crystallinity for a given density. A similar situation occurs with the PBT

crystalline density. Boye (59) proposes 1.39 g/cm^3 and this value has been used by Misra and Stein (7) and by Slagowski (60). Tadokoro (57) proposes the value of 1.404 g/cm^3 and a similar value of 1.406 g/cm^3 is obtained by Mencik (61). In our calculations we have used the value obtained by Alter and Bonart (58), 1.433 g/cm^3, because their WAXS pattern is in very good agreement with the one obtained by us.

The amorphous density for PET is 1.33 g/cm^3 and for PBT is 1.28 g/cm^3. It is apparent that only two decimal digits are significant, which must be kept in mind when interpreting the results. Moreover, because of the difficulty involved in quenching PBT, the samples may not be completely amorphous and therefore the value obtained might be too high.

With the above densities, the crystallization of the pure PBT and PET samples can be easily followed, and this was the main purpose of these density studies: to obtain the absolute degrees of crystallinity of PBT and PET during crystallization and be able later on to establish a correlation between these results and the infrared measurements that would enable us to obtain the degrees of crystallinity of the polymers in the blends through the IR measurements.

The crystallization of some of the blends was also followed by density and an apparent degree of crystallinity is obtained from the following equation

$$X_{app} = \left(\frac{W^{PET} \rho_c^{PET} + W^{PBT} \rho_c^{PBT}}{\rho} \right) \left(\frac{\rho - [W^{PET} \rho_a^{PET} + W^{PBT} \rho_a^{PBT}]}{[W^{PET} \rho_c^{PET} + W^{PBT} \rho^{PBT}] - [W^{PET} \rho_a^{PET} + W^{PBT} \rho_a^{PBT}]} \right) \quad (16)$$

where W^{PET} and W^{PBT} are the weight fractions of PET and PBT in that blend, ρ_c^{PET} and ρ_c^{PBT} are the crystalline densities of the pure polymers and ρ_a^{PBT} and ρ_a^{PET} are their amorphous densities.

The measurement of the apparent degree of crystallinity again gives us information only on the overall crystallization behavior and cannot be used to follow the crystallization of each component separately.

B. Experimental

We will delay the exposition of the sample preparation method to Chapter VI since the samples were used simultaneously in the density and IR studies and the latter being more exhaustive.

The density studies were carried out in two different density columns. The first one had a density range of 1.33 to 1.40 g/cm^3 and was made by establishing a gradient using equal volumes of two mixtures of

carbon tetrachloride and heptane of the following compositions: 70% CCl_4/ 30% C_7H_{16} and 90% CCl_4/10% C_7H_{16}. The second column of a density range 1.26 to 1.40 g/cm^3 was made using the following two mixtures: 63% CCl_4/ 37% C_7H_{16} and 82% CCl_4/18% C_7H_{16}. Both carbon tetrachloride and heptane provide excellent wettability of the samples and do not change their crystallinity by solvent induced crystallization nor appeared to swell the samples. Samples of PBT and PET were kept in the columns for one week without the occurrence of any change in density.

C. Results

The change in density and degree of crystallinity of PET and PBT with log time for the samples crystallized at 200^{o}C, 150^{o}C and 110^{o}C was plotted in Figures 15 and 16. It is possible to observe their sigmoidal shape and how the curves do not superimpose by means of a horizontal shift that would correct for the rate difference, but that the ultimate degree of crystallinity achieved is a function of the annealing temperature. A similar behavior has been observed by Hoffman (62).

In the melt crystallized samples, we can observe how at 200^{o}C the ultimate crystallinity of PET is higher than that of PBT, which depends on the values chosen for the crystalline densities. The behavior upon annealing is different for PET and PBT. PET reaches high degrees of crystallinity, the samples become very turbid, and there is microscopic evidence of the formation of small spherulites. Upon annealing, PBT reaches much lower degrees of crystallinity, the samples do not become turbid and, when viewed under the polarizing microscope, there is just a slight birefringence with no structures observable.

The crystallization of the blends cannot be followed as adequately with the density measurements since both components crystallize separately and the density measurements indicate only the change of the overall density with time.

Figure 17 shows the change in amorphous density, obtained using quenched samples, with blend composition compared to the linear change between both components. The slightly lower density of the blend from the linear extrapolation might suggest incompatibility of the amorphous phases. The deviation is comparable with experimental error and we believe the main reason for lower densities than expected is due to the difficulty in obtaining amorphous PBT, which means that the value for the amorphous density of PBT is too high and, since the PBT component is easier to quench in the blends, lower overall densities for the blends are obtained.

We have plotted in Figures 18, 19 and 20 for the 20/80, 40/60 and 50/50 blends the change of density with log time at the three crystallization temperatures of 200^{o}C, 150^{o}C and 110^{o}C. Their interpretation in terms of the apparent degree of crystallinity, which is also plotted in the same graphs, is difficult, but it is done in these PET rich blends in order to obtain further information about the PET crystallization behavior and final crystallinities in the presence of PBT. Finally, in Figure 21, we have plotted the change in apparent ultimate degree of crystallinity with blend composition at 200^{o}C, 150^{o}C and 110^{o}C (although we believe that at 110^{o}C the crystallization was not completed). We will defer the interpretation of these results to after the IR results have been presented, because both complement each other and cannot be considered separately.

C H A P T E R V I

INFRARED SPECTROSCOPY STUDIES

A. Introduction

All the methods proposed so far provide information on the overall crystallization kinetics of the blends but cannot distinguish the individual rates. Only IR can provide this information by isolating an absorption band which is sensitive to the crystallization of one component but remains unaltered during the crystallization of the other one.

IR has been a widely used method to determine the degree of crystallinity (63-66). The specific extinction coefficient, ε, at each wave number can be calculated as (63)

$$\varepsilon = \frac{1}{d\ell} \log (I/I_0) \qquad (17)$$

where d is the density of the sample, ℓ is its thickness and log (I/I_0) is the optical density.

By knowing the values of the density of the crystalline and amorphouse phases it is possible to obtain the extinction coefficient of these phases and obtain the degree of crystallinity.

$$\varepsilon = X_c \varepsilon_c + (1 - X_c) \varepsilon_a \qquad (18)$$

where ε_c and ε_a are the extinction coefficients of the crystalline and amorphous phases for a given band.

This procedure can be simplified when a standard reference band is available by normalizing the absorption of the crystalline band against the reference band. The variation in thickness and density are thus accounted for.

The crystallization kinetics of PET have been followed by IR by Cobbs and Burton (67). It was observed that the 972 cm^{-1} band is sensitive to the crystallization while the 795 cm^{-1} band remains unchanged. In the case of the PBT/PET blends the 972 cm^{-1} band is affected by the presence of PBT. It therefore cannot be used.

Koenig (68) and Boeiro (69) have studied the PET spectra by Fourier transform IR and assigned the 848 cm^{-1} band to the rocking mode of the trans conformation of the ethylene glycol segments in the crystalline regions. Since this band is unchanged by the presence of the second component (PBT), it will be used to follow the crystallization of PET.

PBT has been recently studied by Koenig (70) who looked at the $-CH_2-$ rocking region. He identified a high energy band at 917 cm^{-1} which showed a marked increase in intensity with crystallization. To follow the crystallization of PBT, we simultaneously monitored the changes in intensity of the 917 cm^{-1} and 810 cm^{-1} bands, but the final results are

plotted in terms of the 917 cm^{-1} band which shows a more sensitive change with crystallization.

The use of the 795 cm^{-1} band as a reference band was rejected since Koenig (68) showed that this band can be assigned to the trans conformation of PET. Instead we chose the 632 band which is assigned to the C-C-C bending mode in the benzene ring (70). In Figure 22 it is seen how the 917, 848, 810 and 795 cm^{-1} bands change in the 60/40 blend crystallized at 90°C for 0, 60 and 600 seconds.

The normalized intensities of the 917 and 848 cm^{-1} bands vs. log time were plotted for each of the blends at the different crystallization temperatures of 200°C, 150°C, 130°C, 110°C and 90°C. The curves obtained are sigmoidal in nature and they level off when the final crystallinity is achieved. Figures 23 and 24 show two typical curves of the change in intensity of the 848 cm^{-1} band for PET crystallized at 200°C and of the 917 cm^{-1} band for PBT crystallized at 200°C with log time.

Because of the limitation of signal to noise ratio, we can follow the crystallization of PBT only for blends having at least 50% PBT. Similarly PET crystallization can be followed only in blends having at least 50% PET.

Because of the different mode of operation of the IR spectrophotometer mentioned before, a different treatment must be given to the IR spectra of those samples crystallized at 200°C from those crystallized at 150°C, 110°C and 90°C. As it will be shown, the values of the intensity of the 917 cm^{-1} band for PET and those of the 848 cm^{-1} band for PBT, although they remain constant, are different from those for the other samples.

The intensity for the PET and PBT crystalline bands in the blends must be corrected to take into account the contribution to those bands of the other component and the dilution effect caused by them. The corrected intensity will reflect the change in crystallinity of the PET and PBT phase individually, based upon the weight of that phase. In other words, the corrected intensity would be the observed intensity if the sample had only one component and it would have crystallized at the same rate and manner as it did in the blend.

The correction is done according to Equations (19) and (20)

$$I_{917_{corr}} = \frac{I_{917_{exp}} - M_{PET}\, I_{917_{PET}}}{M_{PBT}} \qquad (19)$$

$$I_{848_{corr}} = \frac{I_{848_{exp}} - M_{PBT}\, I_{848_{PBT}}}{M_{PET}} \qquad (20)$$

where $I_{917_{corr}}$ and $I_{848_{corr}}$ are the corrected intensities for the 917 and 848 cm^{-1} bands. $I_{848_{exp}}$ and $I_{917_{exp}}$ are their experimental values measured in the blends. $I_{917_{PET}}$ is the value for the intensity of the 917 cm^{-1} band for PET and $I_{848_{PBT}}$ is the value of the intensity of the 848 cm^{-1} band for PBT, neither of which changes with crystallization. M_{PBT} and M_{PET} are the monomer mole fractions for PBT and PET in the blends.

The correction is done graphically through the use of Figures 25 - 28.

For the pure polymers, since the values of the IR crystalline bands and the density are known, a linear correlation is established between the intensity of the crystalline band for each crystallizing polymer and its degree of crystallinity. This relationship is plotted in Figure 29 - 32 for PET and PBT. Two different correlations are obtained for the samples crystallized at 200°C from those at 150°C, 110°C and 90°C because of the previously mentioned change in operating mode.

It is now possible to assign absolute values to the crystallinities of each component in the blends and follow its change with time. For each blend the normalized intensity of the crystalline band of each component is corrected according to Figures 25 - 28 and taking the corrected intensities to Figures 29 - 32, the absolute degrees of crystallinity of each component are obtained.

B. Experimental

Samples of the 100/0, 80/20, 60/40, 50/50, 40/60, 20/80, 10/90 and 0/100 (PBT/PET) blends were desiccated in a vacuum oven at 110°C for 24 hours. They were then compression molded on a Pasadena press at 280°C and 30,000 psi for one minute, after which they were quenched in an ice water mixture and then melted again in the press without pressure for another minute. They were then immediately quenched in the ice water mixture, after which they were crystallized in a fluidized bed at

150°C, 130°C, 110°C and 90°C for 15, 30, 60, 120, 180, 240, 300, 600, 900 and 1,800 seconds following which they were quenched again.

Two other sets of samples of the same blends, after the initial pressing and quenching, were remelted between hot plates at 280°C and transferred immediately to the crystallization bath at 200°C and 150°C. After the same crystallization times they were quenched in the ice water mixture.

The above procedure is very laborious since it involves the preparation of more than 600 samples, but it is necessary if density, IR and microscopy studies are to be performed on the same samples.

The IR spectra were obtained by a Perkin-Elmer Infrared Spectrophotometer, Model 283, in the absorption mode, slit N and suppression mode for the samples crystallized at 200°C and slit 7 with no suppression for the samples crystallized at 150°C, 110°C and 90°C.

The density measurements previously described were performed on these samples.

C. Results

From the sigmoidally-shaped curves showing the change of intensity of the crystalline band of each component with log time, the crystallization half times can be obtained. Figures 33 - 36 show the crystallization half times for the PET component vs. PET percentage for 200°C, 150°C, 130°C and 110°C crystallization temperatures. Figures 37 and 38 show the PBT crystallization half times vs. PBT percentage for the same temperatures.

Because of the nature of the 916 cm^{-1} band, it is possible to obtain the PBT induction times. These are the elapsed times until the crystalline peak appears and they are plotted in Figure 39 as a function of PBT percentage and crystallization temperature.

Finally, since by the described procedure we have been able to assign the absolute degrees of crystallinity to each component in the blend, we have plotted in Figures 40 and 41 the final PET and PBT crystallinities as a function of blend composition obtained at 200°C, 150°C, 130°C, 110°C and 90°C.

The procedure followed to determine the partial crystallinities in the blends involves a series of approximations like the insensitivity of the crystalline bands of one polymer to the crystallization of the second one, the additivity of the intensities of each component and the additivity of the specific volume of each component. It is important to estimate the degree of reliability of these results. To do so we have made an error analysis for the 60/40 and 40/60 blends at 110°C shown in Figures 42 - 45. This analysis is further used to verify the reliability of the theoretical interpretation.

It is also possible to compare the actual measured densities in the crystallized blends with the calculated values from the partial crystallinities according to Equation (21)

$$d_{calc} = [1.455\ X_{PET} + 1.33\ (1 - X_{PET})]\ W_{PET} + [1.43\ X_{PBT} + 1.28\ (1 - X_{PBT})]\ W_{PBT} \qquad (21)$$

where X_{PET} and X_{PBT} are the partial crystallinities of PET and PBT in the blend. W_{PET} and W_{PBT} are the weight fractions of the component in the blend.

Table 12 compares the experimental and calculated densities for a few of the samples. As it is possible to see, the agreement is quite good and the discrepancies are mainly on the third decimal digit whose significance in the pure components was already in doubt.

TABLE 12

Comparison of Calculated and Experimental Densities

Blend	T_c	Time Sec	X_{PBT}	X_{PET}	Density calc	Density expt'l
20/80	150	60	0	36	1.356	1.359
20/80	150	180	0	36	1.356	1.361
20/80	150	300	0	36	1.356	1.362
40/60	150	300	17	40	1.350	1.353
40/60	150	180	16	40	1.349	1.349
40/60	150	60	12	39	1.346	1.348
40/60	150	30	11	39	1.346	1.346
20/80	110	15	0	5	1.325	1.316
20/80	110	300	0	23	1.348	1.348
20/80	110	900	0	37	1.358	1.357
20/80	110	180	0	19	1.339	1.334
20/80	200	90	0	45	1.365	1.364
50/50	200	30	6	10	1.316	1.315
50/50	200	180	23	56	1.357	1.357
50/50	200	300	24	66	1.364	1.360
50/50	150	240	24	43	1.350	1.349
50/50	150	900	15	43	1.343	1.335
80/20	200	300	32	42	1.339	1.330
40/60	200	45	20	36	1.349	1.340
20/80	150	300	0	36	1.356	1.362

Since the crystallization behavior varies with temperature of crystallization, we will approach its interpretation looking at the behavior at each crystallizing temperature separately.

D. Crystallization Under Different Conditions

1. Crystallization at 200°C.

While normally PBT is known to have a faster crystallization rate than PET, at 200°C its undercooling is only 24°C while that of PET is 65°C. Therefore, the crystallization rate at 200°C is higher for PET than for PBT, which we already observed by DLI, and can now be seen by IR and density. While the crystallization half time of PBT in the blends remains constant, that of PET increases with PBT content showing a decrease in the crystallization rate of PET. The same behavior was observed by DLI and can be explained not only as a consequence of a dilution effect resulting in a need for each component to segregate from the mixture in order to crystallize, but also as a consequence of the lower undercooling which reaches a minimum in the 80/20 blend, due to the melting point depression.

The final PBT crystallinity decreases with the increase of the PET content while a reverse effect occurs with the PET crystallinity which increases markedly with the presence of PBT. The variation of apparent degree of crystallinity deduced from density offers further evidence of the same phenomena. The apparent degree of crystallinity of the 20/80 blend is higher than that of the 0/100 blend which is a clear

indication of the increase of PET crystallinity, especially if we consider that there is DSC, WAXS and IR evidence that PBT does not crystallize in this sample. The apparent degrees of crystallinity for the 40/60 and 50/50 blends are also higher than the expected values and confirm the increase in crystallinity of PET since the IR and DSC evidence is that the crystallinity of PBT decreases.

2. Crystallization at 150°C.

The general annealing behavior is characterized by lower crystallinities than for the melt crystallized samples. The rate is dependent on the difference between the annealing temperature and the glass transition temperature. The larger the difference between T_c and T_g, the faster the crystallization rate.

The interpretation of the effect of the difference between T_c and T_g on the ultimate degree of crystallinity depends on the approach taken to explain the nature of the T_g. In terms of the free volume theory (71-75), one expects always to obtain the same ultimate degree of crystallinity regardless of the annealing temperature; the only difference will be that the crystallization will proceed at a higher rate at higher annealing temperatures. However, if the T_g is explained according to Gibbs-DiMarzio (76-78) second order transition theory, it may be expected that not only the crystallization rate depends on the annealing temperature, but also the ultimate degree of crystallinity achieved will vary with the annealing temperatures. At higher annealing temperatures a larger number of configurations are available which allows for individual

rearrangements into different configurations which would facilitate the achievement of higher ultimate degrees of crystallinity.

The above considerations are necessary in order to interpret all the data from the annealing process. It must also be considered that the T_g changes with blend composition according to Figure 2 and therefore even though annealing temperatures will be the same, the difference from the T_g will vary with blend composition.

It is seen that PET crystallization half times decrease with increasing PBT concentration, which decreases the T_g of the blend. Similarly, the crystallization half times for PBT increase with increasing PET content which increases the T_g of the blends. Because of the closeness of the annealing temperature (150^oC) to the temperature of maximum rate of crystallization, both PBT and PET show at this temperature their lowest crystallization half times. Since the distance from the changing T_g is quite high, the changes in crystallization rate are not as strong as those observed at lower annealing temperatures.

The PET crystallinity remains fairly constant with the presence of PBT in the blends. There are two opposite effects at this temperature that probably compensate each other. These are the dilution effect by the PBT and the increase of mobility with the lowering of the T_g.

The results from the apparent crystallinities obtained through density are further evidence of this behavior. The apparent degrees of crystallinity decrease with increasing PBT percentage; they follow very closely the extrapolated values which show no drastic change in the partial crystallinities, especially if it is considered that 150^oC is the

only temperature where there is evidence that PBT crystallizes in the 20/80 blend.

3. Crystallization at 130°C.

As observed at other temperatures, there is a moderate increase in the crystallization half times of the PBT phase with increasing PET presence. Correspondingly, there is a dramatic decrease in the crystallization half time of the PET phase with increasing PBT presence.

The ultimate degrees of crystallinity of each phase in the blends at 130°C fall, as expected, between those at 110°C and 150°C. For the PET phase we observe how at high PET compositions the values of the degree of crystallinity are closer to those obtained at 110°C than to those obtained at 150°C. At lower PET compositions the values obtained at 130°C resemble more those obtained at 150°C. For the PBT phase the behavior is opposite. At high PBT compositions, the degrees of crystallinity at 130°C are closer to those obtained at 150°C than those at 110°C; at lower PBT compositions the results at 130°C become close to those obtained at 110°C.

An explanation to the above effect can be viewed in terms of the effect of the presence of the second component on the T_g of the blend. The blends with very high PET composition have a very high T_g and the difference between T_g and T_c is quite small when T_c = 110°C and 130°C while it is higher when T_c = 150°C. Similarly in the PBT rich blends, the presence of the PET component increases the T_g. For high PBT percentages, the difference between T_g and T_c is quite high for T_c = 150°C

and 130°C while for 110°C it is smaller. As the blend composition changes so does the T_g, increasing the value of $T_c - T_g$ in the PET rich blends and decreasing it for the PBT rich blends. Once the value of $T_c - T_g$ becomes high enough the crystallization behavior becomes very similar for the various T_c and the ultimate degrees of crystallinity of each phase become constant. This happens with the PET rich blends once 40% PBT is present and similarly this constancy of ultimate degree of crystallinity is lost for the PBT phase once 20% PET is present, reflecting in both cases the same effect.

4. Crystallization at 110°C.

The most profound changes in crystallization behavior with blend composition are seen at this crystallization temperature, since it is quite close to the PET T_g = 69°C and distant from the PBT T_g = 29°C.

The PET crystallization half times decrease drastically with PBT percentage, while those of PBT increase with PET content. This reflects the effects of the changing T_g. The effect is larger for PET since it is a slowly crystallizing polymer and this annealing temperature is quite close to its T_g.

The final crystallinity for PBT is lower than that for the other samples and decreases with increasing PET percentage in the blends. At the same time, the PET crystallinity increases with the presence of PBT quite markedly.

Both effects can be accounted for as a consequence of the change in T_g in the blends. Evidence for the increase in the PET crystallinity is also provided by the change in apparent degree of crystallinity with

PBT concentration as calculated from density measurements, although it is our belief that the crystallization might not be completed for the pure PET sample.

5. Crystallization at 90°C.

The crystallization at 90°C is very slow and, since the samples were not crystallized long enough to allow for a definite determination of the crystallization half times, these have not been plotted. The plotted degrees of crystallinity for PBT and PET are those achieved after 80 minutes at the crystallization temperature. Similarly to the previous cases, it is possible to observe how the PBT crystallinity decreases with PET content in the blends, while the crystallinity of PET increases with the increasing concentration of PBT, reflecting again the shift in T_g. As it can be expected, the values reached are much lower than those at higher annealing temperatures.

E. Overall Crystallization Behavior

There is no good theory to explain the ultimate degree of crystallinity reached by polymers and therefore our comments in respect to the effect of the T_g are, to some extent, conjecture. There is another aspect of the crystallization behavior which can be more accurately related to the T_g of the blends and that is the crystallization rate.

If one examines a typical plot of crystallization rate vs. temperature of crystallization (Figure 46), a maximum is observed. While at T_m the nucleation rate is zero, as the temperature is lowered the nucleation rate increases which gives increasing crystallization rates. The rate

increases until the temperature of crystallization becomes so low that crystallization becomes retarded by the decreasing diffusion rates with decreasing temperature. Consequently, a maximum in crystallization rate occurs at some temperature between T_g and T_m. At lower temperatures than this maximum, crystallization rates are diffusion controlled, while at higher temperatures they are nucleation controlled.

In the studies of the crystallization kinetics of polymer diluent mixtures, Boon and Azcue (79) observed how the addition of diluent which lowered the T_g causes a shift in the crystallization maximum towards lower temperatures and an increase of its value. A similar behavior was observed by Nishi and Wang (80).

Similarly in our case we have plotted the crystallization rate obtained from the crystallization half times vs. temperature of crystallization for the different blends (Figures 47 and 48). For the PET crystallization rate, we can observe how the maximum in crystallization rate occurs at lower temperatures as the PBT percent in the blends increases. At the same time the crystallization rate at the maximum increases. This behavior is typical of a polymer to which another polymer which lowers the T_g is added. The maximum is predicted to decrease with higher percentages of the second polymer. In that case, the effect caused by the lowering of the T_g is overcome by the dilution effect caused by the higher percentage of the second component. We will further look at this quantitatively in our next chapter.

The behavior of the PBT phase is the opposite to that of the PET phase. The position of the maximum in the blends is shifted towards

higher temperatures with increasing amounts of PET. At the same time, the value of the maximum is lowered. This behavior reflects again the fact that we are adding to the PBT a polymer of high T_g, PET, increasing the T_g of the amorphous phase and causing these changes on the overall crystallization kinetics curve.

Following the Boon and Azcue approach in order to show that the shift to lower temperatures of the crystallization range of PET upon adding PBT, and that the shift to higher temperatures of the crystallization range of PBT upon adding PET, is mainly a consequence of the depression of the T_m and T_g in the first case and to their increase in the second case, we must introduce a reduced temperature scale, θ, which is defined as

$$\theta = \frac{T - T_g}{T_m - T_g} \qquad (22)$$

The experimental growth rates are plotted as a function of θ in Figures 49 and 50. With this correction all the maximum occur at the same reduced temperature and give us further indication that the changes of crystallization behavior can be accounted for in terms of the changes in T_g and T_m. This provides further evidence of the compatibility of both polymers in the amorphous state and of the existence of only one T_g in the blends which determines the crystallization behavior.

We must recall that both polymers crystallize separately according to their own unit cell structure, but we have observed how in doing so they are affected by the change of the T_g of their amorphous phase. If they were segregated in the amorphous phase, they would crystallize with rates that were independent of the second component. (This neglects effects that may result from their possibly being a finite size of a disperse but incomplete amorphous phase.) The fact that their crystallization behavior is affected by the change of T_g, in a manner determined by the reduced temperature, is consistent with the T_g observed by DSC and shows that the T_g's are really representative of the relaxation of the amorphous phase and is further evidence of compatibility between both polymers.

CHAPTER VII

THEORETICAL INTERPRETATION

The quantitative interpretation of polymer crystallization has been offered by Mandelkern (24,81,82) as an extension of the Turnbull-Fisher expression for nucleation (83,84). The growth rate has generally been described by the equation

$$G = G_o \exp \{-\Delta E/KT\} \exp \{-\Delta F^*/KT\} \qquad (23)$$

where G_o is a constant and ΔE the activation energy for the transport process at the interface. The term $G_o \exp \{-\Delta E/KT\}$ may be considered a jump rate for the molecular rearrangements which are necessary for adding a crystallizing unit to the crystal. The quantity ΔF^* is the work required to form a nucleus of critical size.

The term $G_o \{-\Delta E/KT\}$ can be replaced by the segmental jumpt rate of the molecules in the supercooled phase (85-87). Using the WLF equation for viscous flow, Hoffman (88-94) obtained

$$G = G_o \exp \left\{ - \frac{C_1}{R[C_2 + (T - T_g)]} \right\} \exp \left\{ - \frac{\Delta F^*}{KT} \right\} \qquad (24)$$

C_1 and C_2 are general constants obtained by Van Antwerpen (19) for PET.

If the growth rate is controlled by two-dimensional surface nucleation, ΔF^* is given by (94)

$$\Delta F^* = 4 b_o \sigma \sigma_e / \Delta F \qquad (25)$$

where b_o is the thickness of a monomolecular layer, σ and σ_e are interfacial free energies per unit area parallel and perpendicular, respectively, to the molecular chain direction, and ΔF is the Gibbs free energy difference between the supercooled phase and the crystalline phase per unit volume. The last quantity can be approximated by

$$\Delta F = \Delta H (T_m - T)/T_m \qquad (26)$$

where ΔH is the heat of fusion.

For polymer-diluent mixtures an additional term must be included in calculating the work required to form a nucleus (24). This additional

term, containing ln v_2, represents the probability of selecting the required number of crystalline sequences from a mixture with volume fraction of polymer v_2. For a two-dimensional nucleus ΔF^* can be calculated (79)

$$\Delta F^* = (4\, b_o\, \sigma\, \sigma_e/\Delta F') - 2\sigma\, KT\, (\ln v_2)/b_o\, \Delta F' \qquad (27)$$

where $\Delta F'$ represents the bulk free energy of fusion plus the heat of mixing of molten polymer with the melt at the specified composition. It can be approximated by

$$\Delta F' = \Delta H\, (T_m - T)/T_m \qquad (28)$$

where T_m is the melting point of the crystalline phase in the mixture and ΔH is the heat of fusion as used in Equation (26).

For the growth rate of a polymer-diluent or, in our case of polymer-polymer mixture, we can use the following equation:

$$G = v_2\, b_o \exp\left\{ - \frac{C_1}{R[C_2 + (T - T_g)]} \right\} \exp$$

$$\left\{ \frac{-4\, b_o\, \sigma\, \sigma_e\, T_m}{KT\, \Delta H\, (T_m - T)} + \frac{2\, T_m \ln v_2}{b_o\, \Delta H\, (T_m - T)} \right\} \qquad (29)$$

where T_g is the glass transition of the blend and v_2 is the volume fraction in the blend of the polymer whose crystallization we are studying.

This value of G obtained in this way is representative of the lamellar growth rate. In our case, this data is not available but, instead, we have a crystallization rate related to the overall crystallization and not associated with any specific morphology. There is also an uncertainty in the value of the T_m of each component in the blends since, although there is a slight depression in the melting point of each component as shown by DSC, Hoffman-Weeks plots cannot be obtained because of the recrystallization of PBT. These two factors induced us to study theoretically that portion of the crystallization rate vs. temperature curve which is diffusion controlled. Moreover, most of our experimental data lies in that region, in which we had already gone through the maximum in nucleation rate. Thus, nearly all the nuclei are present and our measurement of the crystallization rate will be a good representation of G since all the chance in crystallinity will be accounted in

terms of lamellar growth and no contribution from the creation of new crystals can be expected.

If we are studying only the diffusion controlled region, G can be approximated by

$$G = v_2 G_o \exp\left(- \frac{C_1}{R[(C_2 + [T - T_g])]} \right) \qquad (30)$$

We can use the following values for the parameters in the above equation (19). R is the gas constant (8.31 J/mole ^oK), C_1 = 6.46 KJ/mole, C_2 = 24^oK and v_2 is the volume fraction of the polymer being studied obtained from the weight fractions using for densities the following values - density of PET = 1.33 g/cm^3 and of PBT = 1.28 g/cm^3.

With the above parameters, the crystallization rate is obtained vs. the temperature of crystallization (Figure 51) for the different blends. Both the PET and PBT crystallization rates are plotted and we can observe how the slope of the curves for the crystallization rate of PET is much higher than that for PBT. The same effect was predicted theoretically. It is also possible to observe how at each of the crystallization temperatures (110^{o}C, 130^{o}C and 150^{o}C) the crystallization rates of PET and PBT, as the blends become rich in the second component, approach each other to reach in the 60/40 and 40/60 values of the same order of magnitude, an effect which has been also observed experimentally.

The model therefore describes quite well qualitatively the crystallization behavior of the blends.

To obtain further quantitative evidence of the agreement, we have plotted in Figures 52 and 53 the PET and PBT crystallization rate vs. composition for the three crystallization temperatures. The theoretical curves have been adjusted to coincide with the experimental value for the pure polymers which accounts for the factor G_o in Equation (30). The agreement is quite good considering the approximations involved.

During crystallization, the composition of the amorphous phase varies due to the different crystallization rates of each component. Therefore, a numerical integration must be performed when theoretically computing the crystallization rate to take into account the change in the composition of the amorphous phase which affects the value of v_2 and of the T_g. This integration was performed, and the results plotted in Figures 54 and 55 are not too different from those previously obtained.

The approximations involved in the above calculations include the neglect of the nucleation term which causes us to neglect also any possible interaction between both polymers. The values of C_1 and C_2 have a certain degree of uncertainty and we have used the PET values for both PET and PBT, and for the values of the blends, which may, in reality, be different. We have also assumed G_o to be constant for each polymer. In fact, it is dependent on molecular weight, on the morphology of the crystalline structure, and it includes a factor which arises from balancing

all the forward and backward reactions in the surface nucleation process which might vary in the blends.

Examining Figures 54 and 55 it can be observed how for PBT the crystallization rate decreases with increasing PET percent, as expected, which is due to the rising T_g and the dilution effect. For PET, the crystallization rate increases with PBT percent. This increase is due to the lowering T_g. The dilution effect, in the range of blends for which data is available, is not high enough to start decreasing the rate; the same behavior is predicted theoretically.

It is therefore our feeling that within the approximations involved, the model describes correctly the crystallization behavior in the diffusion controlled region and that the changes in crystallization rate can be accounted for in terms of the changing glass transition temperature, which, as we have explained, is proof of the compatibility of both polymers in their amorphous phase.

CHAPTER VIII

COMPARISON IN THE CRYSTALLIZATION FROM THE GLASS AND THE MELT

The crystallization studies at low temperatures can either be performed on samples cooled from the melt to the crystallization temperature or on samples which are annealed to the crystallization temperature from the glass. Each method would be indicated for the particular regions where there would be faster equilibration to the crystallization temperature, without having induced crystallinity in the amorphous polymer. In general, crystallization from the melt is better for crystallization temperatures above that of the crystallization rate maximum and crystallization from the glass is better for temperatures lower than the maximum.

We observed that for slowly crystallizing polymers both methods can be used and the growth rates and morphologies obtained will be the same and only dependent upon the crystallization temperature. Since the maximum in nucleation rate occurs at lower temperatures than that of the maximum growth rate, in quenched samples, which are annealed above the first one, very high nucleation densities are achieved which yield samples with a large number of spherulites that do not achieve as large a radius as those samples crystallized from the melt at the same temperature (19,95-97). With polymers which have a high crystallization rate when crystallizing from the melt at low temperatures, upon going through the maximum a substantial crystallization occurs. However, if the same samples

are quenched from the melt to the amorphous state, although a high number of nuclei may be formed, they do not grow since the cooling step is too fast.

The above considerations are usually made, without much experimental evidence, this absence is more evident for the fast crystallizing polymers. Since in our studies we are dealing with a "fast" and "slow" crystallizing polymer, it offers a good opportunity to experimentally verify the above considerations.

Two sets of samples of the different blends were crystallized at 110^{o}C - one from the melt and the other from the glass - and the crystallization half times and degrees of crystallinity were obtained by IR.

The PET crystallization half times vs. PET percent are plotted in Figure 58. Those of PBT are plotted in Figure 59. It is observed how the crystallization rate of PET is the same in the samples crystallized from the melt or the glass. However, the PBT crystallization rate is higher for those samples crystallized from the melt than for those crystallized from the glass.

The ultimate degrees of crystallinity are plotted in Figures 60 and 61 for the PET and PBT phases. For the PET rich blends, the ultimate degrees of crystallinity obtained by both methods are similar although, as the PBT content increases, the T_g is lowered, the rate increases and some discrepancies appear. For PBT the values obtained by both methods are very different. As the PET percentage increases, the rate decreases and the difference in crystallinity obtained through both methods decreases.

One must, therefore, conclude that while for PET both methods yield similar results, for PBT, because of the high crystallization rates, higher degrees of crystallinity and lower crystallization half times are obtained for the samples crystallized from the melt. In the blends these differences are affected by the already observed changes in the crystallization rates.

C H A P T E R I X

TRANS-ESTERIFICATION STUDIES

The presence of only one T_g in the amorphous blends could arise from the trans-esterification reaction occurring between both polymers during the melting process, forming a copolymer of both species. We would then infer compatibility between both polymers in the amorphous state because of the existence of only one T_g which would actually be due to the trans-esterification reaction yielding a blend compatibilized by the copolymer.

The arguments in favor of compatibility which arise from the crystallization behavior cannot be easily discussed in terms of the trans-esterification reaction occurring. If this occurs, it is expected to affect the crystallization behavior. It is therefore important to know how much it may affect the crystallization data previously obtained.

The trans-esterification reaction is very fast in the presence of a catalyst (98-100). In our case, the polymers have been stabilized and no catalyst is present. However, during melt blending they are kept at high temperatures ($280^{o}C$) for a few minutes at which condition, therefore, trans-esterification may occur even in the stabilized polymers (101-104). In this section we discuss the time dependence for this trans-esterification reaction to occur in the melt.

Flory has shown (98-100) how, if the two initial polyesters have different molecular weights, the melt viscosity depends on the degree of trans-esterification. Actually, as the reaction occurs, randomization of the two polymers takes place and it proceeds until they become Flory distributed (polydispersity = 2). Since $\overline{M}_n$ remains constant, we are not creating nor destroying polymer molecules; the polydispersity is decreased because of the lowering of $\overline{M}_w$. Therefore, a decrease of the melt viscosity is expected as the trans-esterification reaction occurs. A similar effect is observed in the intrinsic viscosity for the same reason. Kotliar (105,106) has studied theoretically the trans-esterification reaction and predicted the changes in intrinsic viscosity with the number of interchanges per number average molecule for the different Mark-Houwink exponents and the different ratios of initial molecular weight ratio of the blend components.

In our system, we have measured the intrinsic viscosities of the 50/50 blend in a 60% phenol 40% 1,1,2,2 tetrachloro ethane mixture for the samples kept at different times in the melt at 280^{o}C (Figure 62).

It is possible to observe how, for up to three minutes in the melt, there is no substantial change in the intrinsic viscosity, but there is a very appreciable drop at longer times.

The trans-esterification reaction is expected to affect the crystallization behavior, decreasing the ultimate degree of crystallinity and the crystallization rate with the occurrence of the randomization reaction. To study the effect on the crystallization, we have isothermally crystallized samples of the 50/50 blend at 110^{o}C, which had been kept in the melt for different times. The crystallization was followed by IR according to

the procedure previously described. The crystallization half times for the PBT phase in the 50/50 blend are plotted in Figure 63, where we again observe a sharp increase in crystallization half times after three minutes in the melt. The same behavior can be observed for the PET phase (Figure 64) where, after three minutes in the melt, the crystallization half times increase sharply indicating that the trans-esterification reaction is occurring. Further evidence of the same effect is obtained by looking at the ultimate degrees of crystallinity for the PBT and PET phase with time in the melt as seen in Table 13.

Table 13

Ultimate Degrees of Crystallinity

Time (min)	PBT %	PET %
2_{solu}	8	30
2_{extr}	7	28
3	7	28
5	5	20
7	5	18
10	4	15

The PBT degrees of crystallinity are very low and their accuracy is therefore not good, but those of PET are more easily measured and

they show a marked decrease after three minutes in the melt. No significant different behavior is observed in the solvent blended samples. From the above experiments, it is possible to conclude that no significant trans-esterification occurs within the first three minutes in the melt; after this time trans-esterification occurs and the crystallization behavior is seriously affected. Similar results have been obtained by Budin (104) who does not observe any significant trans-esterification after a few minutes in the melt.

In all our crystallization studies the samples were consistently kept in the melt for two minutes. Therefore, no significant effect from the trans-esterification reaction is expected and we do not believe that the compatibility arises from the presence of the copolymer.

We tried to obtain further evidence of this behavior from thin layer chromatography studies. These studies were performed by preparing 5% solutions in 60% phenol-40% tetrachloro ethane, which were spotted onto an Analtech silica gel 6.F plate (107), dried at 100^{o}C in a vacuum oven, cooled, and developed in a mixture of phenol-tetrachloro ethane-methanol (108). The results were not conclusive but they showed a different behavior for the blend kept 10 minutes in the melt while the solvent blended samples and those extrusion blended showed a similar behavior.

C H A P T E R X

EFFECT OF THE PROCESSING CONDITIONS ON THE KINETICS OF CRYSTALLIZATION

The blends, on which all the crystallization studies were performed, had been obtained by co-extrusion of both polymers and had been stabilized. It is important to determine whether the processing conditions may influence the crystallization behavior. Therefore, a series of crystallization studies were made on three blends which had been processed under different conditions. The information on the processing conditions was provided by the General Electric Company.

The first sample was a 60/40 (PBT/PET) blend which had been processed at different screw speeds. The second sample was a 40/60 (PBT/PET) blend which had been processed in a similar way. Neither of the blends contained any stabilizer in order to maximize the possible influence of the processing conditions. The different screw speeds and residence times at $520^{o}F$ ($271^{o}C$) are given in Table 14.

Table 14

Screw Speeds and Residence Times in the Extruder

Screw Speed rpm	Residence Time sec
20	100
40	50
60	38
80	25
100	20

In order to measure the effect of the stabilizer, we performed the studies on five samples of the 75/25 (PBT/PET) blend in which the stabilizer concentration was 0, 0.5, 0.10, 0.20 and 0.50%.

The three sets of samples were crystallized at 110^{o}C and their crystallization was followed by IR according to the process previously outlined.

In the first set of blends, the crystallization behavior of the PBT component was followed. The final degrees of crystallinity and crystallization half times were obtained which are plotted in Table 15.

Table 15

PBT Crystallization Behavior in the 60/40 Blend

Screw Speed rpm	Degree of Crystallinity %	Crystallization Half Times sec
20	19.0	20
40	17.5	30
60	17.5	30
80	17.5	40
100	16.5	40

The changes are within experimental error for screw speeds from 40 rpm up. However, for 20 rpm, giving the longest residence time, an increase in crystallinity and rate is observed. The samples presented a slight brown appearance, showing that some degradation must have occurred; it is known that PBT degrades, releasing THF and reducing the molecular weight which would increase the rate. The degradation effect, as evidenced by the brown appearance, is probably accelerated by the presence of air. For all the other screw speeds, there is no effect on the crystallization behavior of the PBT component.

The crystallization behavior of the PET component in the 40/60 blend is recorded in Table 16.

Table 16

PET Crystallization Behavior in the 40/60 Blend

Screw Speed rpm	Degree of Crystallinity %	Crystallization Half Times sec
20	38.8	50
40	39.0	55
60	39.0	50
80	39.2	65
100	38.8	40

No substantial change is observed in the crystallization behavior of the PET component with varying screw speeds.

Finally, the PBT crystallization behavior in the blends 75/25 (100 rpm) with different amounts of stabilization was studied. The results are recorded in Table 17.

Table 17

PBT Crystallization Behavior in the 75/25 Blend

Stabilizer Concentration %	Degree of Crystallinity %	Crystallization Half Times sec
0	16.5	30
0.05	15.5	20
0.1	17.5	30
0.2	16.5	30
0.5	18.0	20

In these results we again observe no significant changes, within experimental error, in the crystallization behavior. Our conclusion is, therefore, that the processing conditions studied do not affect the crystallization results. Exception must be made in the PBT rich blends which, if they are kept in the melt for 100 sec or more in contact with air, undergo degradation evidenced by the brown coloration that appears. The requirement of contact with air must be underlined since no evidence of degradation for those times is seen in samples which are not kept in contact with air.

Since all our samples were prepared at 60 rpm, no influence in the crystallization behavior by the processing conditions is expected.

C H A P T E R X I

DYNAMIC-MECHANICAL STUDIES

Although it was not the main purpose of the present study to describe the mechanical properties of the PBT/PET blends, dynamic-mechanical studies can provide us with information about the relaxation behavior of the blends and from it we can get a more complete knowledge of their compatibility.

When a stress or a strain is applied to a viscoelastic material, part of the energy is stored elastically and part is lost in the form of heat. The ratio of the energy lost to that stored is a measure of the damping characteristics of the material. In the Rheovibron, a sinusoidal strain of fixed frequency is applied to one end of a small sample, held in slight tension, and the response or stress is measured at the other end by a transducer. The stress in phase and 90^{o} out of phase with the strain and the phase angle are measured over a wide temperature range.

The samples, which have been desiccated for 24 hours, are pressed between aluminum foil and after two minutes in the melt they are quenched in an ice water mixture. Since these samples are thicker (10 to 15 mils), the quenching process is not perfect and we expect some crystallites to be formed in the low T_g, PBT rich blends.

The samples are placed in a Rheovibron Model DDV-II and the low temperature accessory is placed in position and filled with dry ice. The range of temperatures studied therefore starts at $0^{o}C$ and would clearly cover the PBT relaxation.

Directly from the Rheovibron one obtains the value of tanδ which is the ratio between the loss modulus and the elastic modulus, as well as the value of G*. From these values it is possible to obtain the elastic and loss modulus.

$$G' = G^* \cos\delta \qquad (31)$$

$$G'' = G^* \sin\delta = G' \tan\delta \qquad (32)$$

The results are plotted in Figures 65 - 74. We have shown the results obtained at 110 Hz. Similar results were obtained at 35 Hz. The complex modulus G* is plotted in Figures 65 and 66 for the different blends. These plots show the fall in the complex modulus with temperature when the T_g is reached. An important feature is observed; when the temperature reaches the T_g the modulus starts to decrease, with higher temperatures the modulus increases in value again, it levels off and, finally, with further increases in temperature it decreases again. This behavior is observed in the blends and is most pronounced

in the 20/80 blend. It is our belief that this increase in modulus with temperature is due to an increase in the PET crystallinity in the blends which occus during the experiment. This increase is favored by the lowering of the T_g in the blends and by the increase in crystallization rate induced by the presence of PBT as already discussed.

The evidence for the crystallization arises from the examination of the samples during the experiment which become white as the modulus starts to increase. This whitening of the sample is most pronounced in the 20/80 blend which has the highest PET concentration. This increase in crystallinity is mostly due to the PET component because the PBT, when annealed, does not become white. The drop in modulus with the T_g occurs at lower temperatures for the 0/100, 20/80, and 40/60 blends. For the PBT rich blends the values are quite close and this is mainly due to the fact that the PET component is not completely amorphous which increases the T_g in the PBT rich blends.

The values of tanδ with temperature are recorded in Figures 67 and 68 for 110 Hz. Only one relaxation is observed in the blends which is further evidence of their compatibility. It is possible to observe how, as we proceed from the PET rich samples to those rich in PBT, the tanδ curves become broader and the value of the maximum decreases. This behavior shows an increase in the crystallinity of the samples which was expected with the lower T_g's due to the inefficiency of the quenching process (109-111).

Finally, the T_g vs. blend composition is plotted for the different blends at the two frequencies in Figures 73 and 74. The values are obtained from the tanδ and the loss modulus. In the PBT rich blends the T_g's are very similar because the samples had some crystallinity induced by the quenching process. With higher PET concentrations, the T_g's increase until they reach the value for pure PET. The existence of only one glass transition in the blends is further evidence of their compatibility. These results must be compared with those obtained by DSC. The T_g values for the PET rich blends are similar and the differences arise from the selection of frequencies. The values for the PBT rich blends are higher than those obtained by DSC. The differences, as mentioned before, are not only due to the selection of frequency but mainly to the fact that the quenching process, to obtain thick enough samples, is inefficient. Some crystallization occurs mainly in the PBT phase changing the composition of the amorphous phase and the T_g.

CHAPTER XII

CONCLUSIONS

1. PBT and PET crystallize separately in the blends.

2. PBT and PET show only one glass transition temperature in the amorphous blends. Its value is intermediate between those of the pure polymers.

3. The spherulitic morphology of PBT and PET is preserved upon the addition of small amounts of the other components. With higher amounts, the spherulites become coarser and more disordered and finally the spherulitic morphology is lost in the blends of intermediate composition.

4. The overall crystallization rate at high temperatures is depressed with the addition of the second component reaching a minimum in the 85/15 blend.

5. The crystallization kinetics of each component in the blends can be determined by the use of IR spectroscopy.

6. At high temperatures both the PBT and PET crystallization rates are decreased with the presence of the second component.

7. At low temperatures, the crystallization rate of PET is increased with increasing PBT percent while that of PBT is decreased with increasing amounts of PET.

8. The crystallization rate curves vs. temperature curves for PET show a shift of the maximum toward lower temperatures and an increase of its value with increasing amounts of PBT. A similar shift toward higher temperatures is observed for the PBT crystallization. The value of the maximum decreases with increasing concentration of PET. The shift in the maximum in crystallization rate can be corrected by plotting the crystallization rate vs. a reduced temperature which takes into account the change in T_g in the blends.

9. The above effects were theoretically accounted for by following Mandelkern's approach to the kinetics of crystallization of a polymer diluent mixture, adapted to the diffusion controlled region.

10. Because of the strong influence of the other component to the kinetics of crystallization of PBT and PET, which is consistent with the single T_g observed in the amorphous blends, compatibility between both polymers in their amorphous state was concluded.

11. For a slowly crystallizing polymer (PET), crystallization from the glass or the melt, at temperatures below those of the maximum, yields the same crystallization half times and ultimate degrees of crystallinity. A different behavior is observed for a fast crystallizing polymer (PBT) which, when crystallized from the melt, shows much higher crystallization rates and ultimate crystallinities.

12. The trans-esterification reaction for up to 3 minutes in the melt does not occur in a significant amount to alter either the crystallization kinetics or intrinsic viscosity of the blends.

13. The studied processing conditions did not affect the crystallization behavior of the blends.

CHAPTER XIII

SUGGESTIONS FOR FUTURE RESEARCH

1. The compatibility of both polymers in their amorphous state could be further studied by neutron scattering.

2. The reasons for compatibility between both polymers could be studied, through Fourier transform infrared spectroscopy of the blends, which might be able to establish the interactions between both polymers.

3. The occurrence of the trans-esterification reaction between both polymers when the blends are kept a long time in the melt could be further studied by thin layer chromatography and gel permeation chromatography.

4. The composition-physical properties relationship for the different blends could be studied, varying crystallization conditions and degree of trans-esterification.

5. Low angle x-ray scattering studies could be conducted to estimate the variation of lamellar dimensions with the composition of the different blends.

6. Studies on the morphologies of the different structures induced during crystallization could be performed by using a scanning electron microscope. Special attention should be given to the already seen highly branched spherulites and the other disordered structures.

BIBLIOGRAPHY

1. C. J. Ong, Ph.D. Dissertation, University of Massachusetts, Amherst, 1974.

2. C. J. Ong and F. P. Price, J. Polym. Sci., Symposium Series, 1977.

3. F. H. Khambatta, Ph.D. Dissertation, University of Massachusetts, Amherst, 1976.

4. F. H. Khambatta, T. Russell, F. Warner and R. S. Stein, J. Polym. Sci., Polym. Phys. Ed. 14, 1391 (1976).

5. W. Wenig, F. E. Karasz and W. J. MacKnight, J. Appl. Phys. 46, 4194 (1975).

6. F. P. Warner and R. S. Stein, J. Polym. Sci., Polym. Phys. Ed., in press.

7. A. Misra and R. S. Stein, Bull. Am. Phys. Soc., Ser. II, 20, 391 (1975).

8. A. Misra and R. S. Stein, Report No. 2 to the General Electric Company, 1974.

9. A. Wasiak and R. S. Stein, Report No. 3 to the General Electric Company, 1975.

10. S. Y. Hobbs and C. F. Pratt, Report 74CRD276, General Electric Company, 1974.

11. A. Keller, J. Polym. Sci. 17, 291 (1955).

12. M. J. Kolb and E. F. Izard, J. Appl. Phys. 20, 571 (1949).

13. W. M. Cobbs and R. B. Burton, J. Polym. Sci. 12, 275 (1953).

14. A. Keller, G. R. Lester and L. B. Morgan, Phil. Trans. Roy. Soc. (London), A247, 1 (1954).

15. F. D. Hartley, F. W. Lord and L. B. Morgan, Phil. Trans. Roy. Soc. A247, 23 (1954).

16. L. B. Morgan, Phil. Trans. Roy. Soc. A247, 13 (1954).

17. K. G. Mayhan, W. J. James and W. Bosch, J. Appl. Polym. Sci. 9, 3605 (1965).

18. G. S. Fielding-Rusell and P. S. Pillai, Die Makromolekulare Chemie 135, 263 (1970).

19. F. VanAntwerpen and D. W. VanKrevelen, J. Polym. Sci., Polym. Phys. Ed. 10, 2423 (1972).

20. F. VanAntwerpen and D. W. VanKrevelen, J. Polym. Sci., A-2, 10, 2409 (1973).

21. F. VanAntwerpen and D. W. VanKrevelen, J. Polym. Sci., A-2, 10, 2423 (1973).

22. A. Misra, Ph.D. Dissertation, University of Massachusetts, Amherst, 1976 .

23. A. Misra and R. S. Stein, J. Polym. Sci., B, 10, 473 (1972).

24. L. Mandelkern, "Crystallization of Polymers," McGraw-Hill, New York, Chapter 8, 1964.

25. Z. Mencik, J. Polym. Sci., Polym. Phys. Ed. 13, 2173 (1975).

26. R. P. Daubeny, C. W. Bunn and C. J. Brown, Proc. Royal Soc. (London), A226, 531 (1959).

27. H. G. Kilian, H. Halboth and E. Jenckel, Kolloid-Zeitschrift 172, 2, 166 (1960).

28. L. Mandelkern, G. M. Martin and F. A. Quinn, J. Res. Nat. Bur. Stand. 58, 137 (1959).

29. T. G Fox and S. Loshaek, J. Polym. Sci. 15, 371 (1955).

30. A. Keller, J. Polym. Sci. 17, 291 (1955).

31. R. S. Stein and M. B. Rhodes, J. Appl. Phys. 31, 1873 (1960).

32. R. S. Stein in "Structure and Properties of Polymer Films," ed. by R. W. Lenz and R. S. Stein, Plenum, New York, p. 1, 1973.

33. J. H. Magill, Polymer 2, 221 (1961).

34. J. H. Magill, Polymer 3, 35 (1962).

35. C. F. Pratt and S. Y. Hobbs, Internal Report, General Electric Company.

36. S. Clough, M. B. Rhodes and R. S. Stein, J. Polym. Sci. C, 18, 1 (1967).

37. F. L. Binsberger, J. Macromol. Sci., Physics, B4 (4), 837 (1970).

38. A. Ziabicki, Kolloid 219, 2 (1967).

39. M. J. Avrami, J. Chem. Phys. 7, 1103 (1939).

40. L. B. Morgan, J. Appl. Chem. 4, 160 (1954).

41. W. A. Johnson and R. F. Mehl, Trans. AIME, A-16, 135 (1939).

42. M. Avrami, J. Chem. Phys. 8, 212 (1940).

43. M. Avrami, J. Chem. Phys. 9, 177 (1941).

44. C. F. Pratt and S. Y. Hobbs, Polymer 17, 12 (1976).

45. A. J. Kovacs and S. Y. Hobbs, J. Appl. Polym. Sci. 16, 301 (1972).

46. G. Arnei and J. A. Sauer, Thermochim. Acta 15, 29 (1976).

47. E. Balizer, private communication.

48. E. Hunter and W. G. Oakes, Trans. Faraday Soc. 41, 56 (1945).

49. M. Gubler and J. Kovacs, J. Polym. Sci. 34, 551 (1959).

50. H. Wilski, Kunstoffe 54, 10 (1964).

51. M. J. Richardson, P. J. Flory and J. B. Jackson, Polymer 4, 221 (1963).

52. A. Charlesby and L. Callaghan, Phys Chem. Solids 4, 227 (1958).

53. R. Chiang and P. J. Flory, J. Am. Chem. Soc. 83, 2857

54. L. E. Nielson, J. Appl. Phys. 25, 1209 (1959).

55. J. G. Faton and L. Mandelkern, J. Phys. Chem. 69, 417 (1965).

56. C. W. Bunn and C. J. Brown, Proc. Royal Soc. 226A, 531 (1954).

57. M. Kokondu, Y. Sakakibara and H. Tadokoro, Macromolecules 9, 226 (1976).

58. V. Alter and R. Bonart, Colloid and Polym. Sci. 254, 348 (1976).

59. C. A. Boye and J. R. Overton, Bull. Am. Phys. Soc., Ser. II, 10, 352 (1974).

60. E. L. Slagowski and E. P. Chang, J. Appl. Phys., to be published.

61. Z. Mencik, J. Polym. Sci., Polym. Phys. Ed. 13, 2173 (1975).

62. J. D. Hoffman and J. J. Weeks, J. Chem. Phys. 37, 8, 1723 (1962).

63. T. Okada and L. Mandelkern, J. Polym. Sci., A2, 5, 239 (1967).

64. H. Hendus and G. Schnell, Kunstoffe 51, 69 (1961).

65. V. N. Nikitin and E. I. Pokrovskii, Dokl. Akad. Nauk USSR 95, 109 (1954).

66. M. C. Tobin and M. J. Carrano, J. Polym. Sci. 24, 93 (1957).

67. W. H. Cobbs, Jr. and R. L. Burton, J. Polym. Sci. X, 3, 275 (1953).

68. L. D'Esposito and J. L. Koenig, J. Polym. Sci., Polym. Phys. Ed. 14, 1731 (1976).

69. S. Bahl, D. Cornell and F. Boerio, J. Polym. Sci., Polym. Lett. 12, 131 (1974).

70. B. Stambaugh and J. L. Koenig, J. Polym. Sci., Polym. Lett. 15, 299 (1977).

71. A. K. Doolittle, J. Appl. Phys. 22, 471 (1951).

72. A. K. Doolittle and D. B. Doolittle, J. Appl. Phys. 26, 901 (1957).

73. H. H. Cohen and D. Turnbull, J. Chem. Phys. 31, 1164 (1959).

74. F. Bueche, J. Chem. Phys. 29, 418 (1956).

75. F. Bueche, "The Physical Chemistry of Polymers," Interscience, New York, 1962.

76. J. H. Gibbs and E. A. DiMarzio, J. Chem. Phys. 28, 373 (1958).

77. G. Adam and J. H. Gibbs, J. Chem. Phys. 43, 139 (1965).

78. R. N. Haward, "The Physics of Glassy Polymers," John Wiley, New York, 1973.

79. J. Boon and J. M. Azcue, J. Polym. Sci., A-2, 6, 885 (1968).

80. T. T. Wang and N. Nishi, Macromolecules 10, 2, 621 (1977).

81. L. Mandelkern, F. Quinn and P. J. Flory, J. Appl. Phys. 25, 7, 830 (1954).

82. L. Mandelkern, J. Appl. Phys. 26, 6, 443 (1955).

83. D. Turnbull and J. C. Fisher, J. Chem. Phys. 17, 71 (1949).

84. S. Glasstone, K. J. Laidler and H. Eyring, "The Theory of Rate Processes," McGraw-Hill, New York, 1941.

85. M. Williams, R. Landel and J. Ferry, J. Am. Chem. Soc. 77, 3701 (1955).

86. T. G Fox, S. Gratch and S. Loeshak, "Viscosity Relationships for Polymers in Bulk and Concentrated Solutions," in "Rheology, Theory and Practice," ed. by F. R. Eirich, Academic Press, New York, 1957.

87. J. D. Ferry, "Viscoelastic Properties of Polymers," John Wiley, New York, 1961.

88. J. D. Hoffman and J. Weeks, J. Chem. Phys. 37, 8, 15 (1952).

89. J. D. Hoffman, L. J. Frolen, G. S. Ross and J. L. Lauritzen, J. Res. Natl. Bur. Stand. 79A, 6, 671 (1975).

90. J. D. Hoffman and J. L. Lauritzen, J. Res. Natl. Bur. Stand. 65A, 297 (1961).

91. J. L. Lauritzen and J. D. Hoffmann, J. Res. Natl. Bur. Stand. 64A, 73 (1960).

92. J. D. Hoffman, G. T. Davis and J. L. Lauritzen in "Treatise on Solid State Chemistry," ed. by N. B. Hannay, Plenum Press, New York, Vol. 3, 1976.

93. J. L. Lauritzen and J. D. Hoffman, J. Appl. Phys. 44, 4340 (1973).

94. J. D. Hoffman, Soc. Plastics Eng. Trans. 4, 315 (1964).

95. F. VanAntwerpen, Ph.D. Dissertation, Delft, Netherlands, 1971.

96. J. H. Magill, J. Appl. Phys. 35, 3749 (1965).

97. J. Majer, Kunstoffe 55, 111 (1965).

98. P. J. Flory, J. Am. Chem. Soc. 62, 9, 1057 (1940).

99. P. J. Flory, J. Am. Chem. Soc. 62, 9, 2255 (1940).

100. P. J. Flory, J. Am. Chem. Soc. 64, 2205 (1952).

101. P. Kresse, Faserforsch. Textiltech. 11, 353 (1960).

102. K. Yoda, Makromol. Chem. 130, 311 (1970).

103. M. Murano and R. Yamadero, Polym. J. 2, 8 (1971).

104. J. Budin and J. Vanicek, "Proceedings of the First European Symposium on Thermal Analysis," ed. by D. Dollimore, Heyden, London, 1976.

105. A. M. Kotliar, J. Polym. Sci., Polym. Chem. Ed. 13, 973 (1975).

106. A. M. Kotliar, J. Polym. Sci., Polym. Chem. Ed. 11, 1157 (1973).

107. L. H. Peebles, Jr., M. W. Huffman and C. T. Ablett, J. Polym. Sci., A-2, 7, 479 (1969).

108. E. E. Paschke, B. A. Poidlingmeyer and J. G. Bergmann, J. Polym. Sci., Polym. Chem. Ed. 15, 983 (1977).

109. M. Takayanagi, "Proceedings of the Fourth International Congress of Rheology," Part I, Interscience, New York, 1965, p. 161.

110. K. M. Sinnot, Polym. Eng. & Sci. 2, 65 (1962).

111. M. Takayanagi, J. Soc. Materials Sci., Japan, 414, 343 (1955).

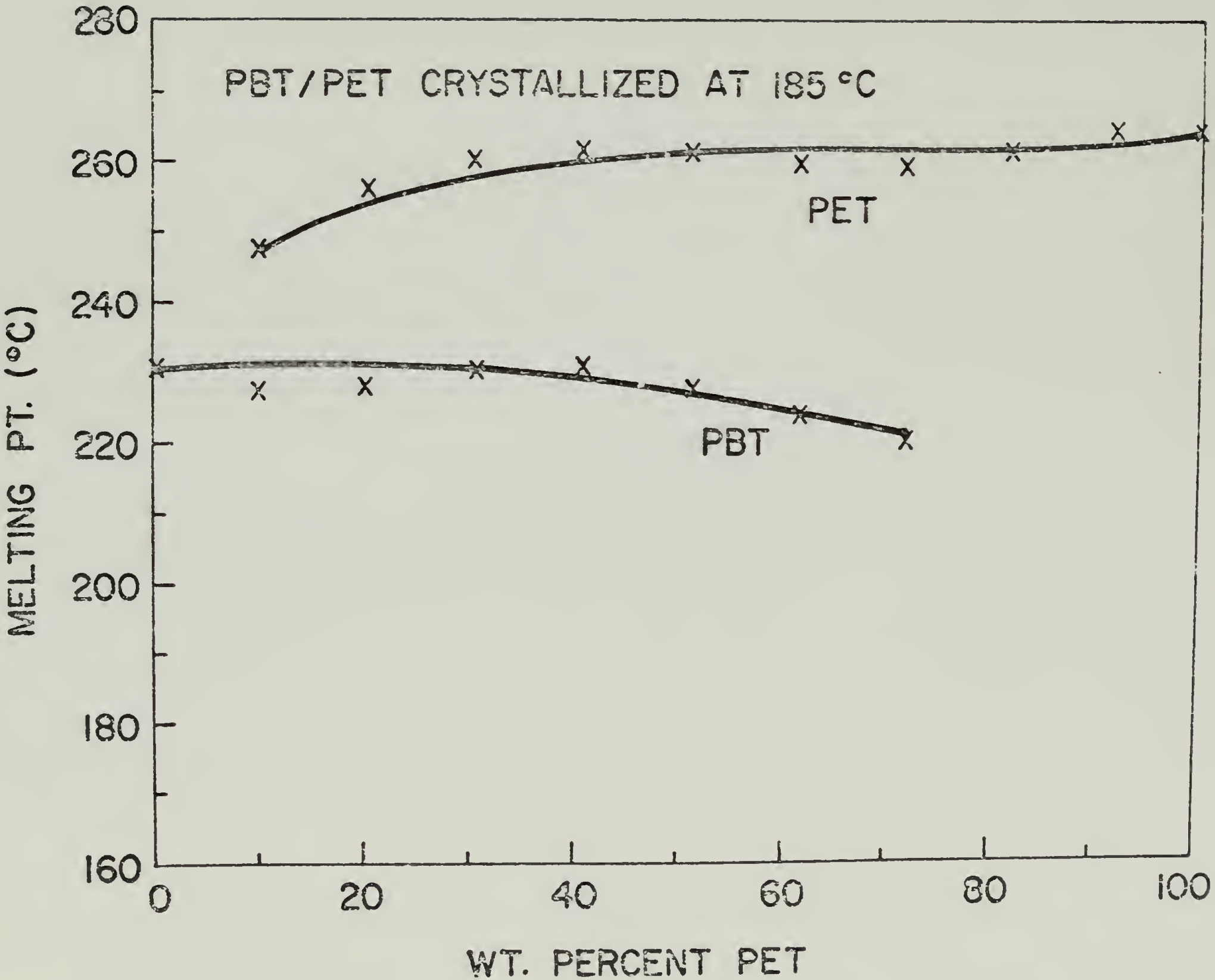
PBT/PET CRYSTALLIZED AT 185 °C
PET
PBT
MELTING PT. (°C)
280
260
240
220
200
180
160
0
20
40
60
80
100
WT. PERCENT PET

Figure 1

PBT / PET BLENDS GLASS TRANSITION TEMPERATURES.

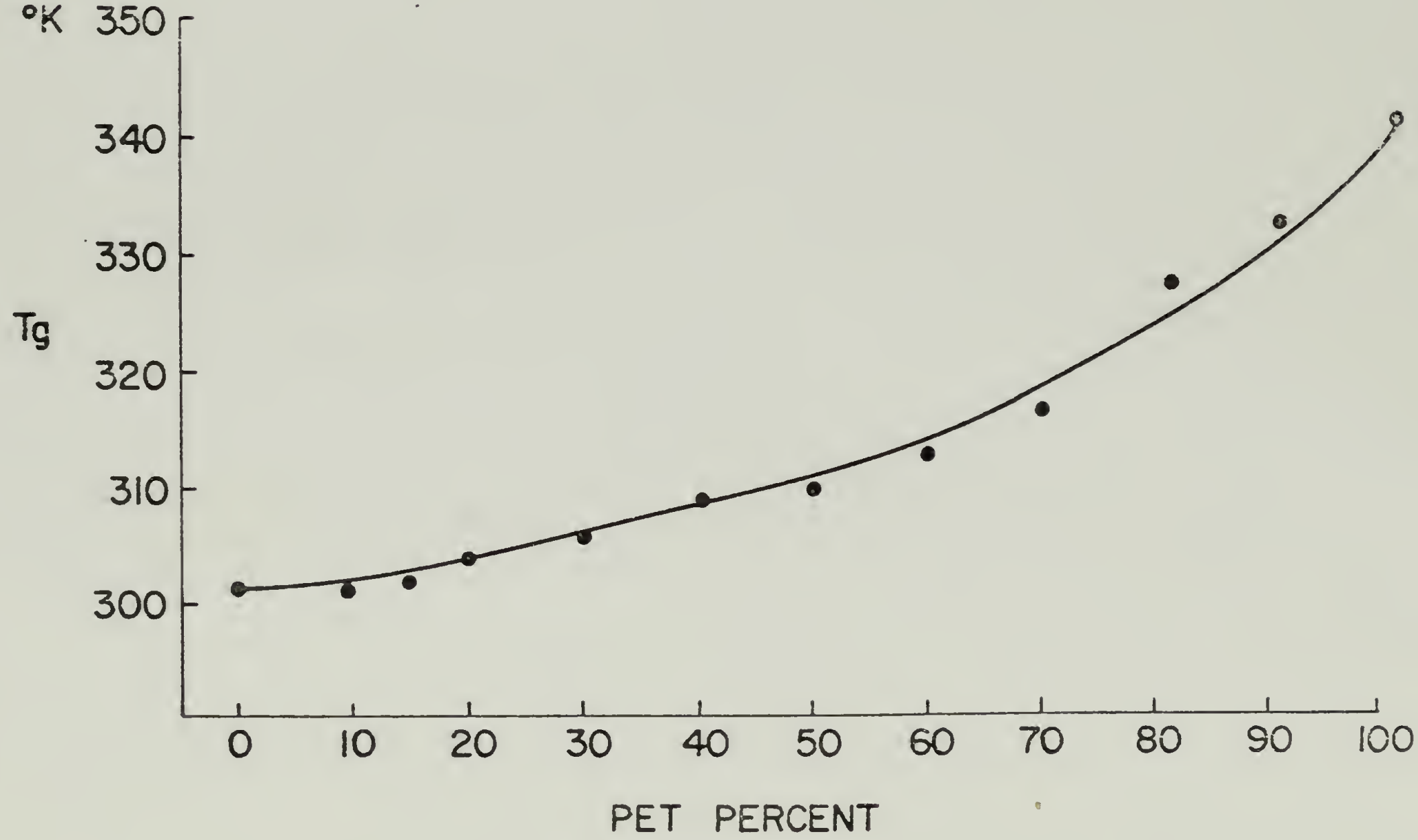

Figure 2

Figure 3

a

b

c

d

Figure 4

a

b

c

d

Figure 5

a

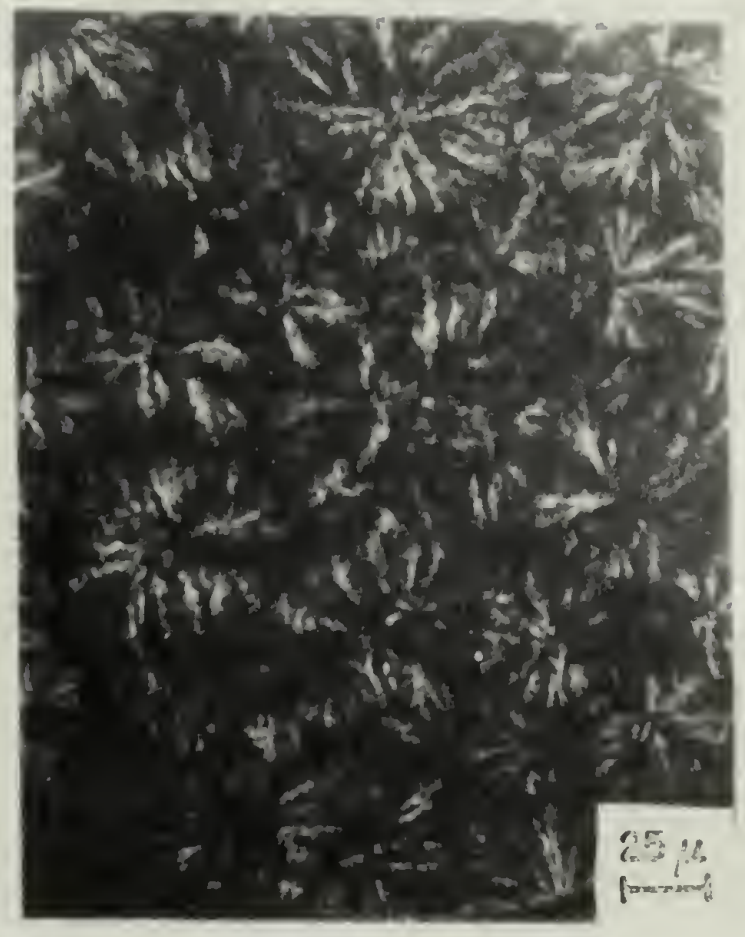

b

c

d

Figure 6

PBT/PET $T_c = 130°C$

100/0

80/20

60/40

50/50

40/60

20/80

0/100

Figure 7

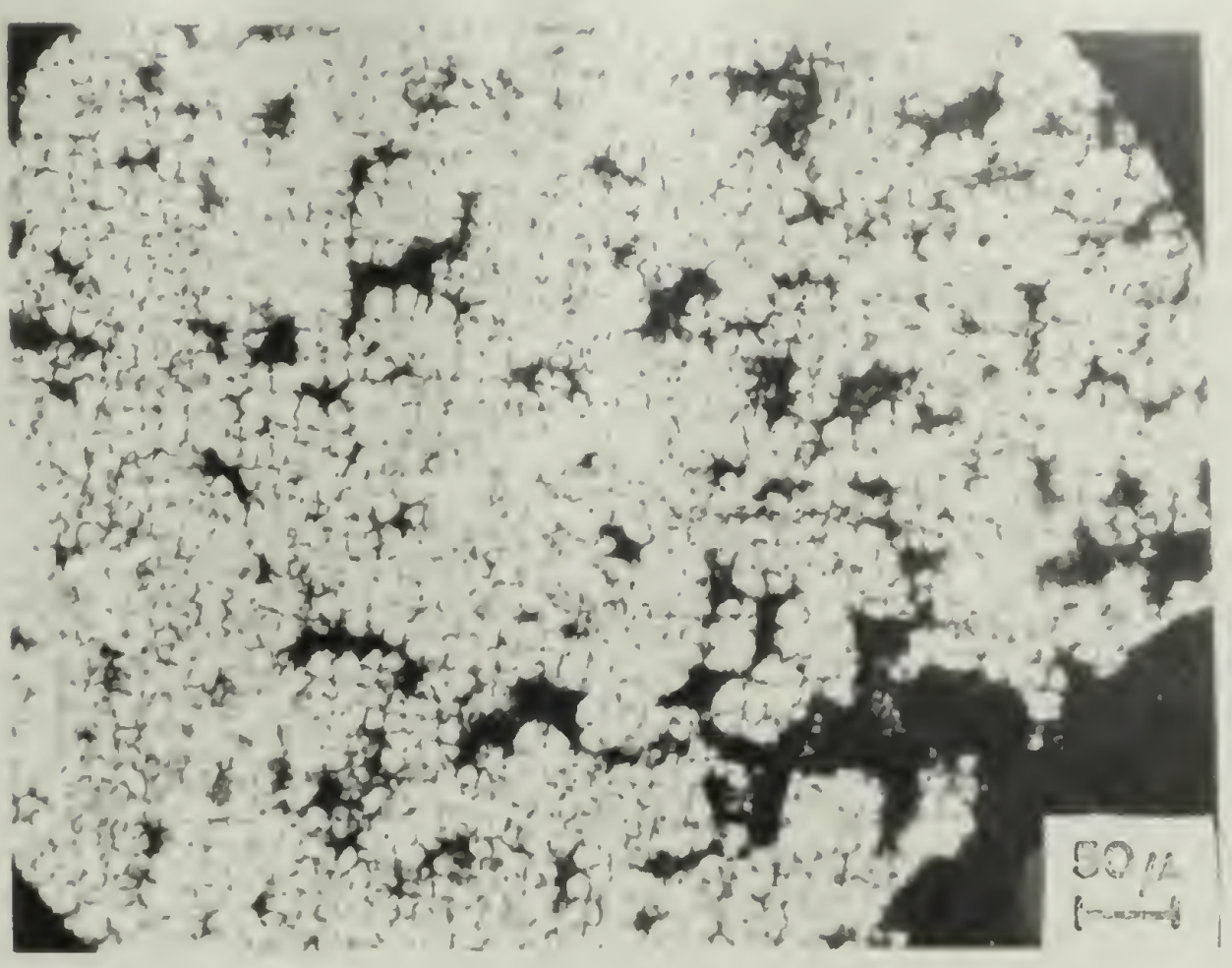

0/100

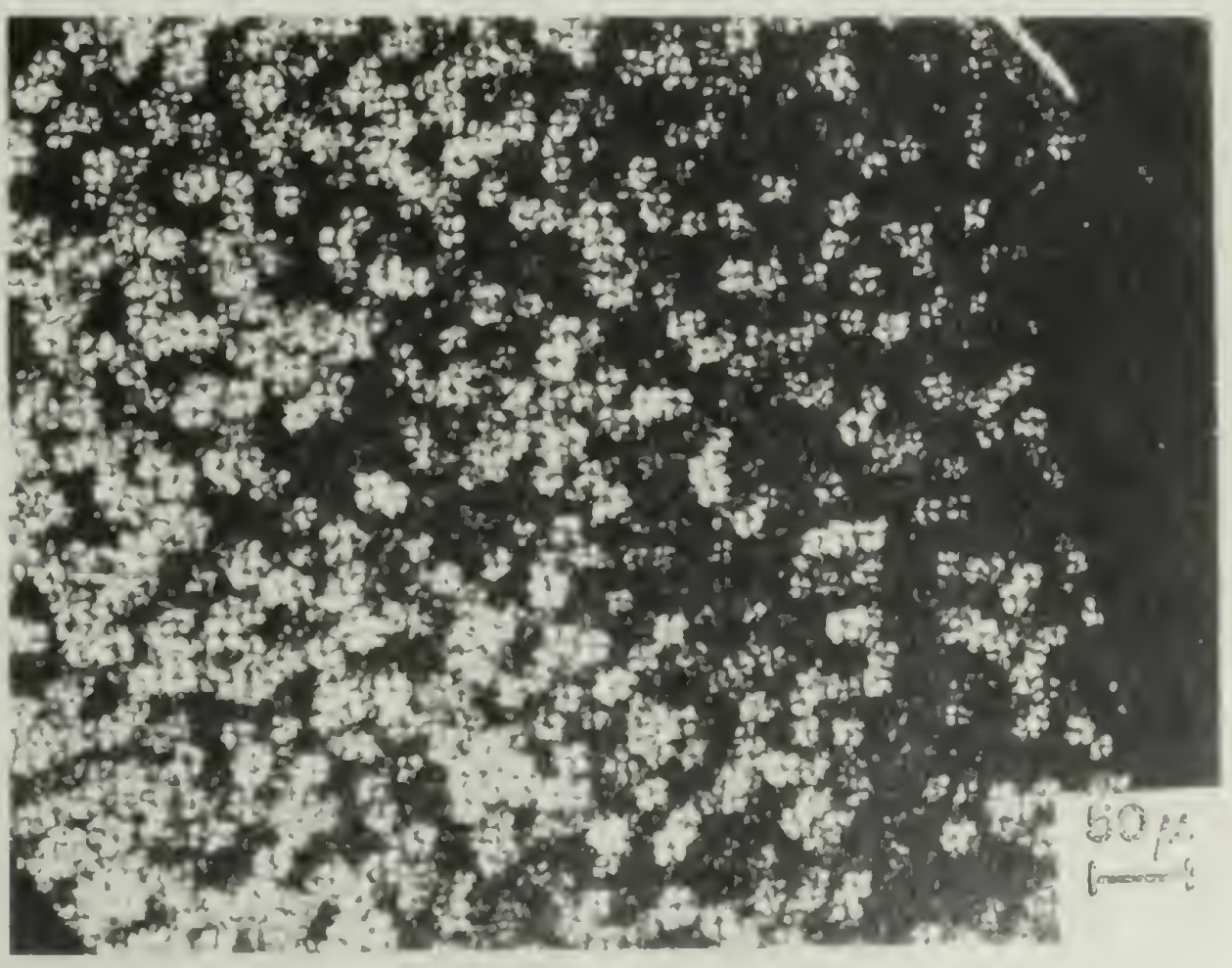

Figure 8

20/80

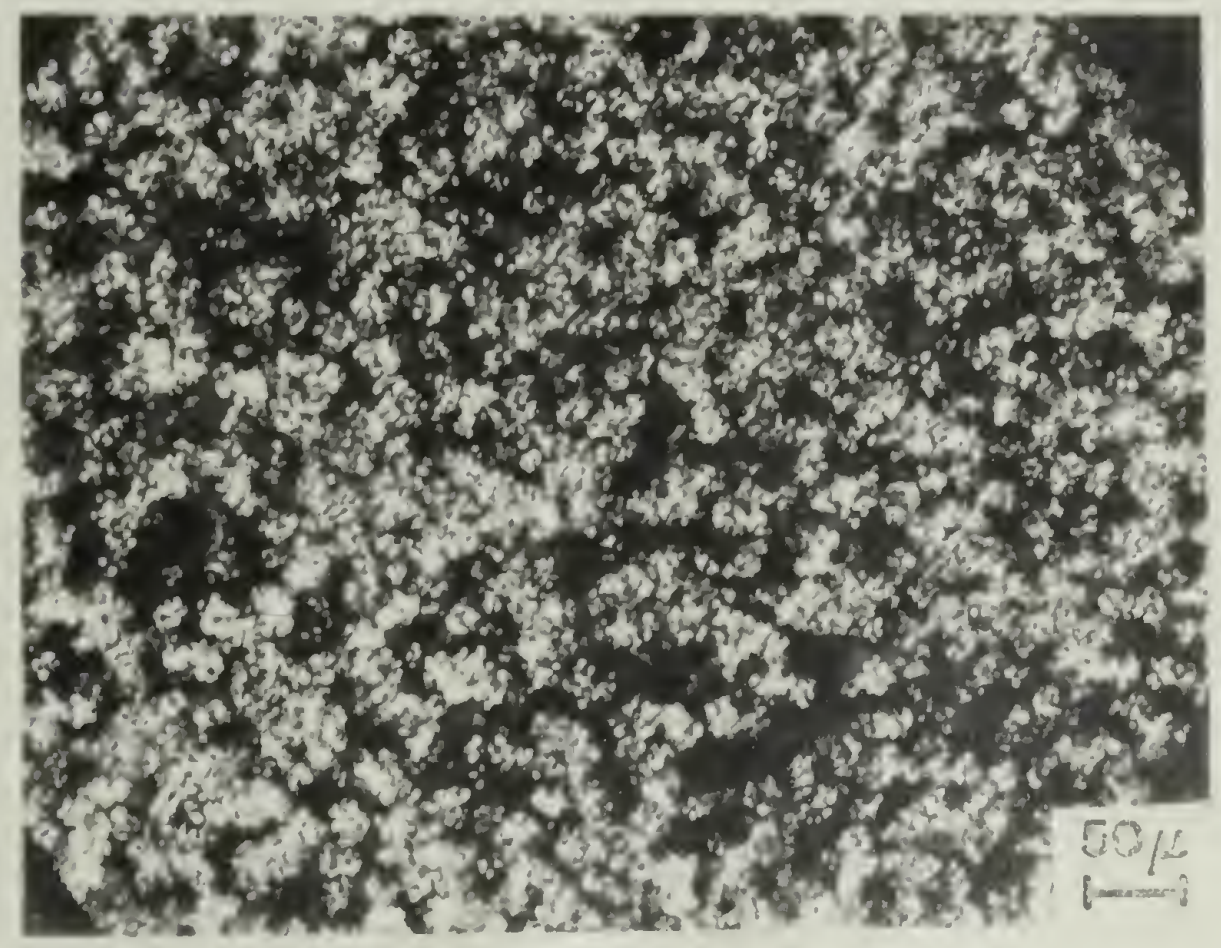

40/60

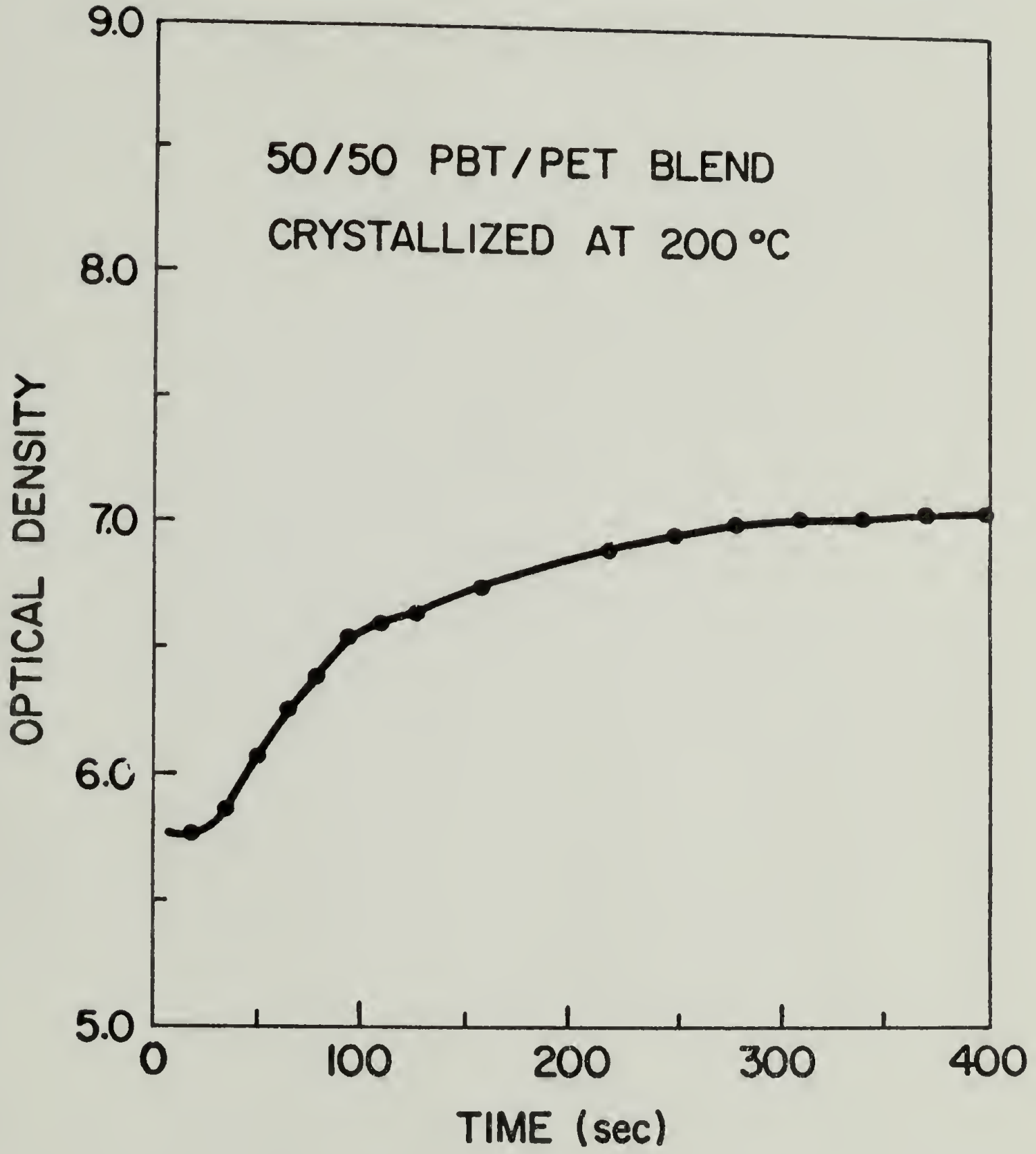
50/50 PBT/PET BLEND
CRYSTALLIZED AT 200 °C
OPTICAL DENSITY
9.0
8.0
7.0
6.0
5.0
0
100
200
300
400
TIME (sec)

Figure 9

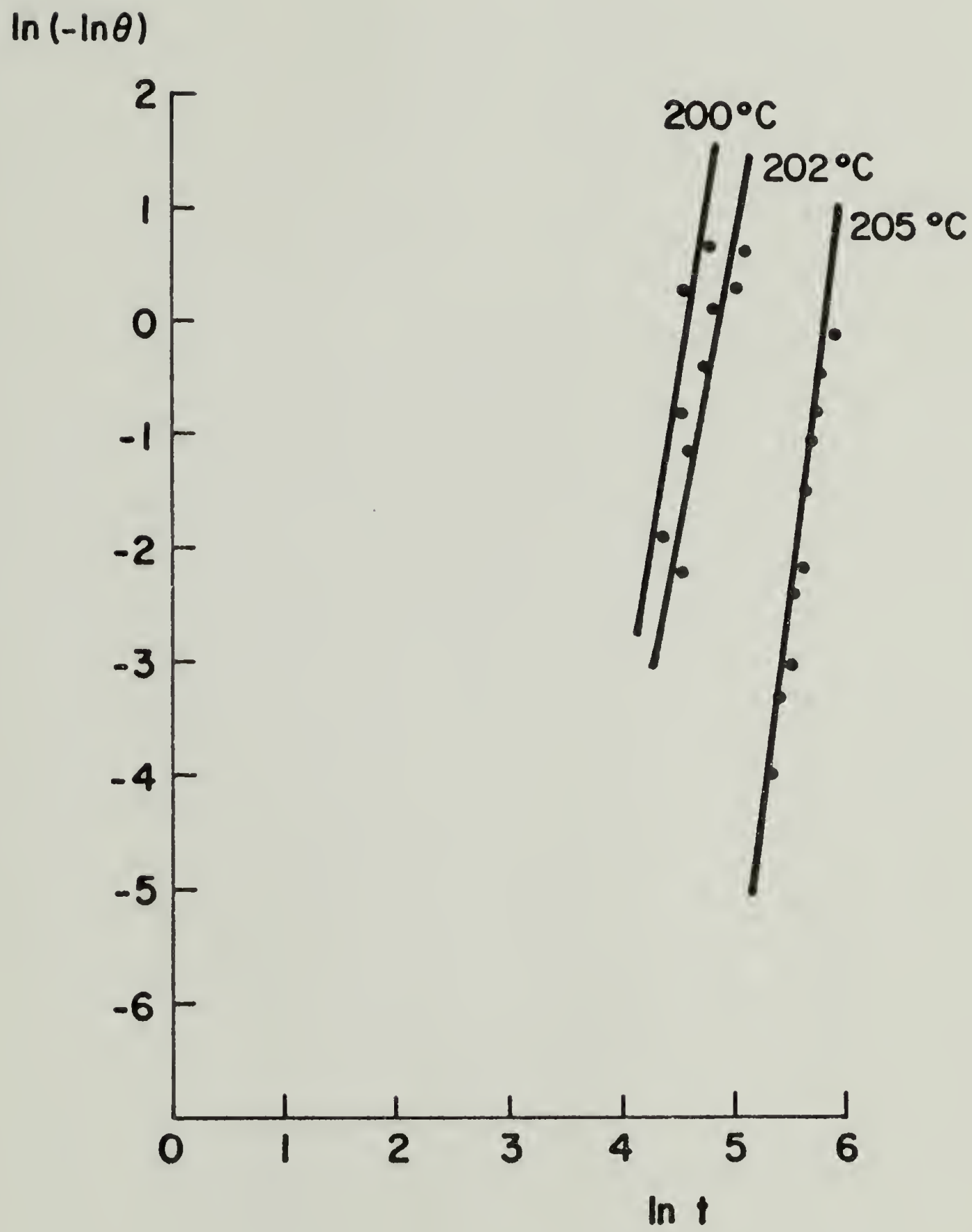

Figure 10

MELTING POINTS AS DETERMINED BY DLI

HEATING RATE 10 °C/min.

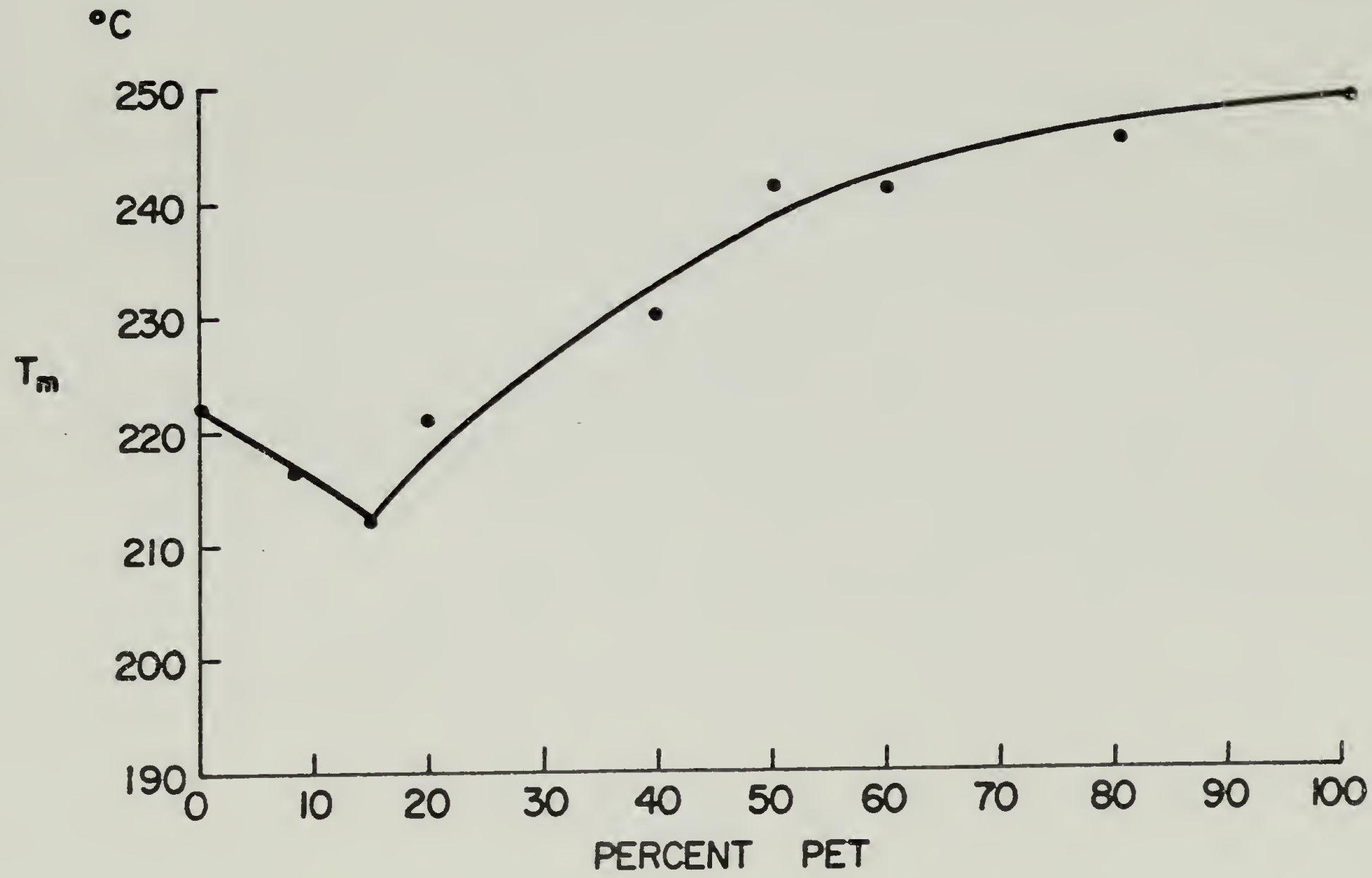

Figure 11

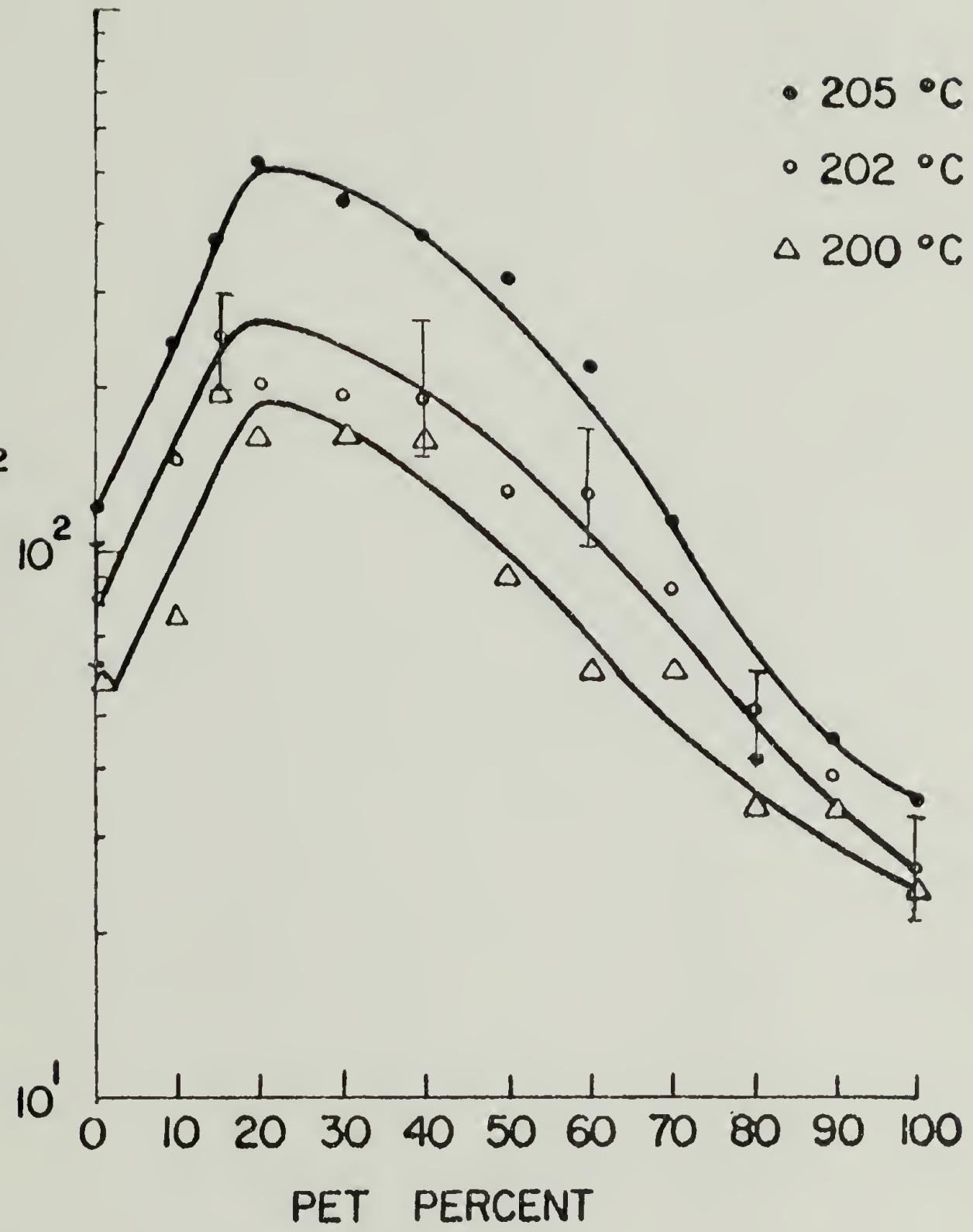
• 205 °C
° 202 °C
△ 200 °C
$t_{1/2}$
10^2
10^1
0 10 20 30 40 50 60 70 80 90 100
PET PERCENT

Figure 12

INDUCTION TIMES VS. BLEND COMPOSITION

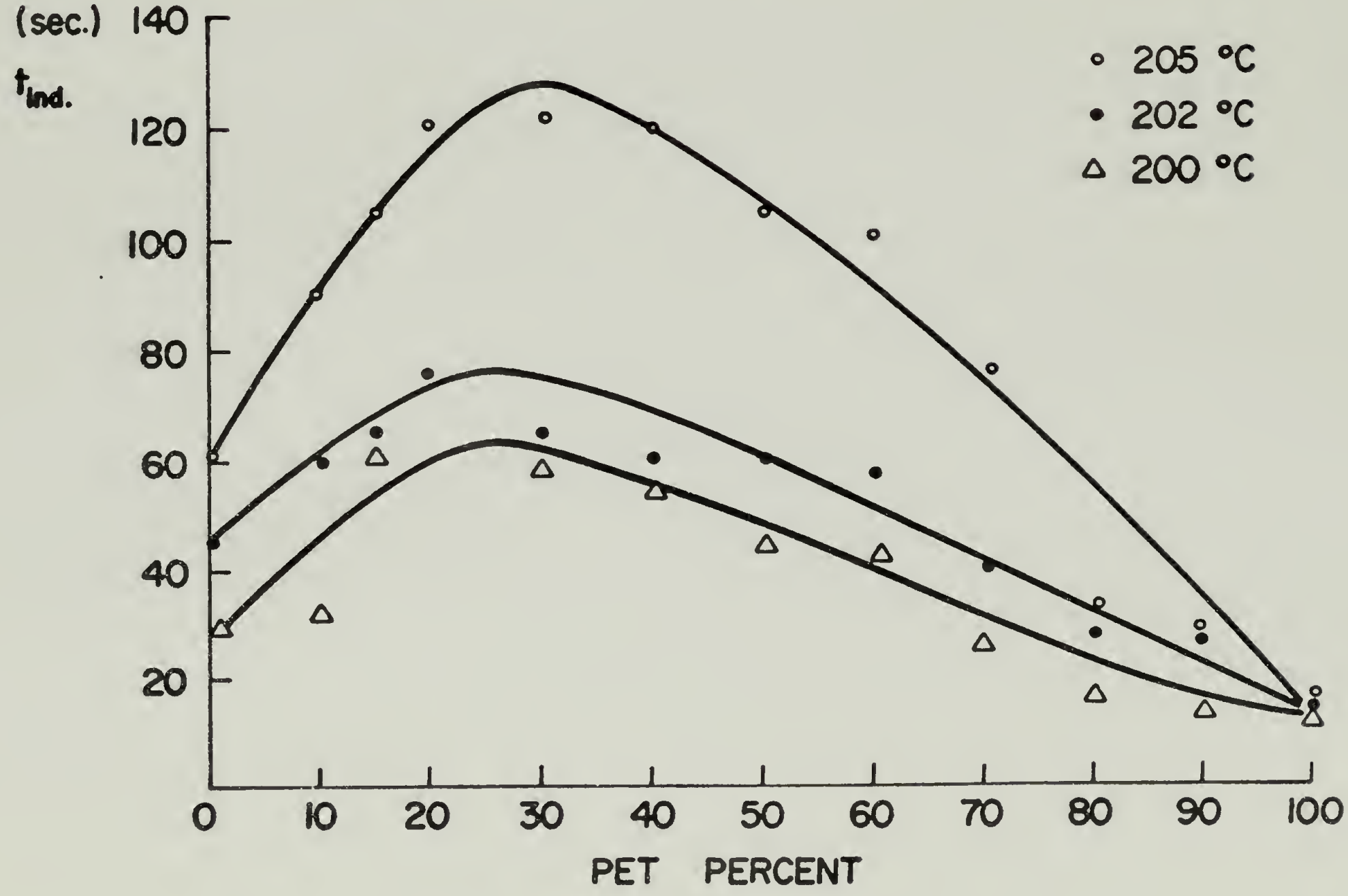

Figure 13

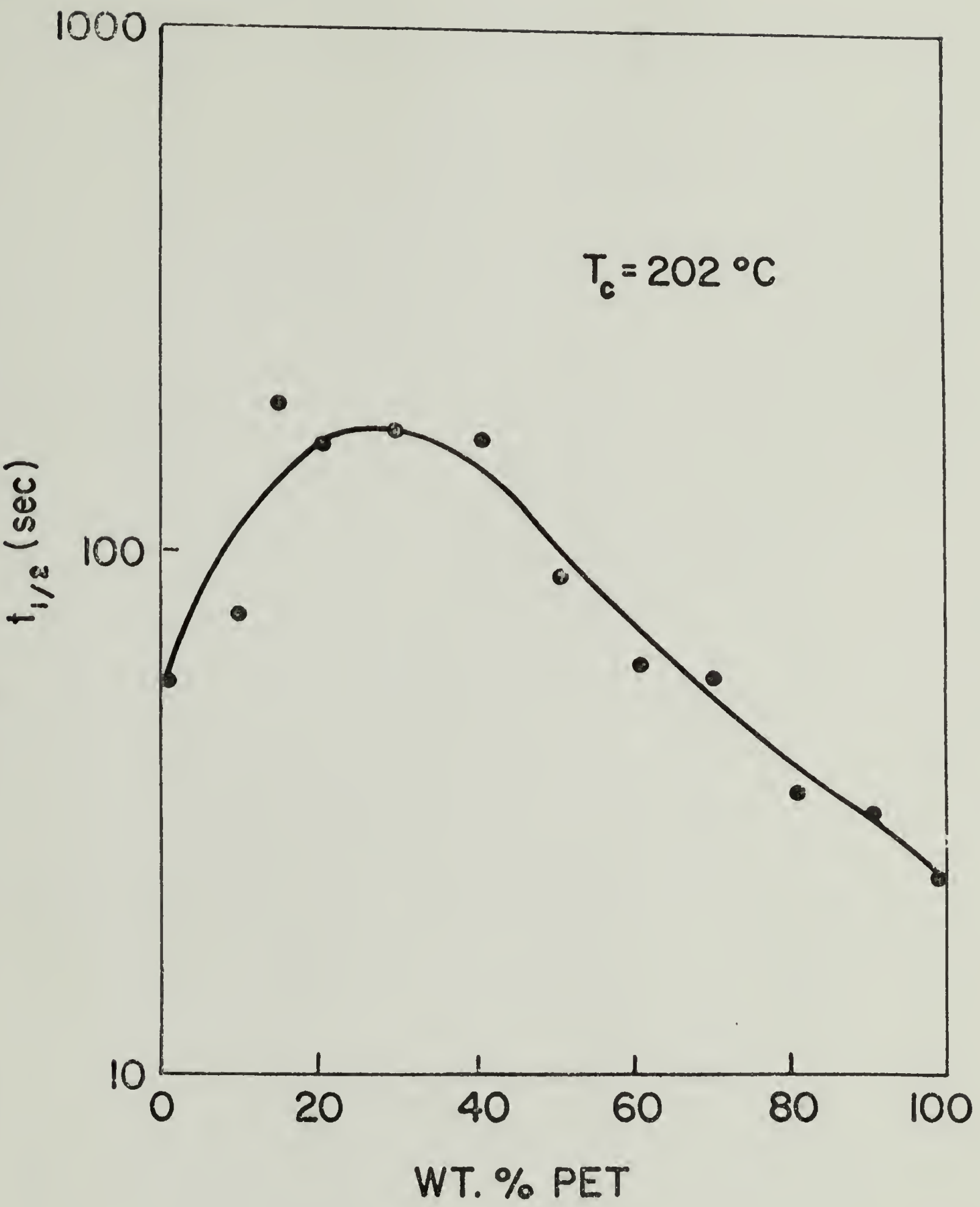

Figure 14

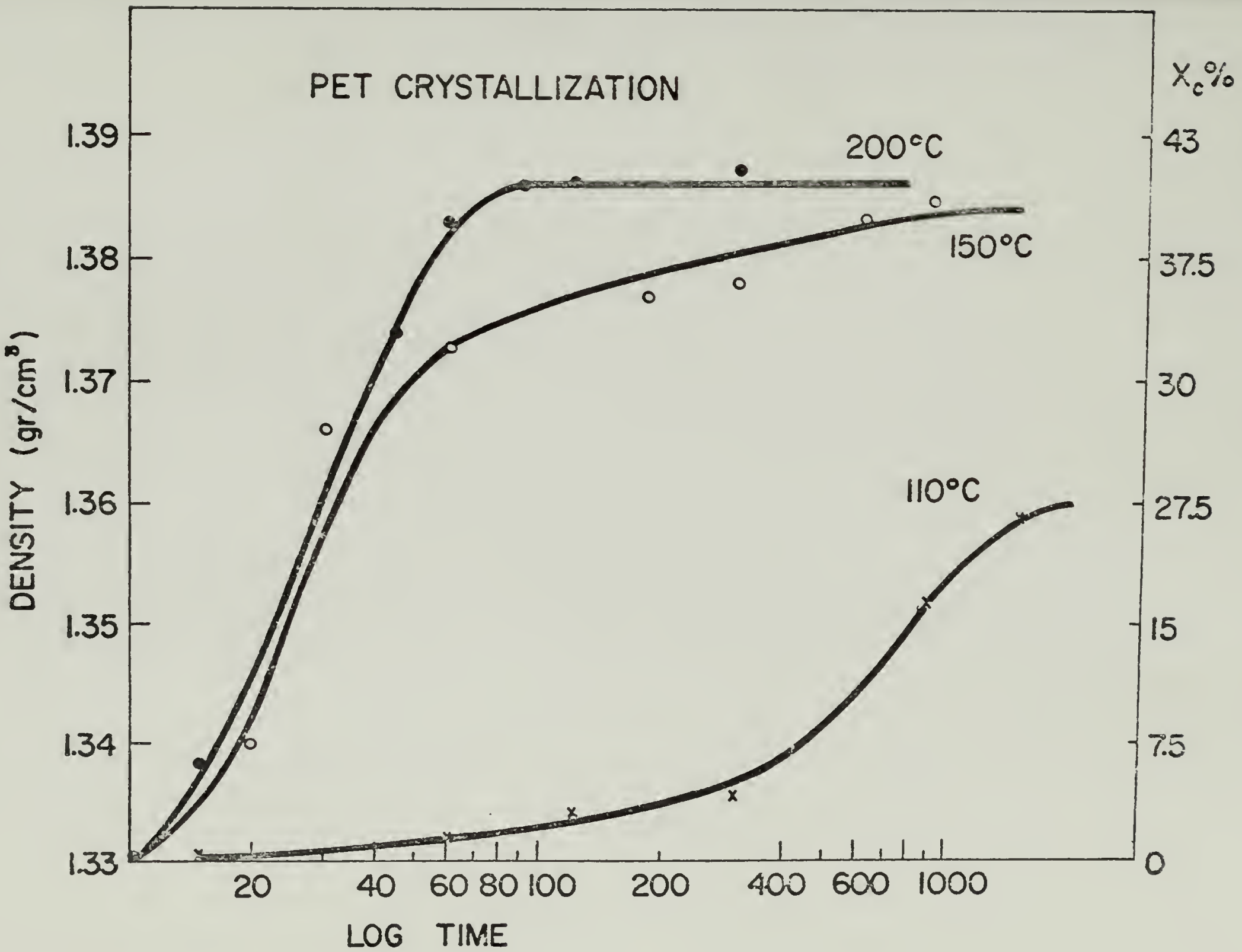
PET CRYSTALLIZATION
DENSITY (gr/cm³)
1.39
1.38
1.37
1.36
1.35
1.34
1.33
X_c%
43
37.5
30
27.5
15
7.5
0
200°C
150°C
110°C
20
40
60
80
100
200
400
600
1000
LOG TIME

Figure 15

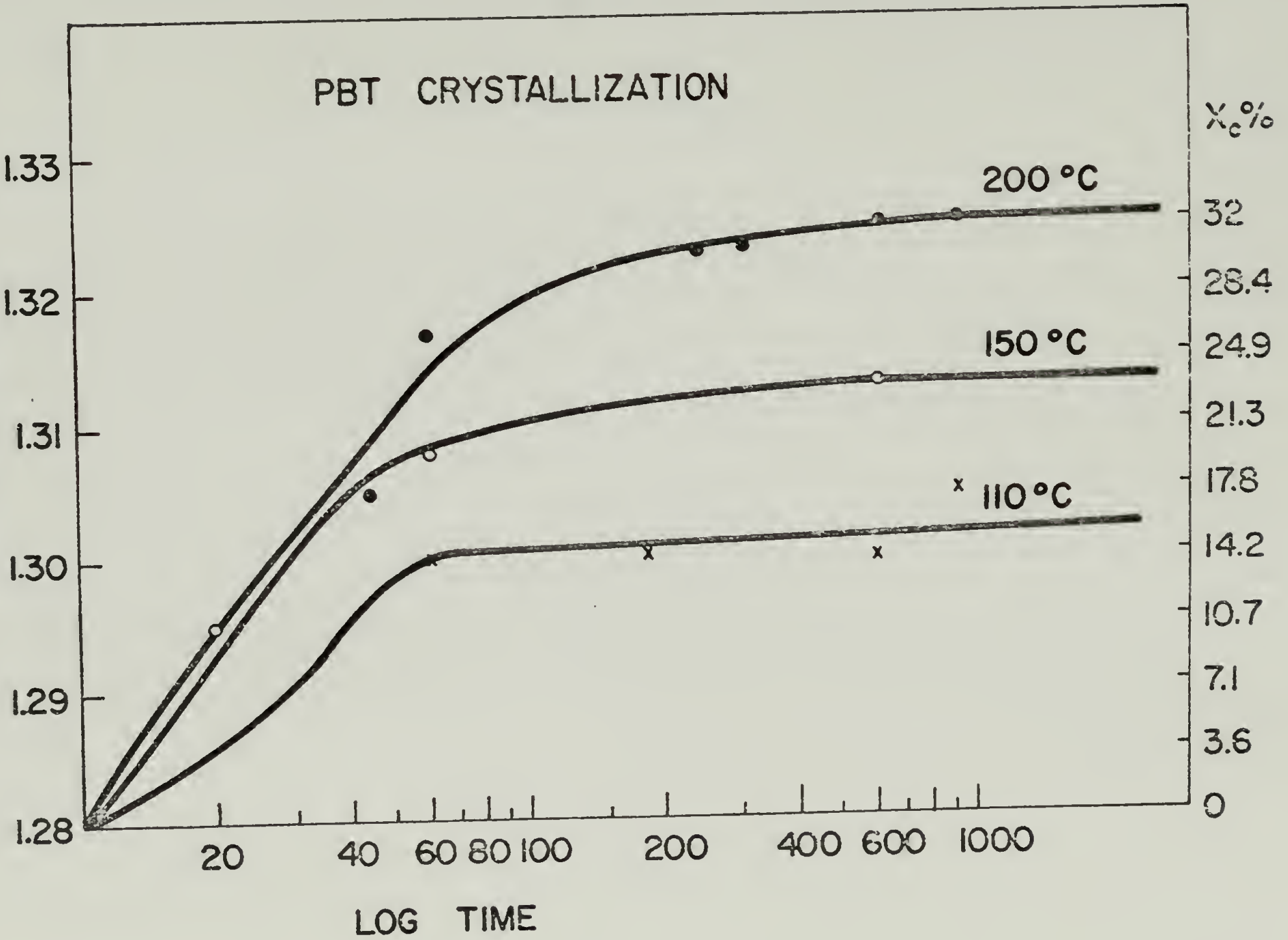
PBT CRYSTALLIZATION
DENSITY (gr/cm³)
1.33
1.32
1.31
1.30
1.29
1.28
200 °C
150 °C
110 °C
X
X_c%
32
28.4
24.9
21.3
17.8
14.2
10.7
7.1
3.6
0
20
40
60
80
100
200
400
600
1000
LOG TIME

Figure 16

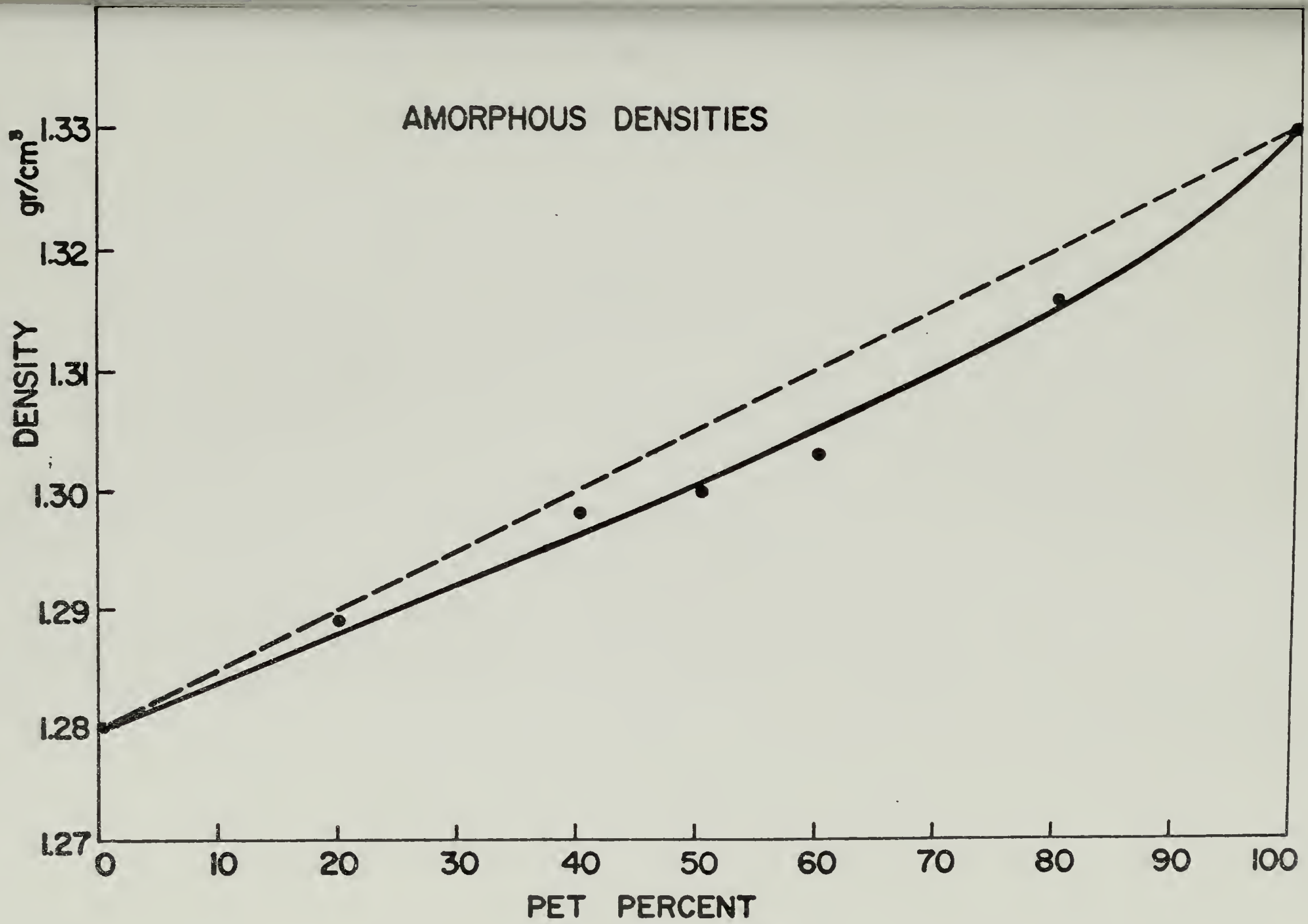
AMORPHOUS DENSITIES
DENSITY gr/cm³
1.33
1.32
1.31
1.30
1.29
1.28
1.27
0
10
20
30
40
50
60
70
80
90
100
PET PERCENT

Figure 17

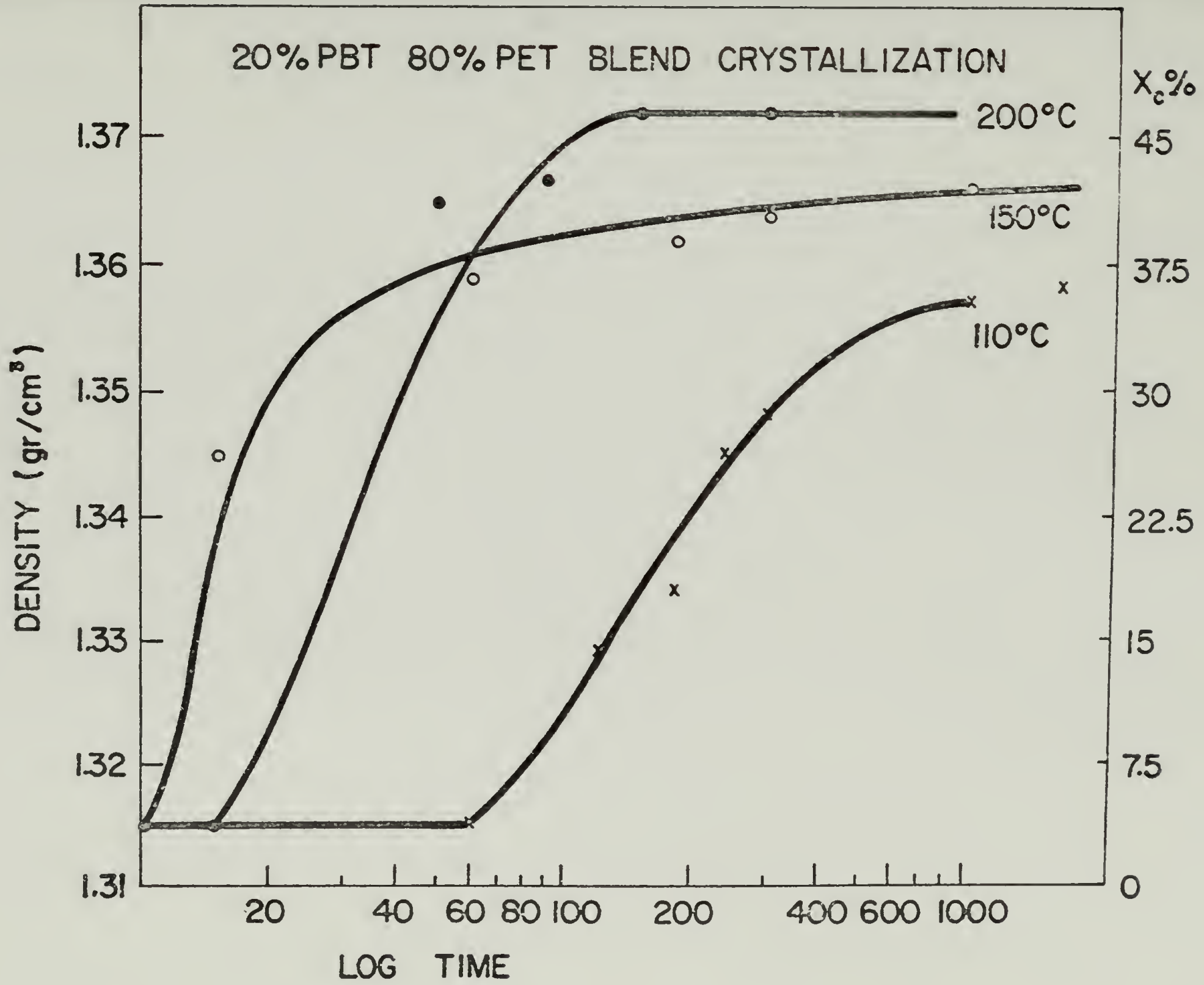
20% PBT 80% PET BLEND CRYSTALLIZATION
200°C
150°C
110°C
DENSITY (gr/cm³)
1.37
1.36
1.35
1.34
1.33
1.32
1.31
X_c%
45
37.5
30
22.5
15
7.5
0
20
40
60
80
100
200
400
600
1000
LOG TIME

Figure 18

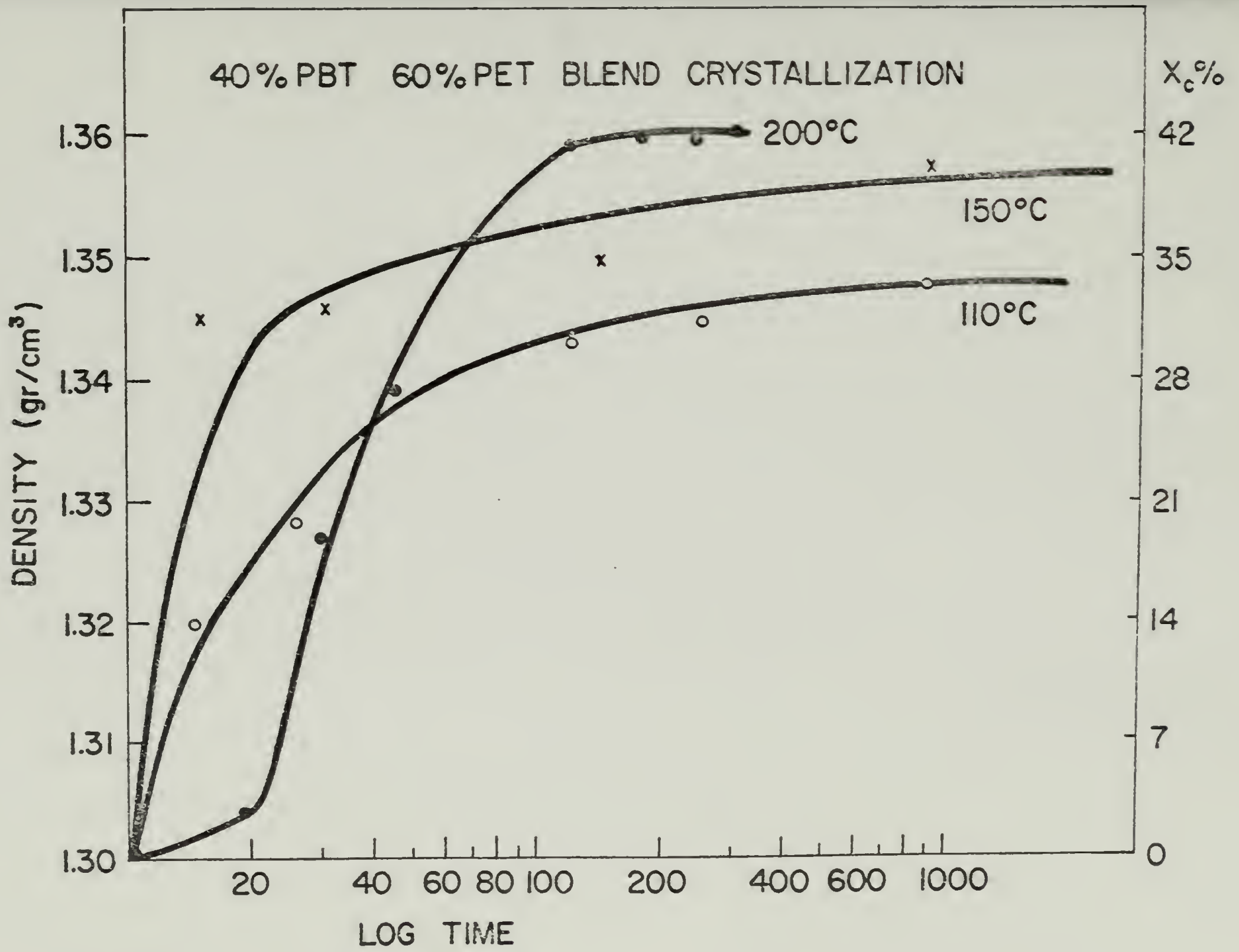
40% PBT 60% PET BLEND CRYSTALLIZATION
200°C
150°C
110°C
DENSITY (gr/cm³)
1.36
1.35
1.34
1.33
1.32
1.31
1.30
X_c%
42
35
28
21
14
7
0
20
40
60
80
100
200
400
600
1000
LOG TIME

Figure 19

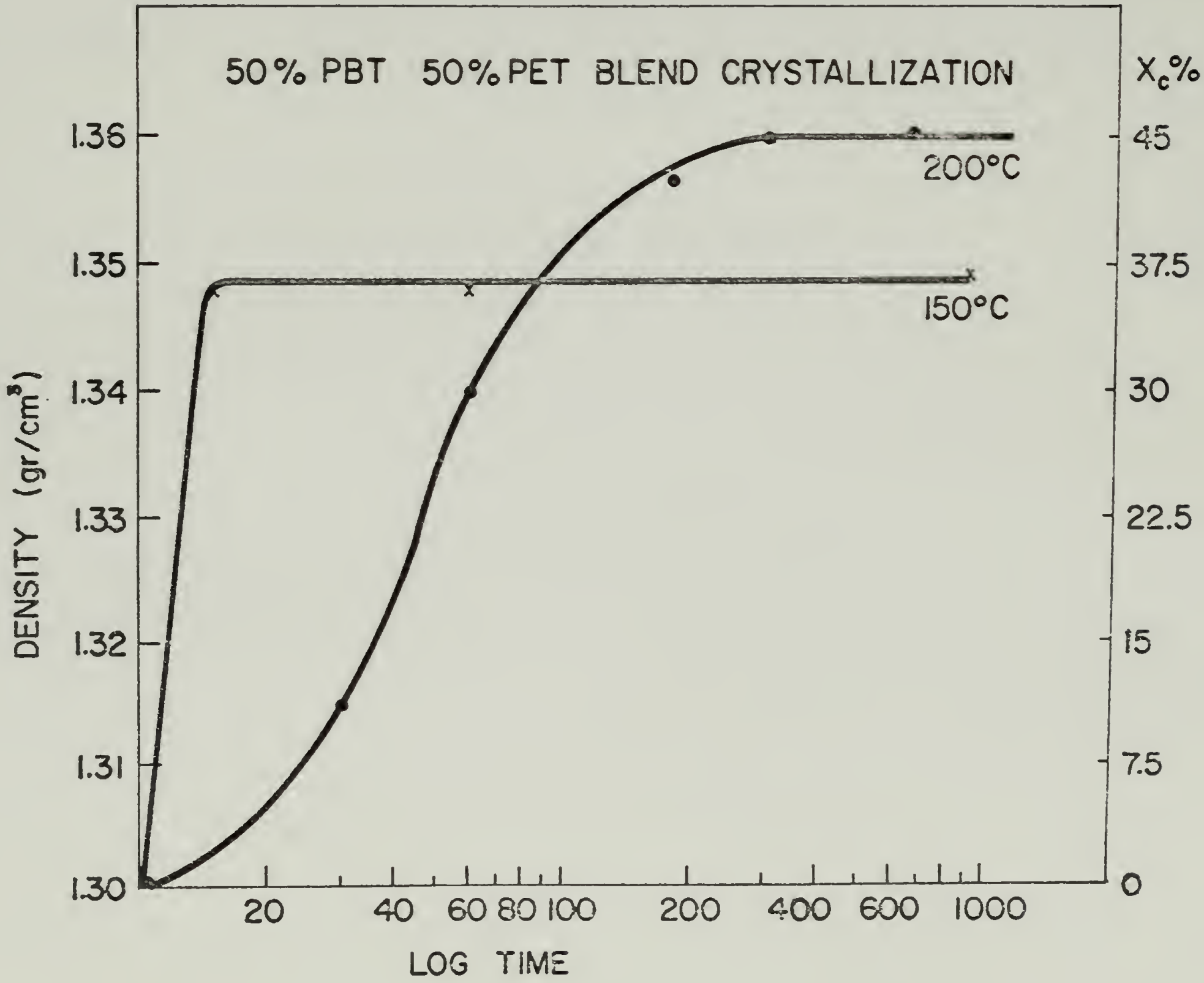
50% PBT 50% PET BLEND CRYSTALLIZATION
X_c%
1.36
1.35
1.34
1.33
1.32
1.31
1.30
DENSITY (gr/cm³)
45
37.5
30
22.5
15
7.5
0
200°C
150°C
20
40
60
80
100
200
400
600
1000
LOG TIME

Figure 20

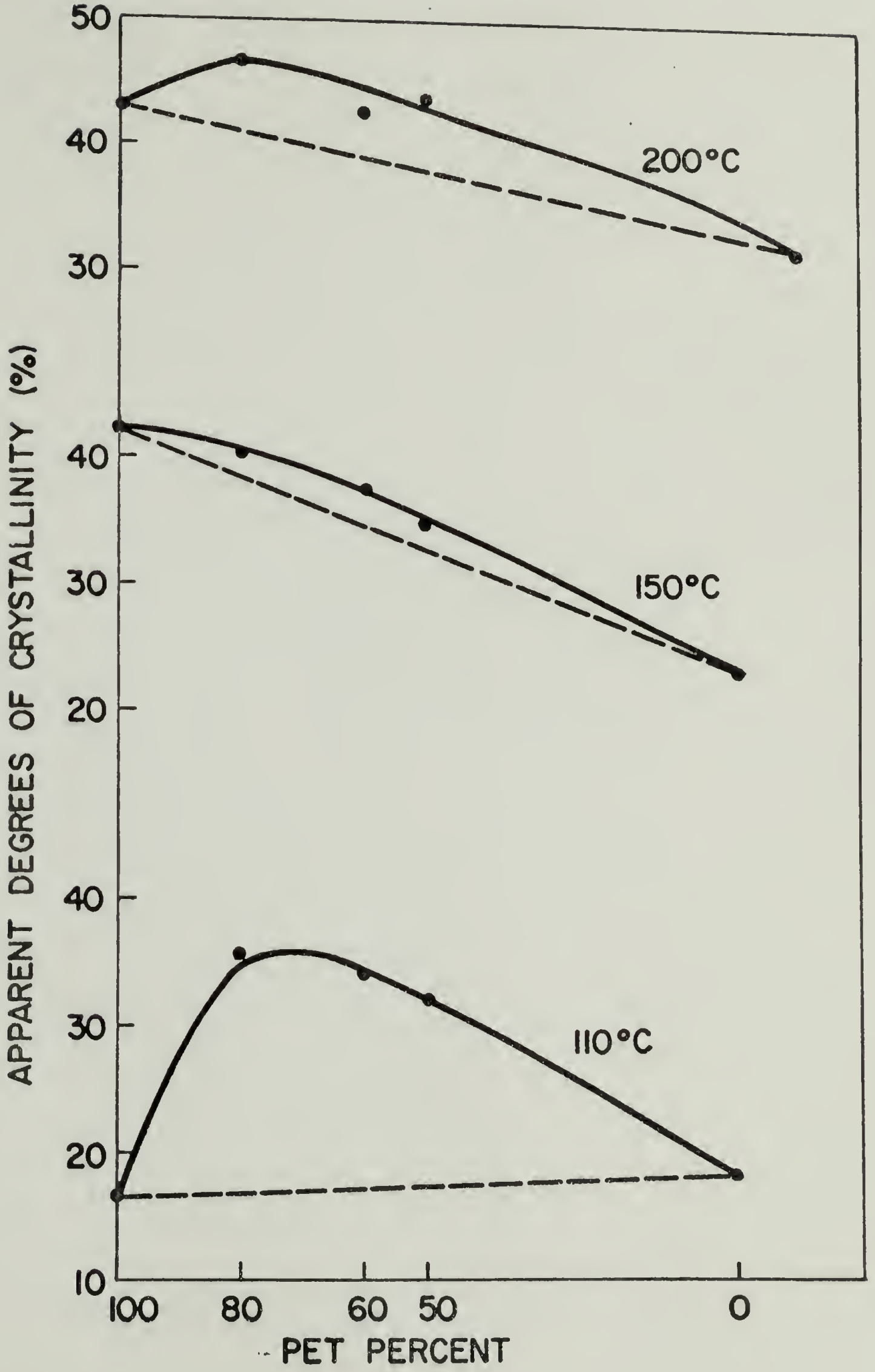
50
40
30
40
30
20
40
30
20
10
APPARENT DEGREES OF CRYSTALLINITY (%)
200°C
150°C
110°C
100
80
60
50
0
PET PERCENT

Figure 21

IR SPECTRA FOR THE 60% PBT 40% PET BLEND CRYSTALLIZED AT 90°C

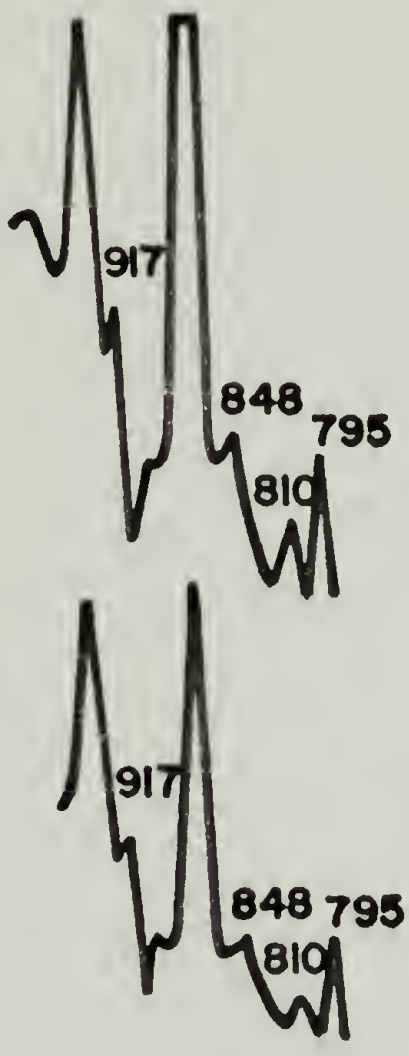

Annealed 600 sec

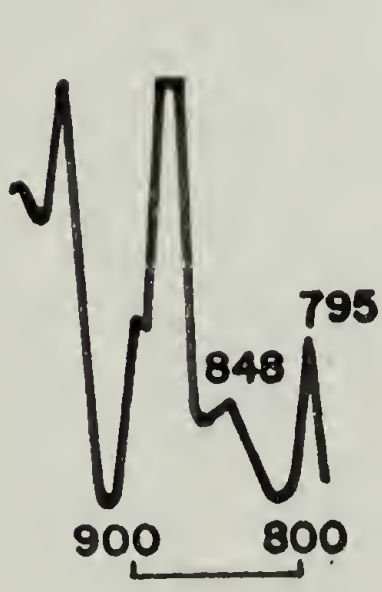

Annealed 60 sec

Quenched

Figure 22

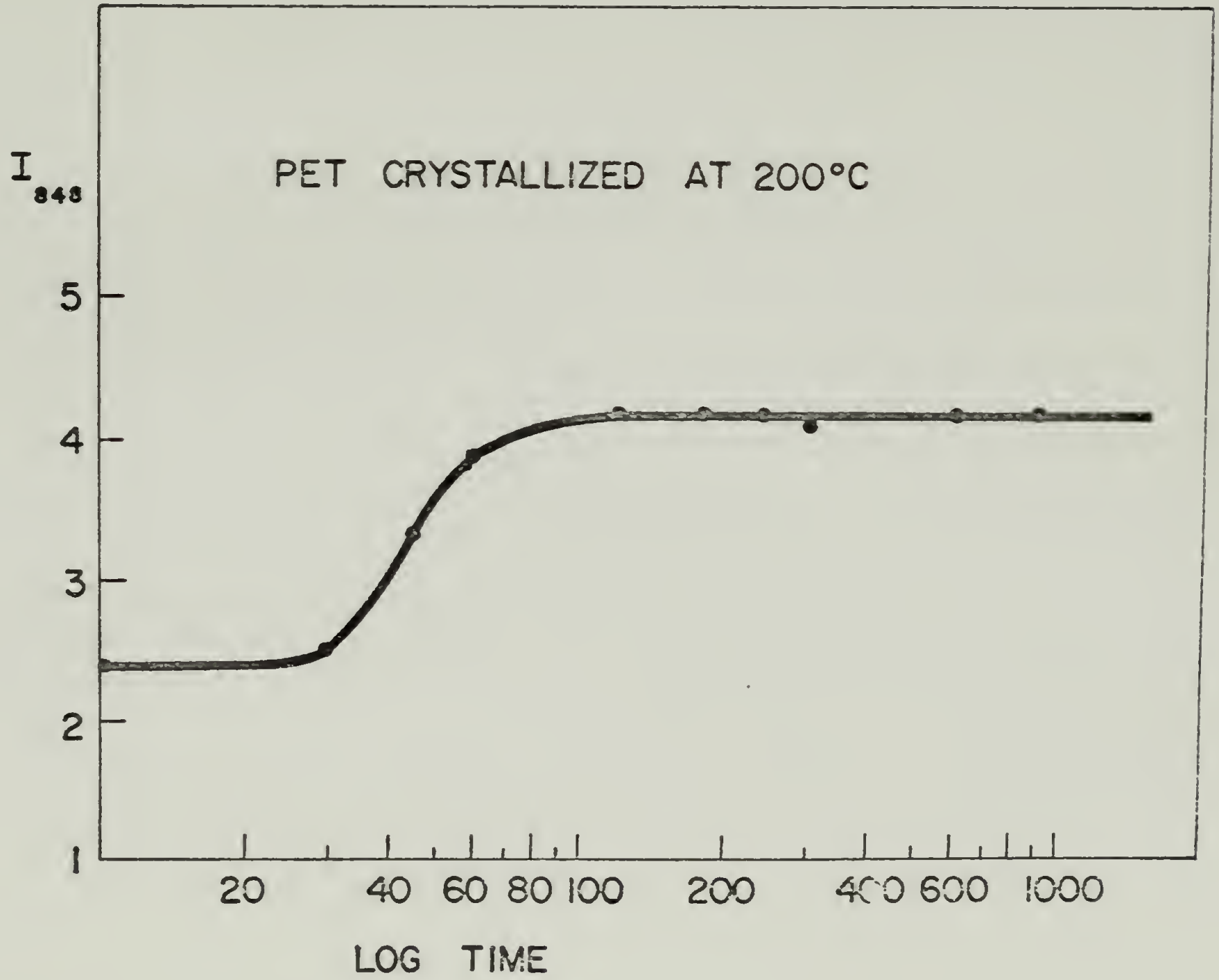
PET CRYSTALLIZED AT 200°C
I_{848}
5
4
3
2
1
20
40
60
80
100
200
400
600
1000
LOG TIME

Figure 23

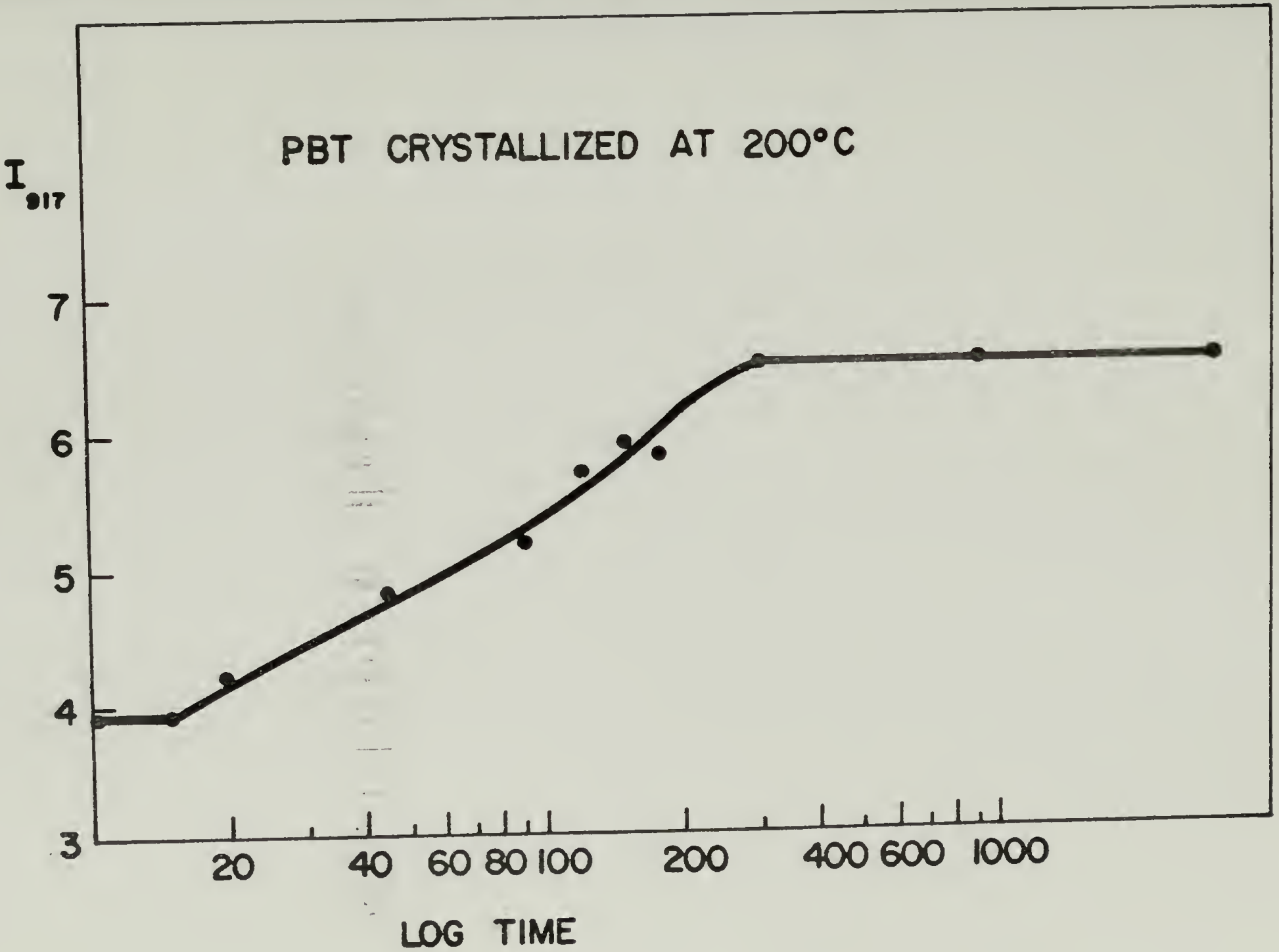
PBT CRYSTALLIZED AT 200°C
I_{917}
7
6
5
4
3
20
40
60
80
100
200
400
600
1000
LOG TIME

Figure 24

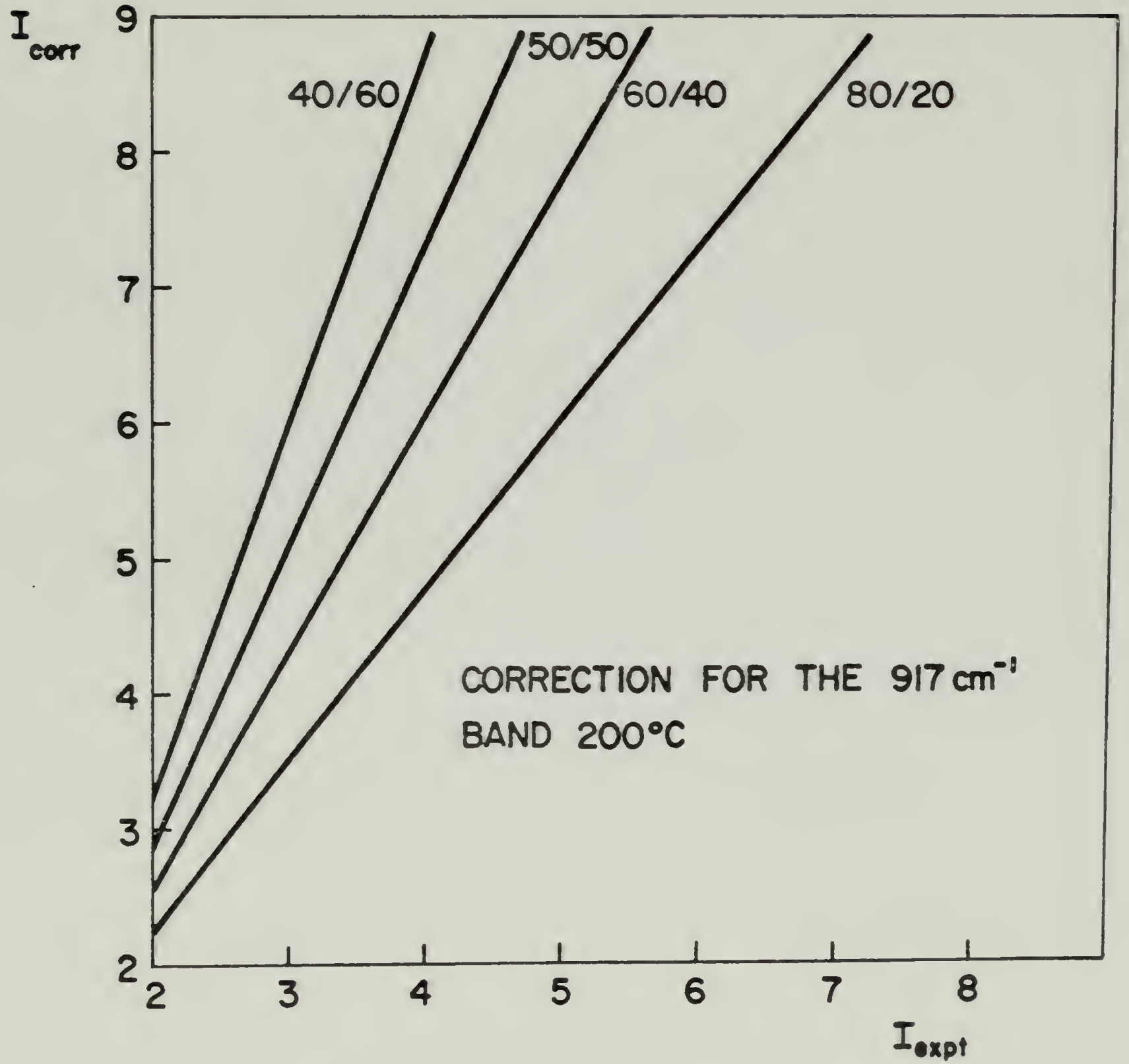
I_{corr}
9
8
7
6
5
4
3
2
40/60
50/50
60/40
80/20
CORRECTION FOR THE 917 cm^{-1}
BAND 200°C
2
3
4
5
6
7
8
I_{expt}

Figure 25

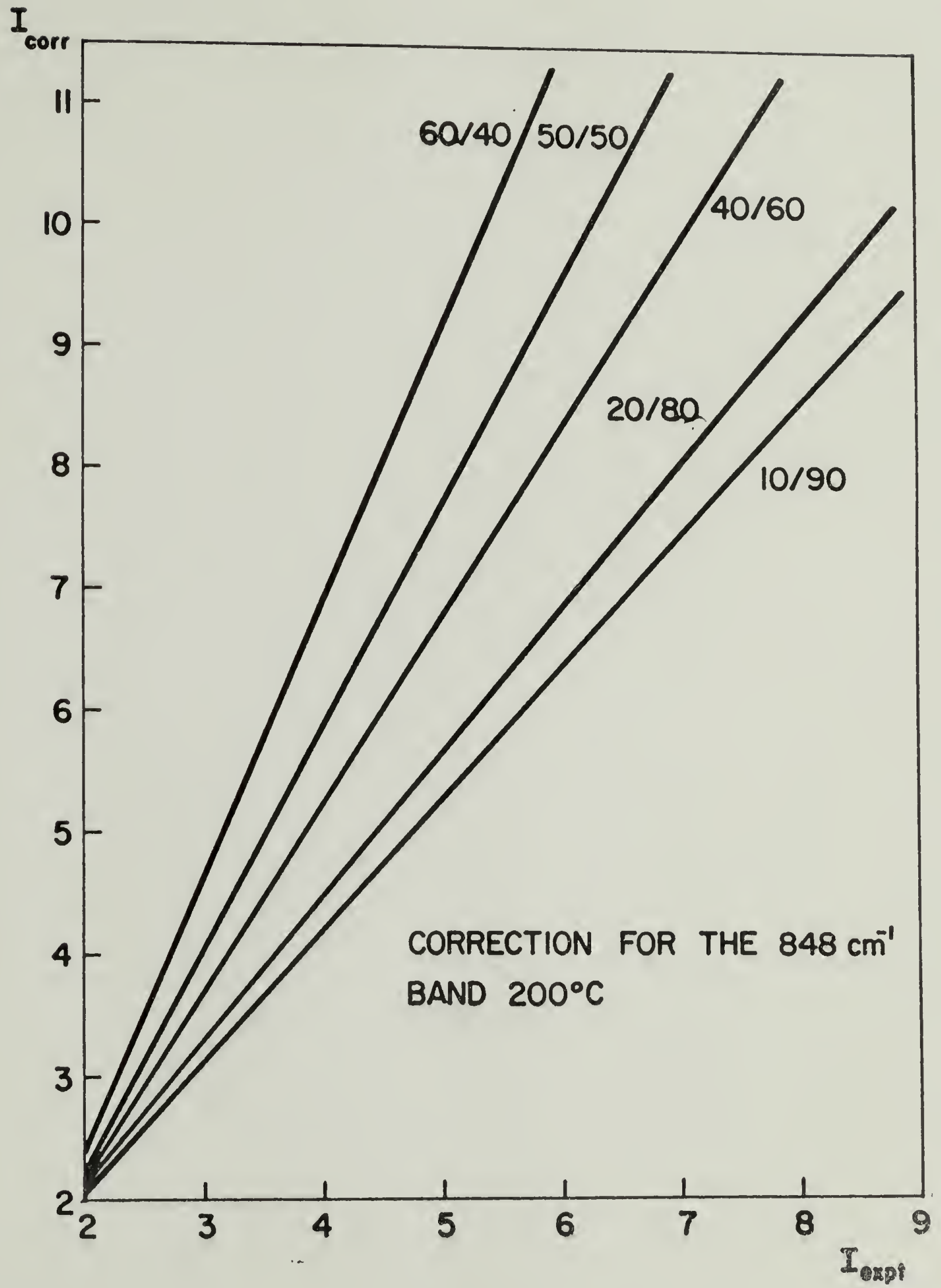
I corr
11
10
9
8
7
6
5
4
3
2
60/40
50/50
40/60
20/80
10/90
CORRECTION FOR THE 848 cm⁻¹
BAND 200°C
2
3
4
5
6
7
8
9
I expt

Figure 26

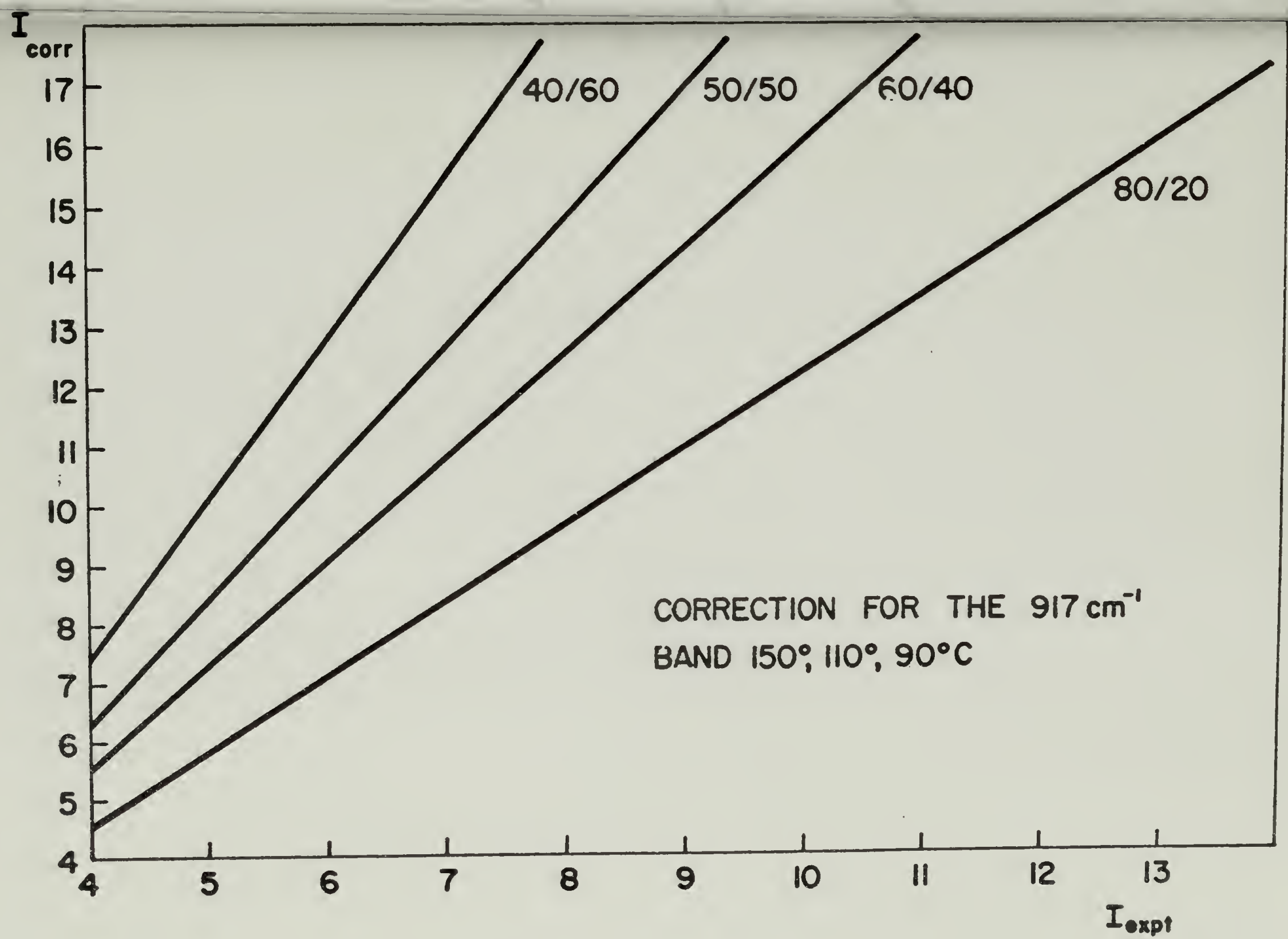
I corr
17
16
15
14
13
12
11
10
9
8
7
6
5
4
40/60
50/50
60/40
80/20
CORRECTION FOR THE 917 cm⁻¹
BAND 150°, 110°, 90°C
4
5
6
7
8
9
10
11
12
13
I expt

Figure 27

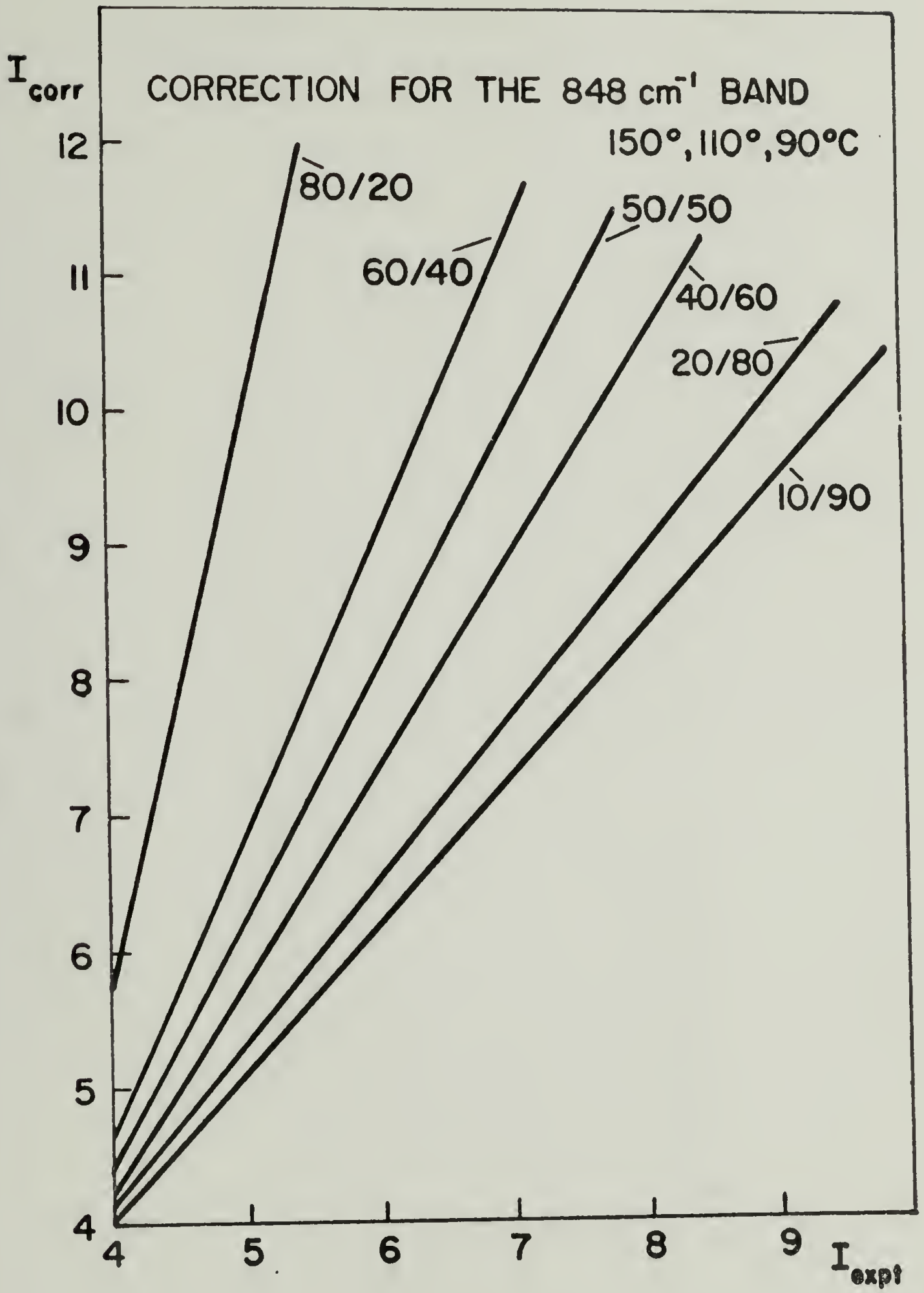
I_{corr}
CORRECTION FOR THE 848 cm^{-1} BAND
150°,110°,90°C
80/20
60/40
50/50
40/60
20/80
10/90
12
11
10
9
8
7
6
5
4
4
5
6
7
8
9
I_{expt}

Figure 28

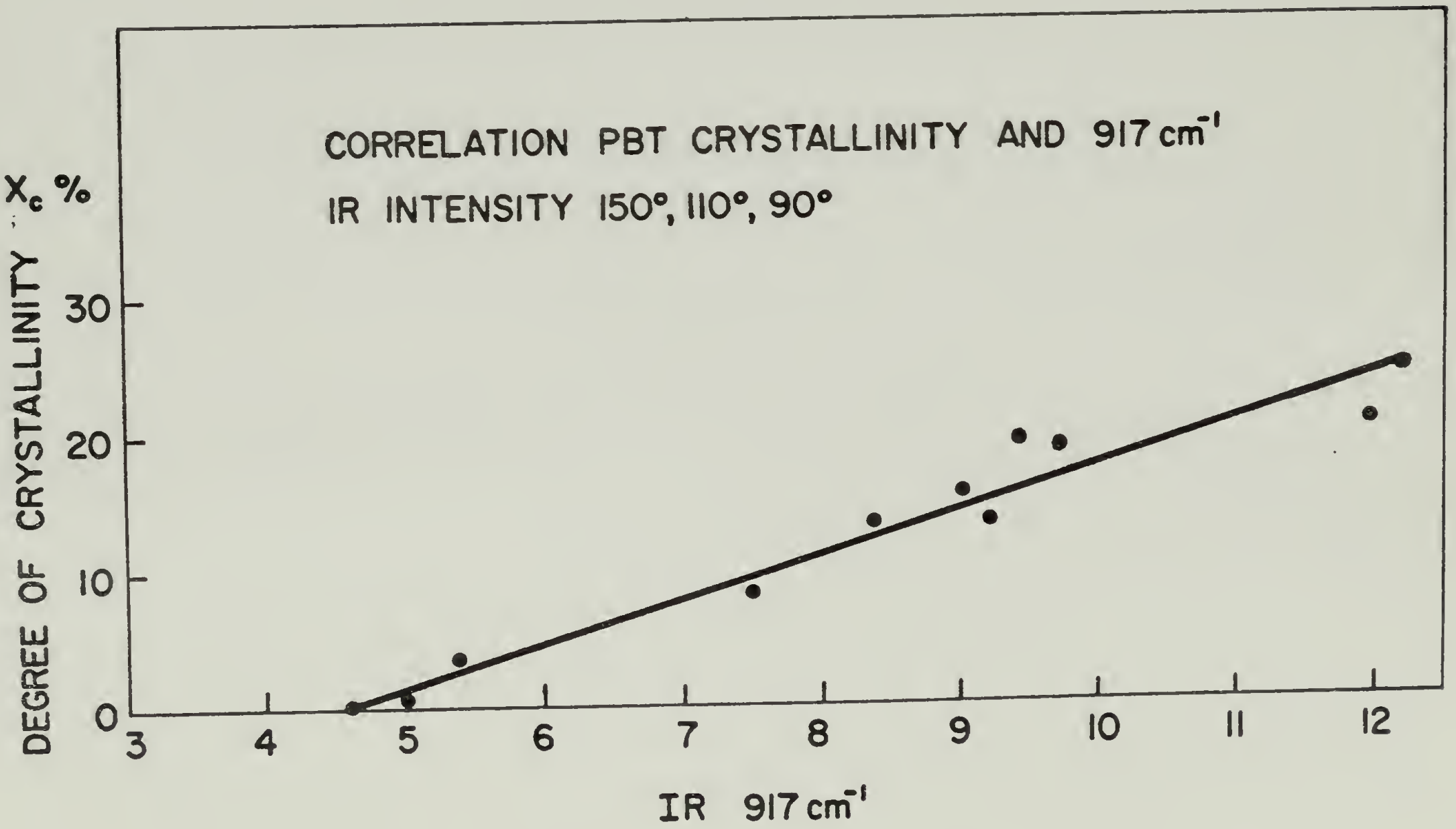
CORRELATION PBT CRYSTALLINITY AND 917 cm⁻¹
IR INTENSITY 150°, 110°, 90°
DEGREE OF CRYSTALLINITY X_c %
0
10
20
30
3
4
5
6
7
8
9
10
11
12
IR 917 cm⁻¹

Figure 29

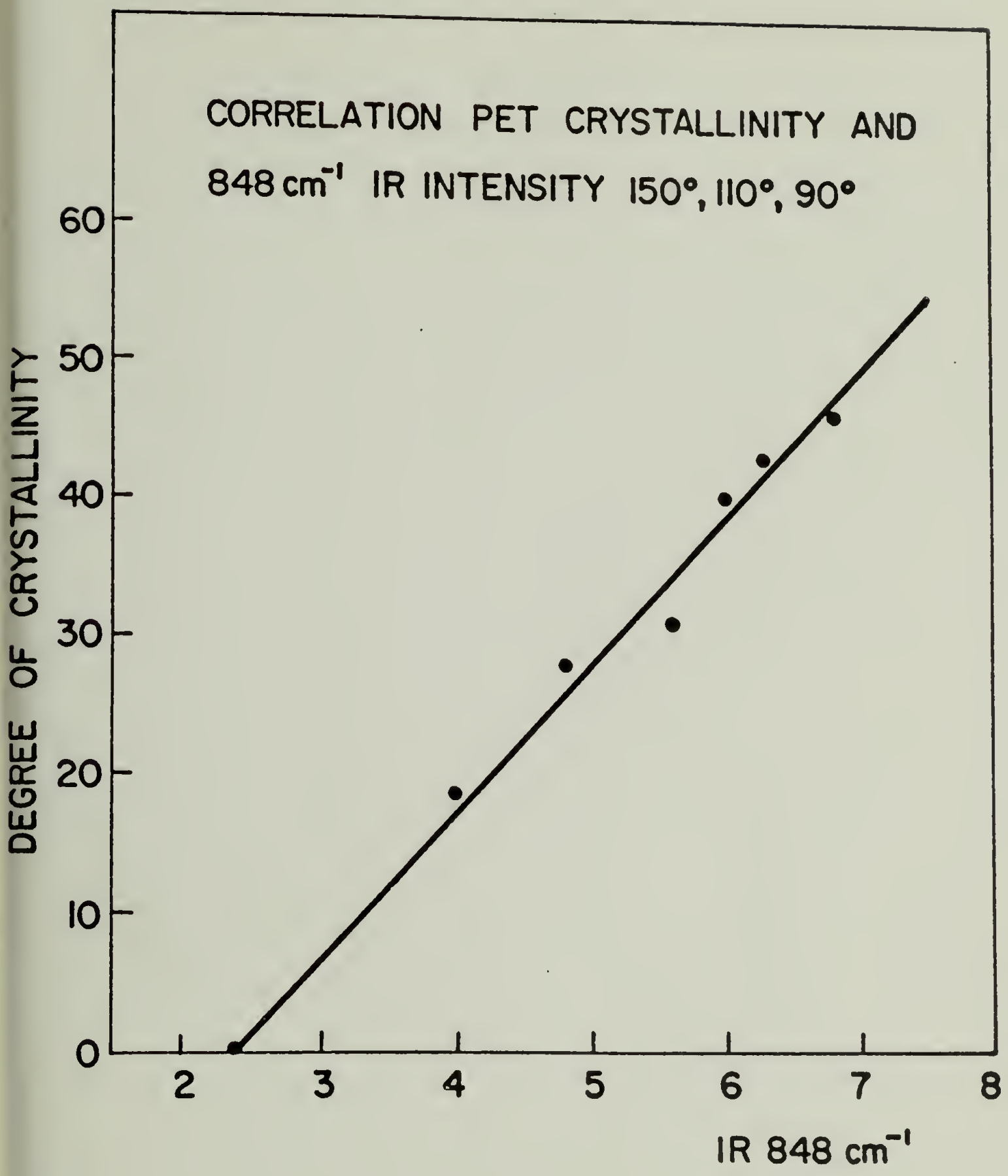
CORRELATION PET CRYSTALLINITY AND
848 cm⁻¹ IR INTENSITY 150°, 110°, 90°
DEGREE OF CRYSTALLINITY
60
50
40
30
20
10
0
2
3
4
5
6
7
8
IR 848 cm⁻¹

Figure 30

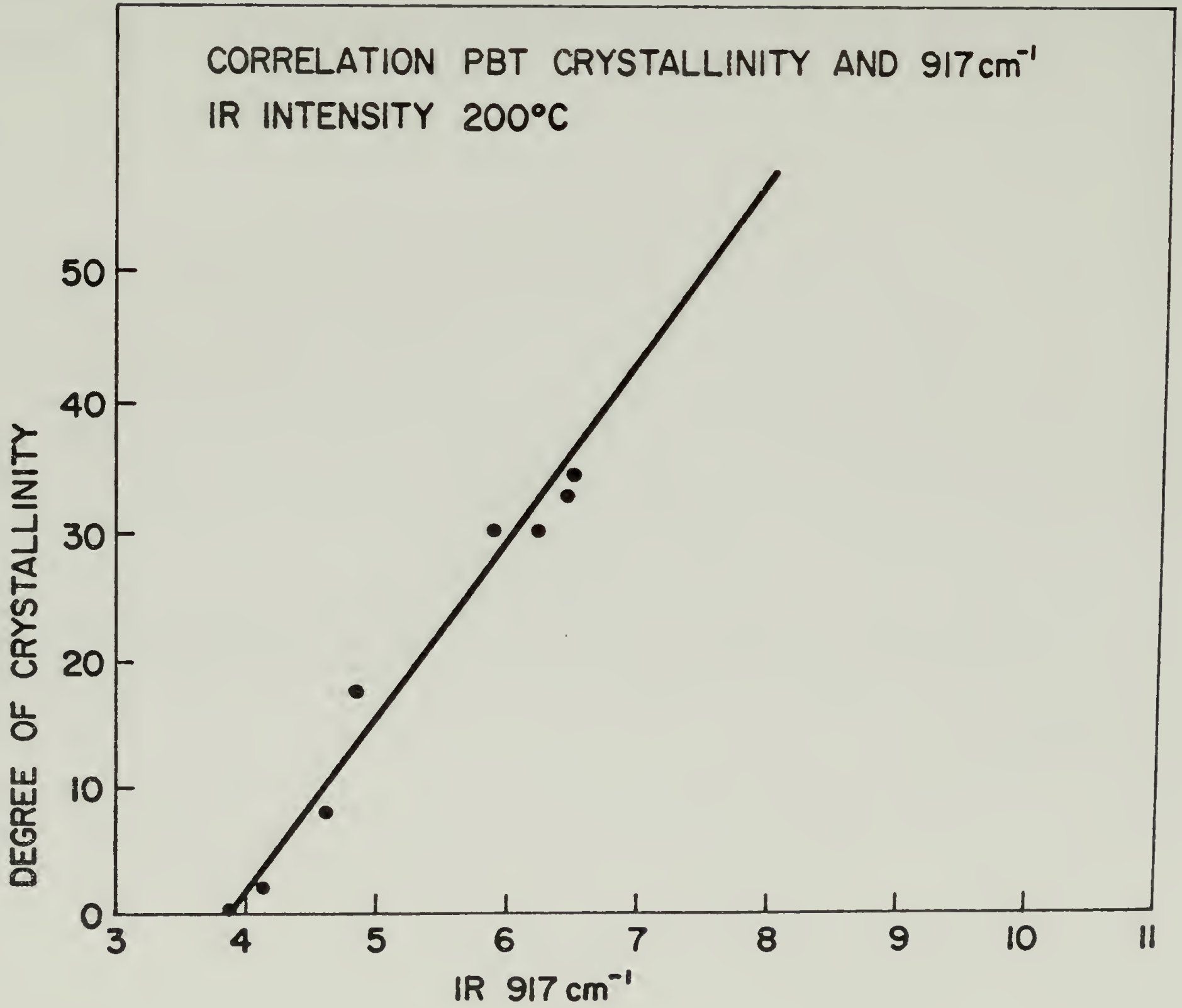
CORRELATION PBT CRYSTALLINITY AND 917cm⁻¹
IR INTENSITY 200°C
DEGREE OF CRYSTALLINITY
0
10
20
30
40
50
3
4
5
6
7
8
9
10
11
IR 917 cm⁻¹

Figure 31

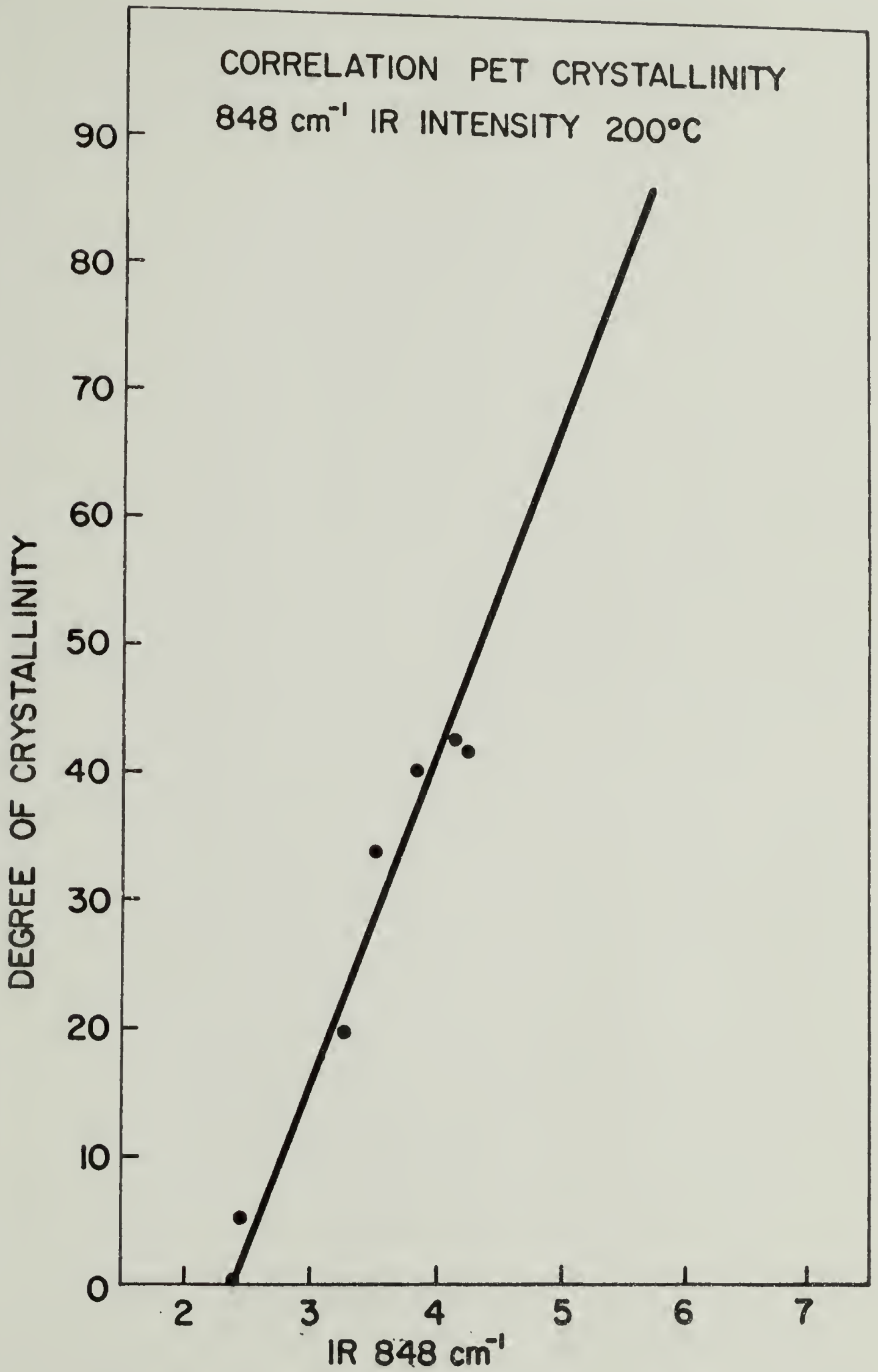
CORRELATION PET CRYSTALLINITY
848 cm⁻¹ IR INTENSITY 200°C
DEGREE OF CRYSTALLINITY
0
10
20
30
40
50
60
70
80
90
2
3
4
5
6
7
IR 848 cm⁻¹

Figure 32

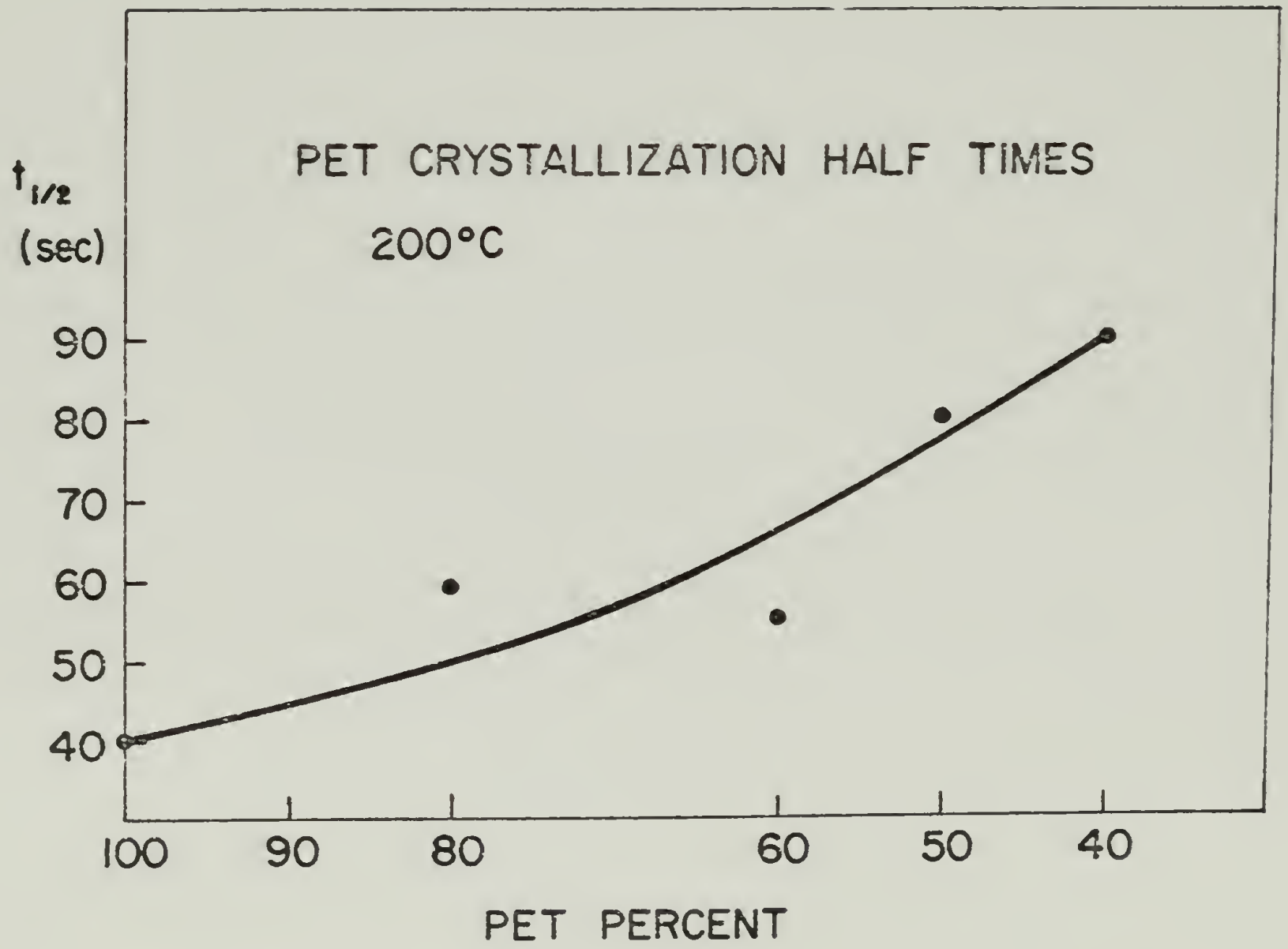
PET CRYSTALLIZATION HALF TIMES
200°C
$t_{1/2}$
(sec)
90
80
70
60
50
40
100
90
80
60
50
40
PET PERCENT

Figure 33

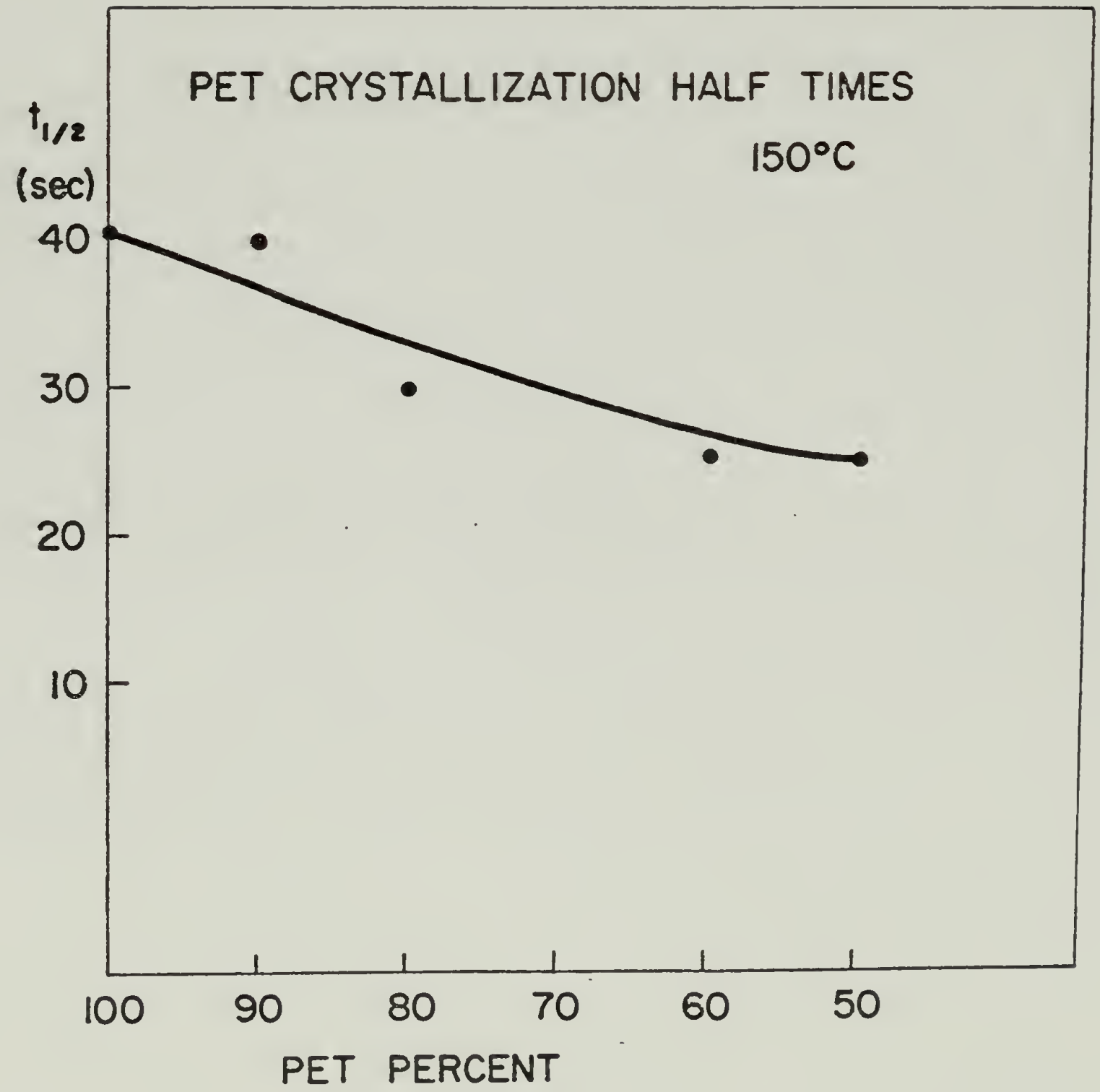
PET CRYSTALLIZATION HALF TIMES
150°C
$t_{1/2}$
(sec)
40
30
20
10
100
90
80
70
60
50
PET PERCENT

Figure 34

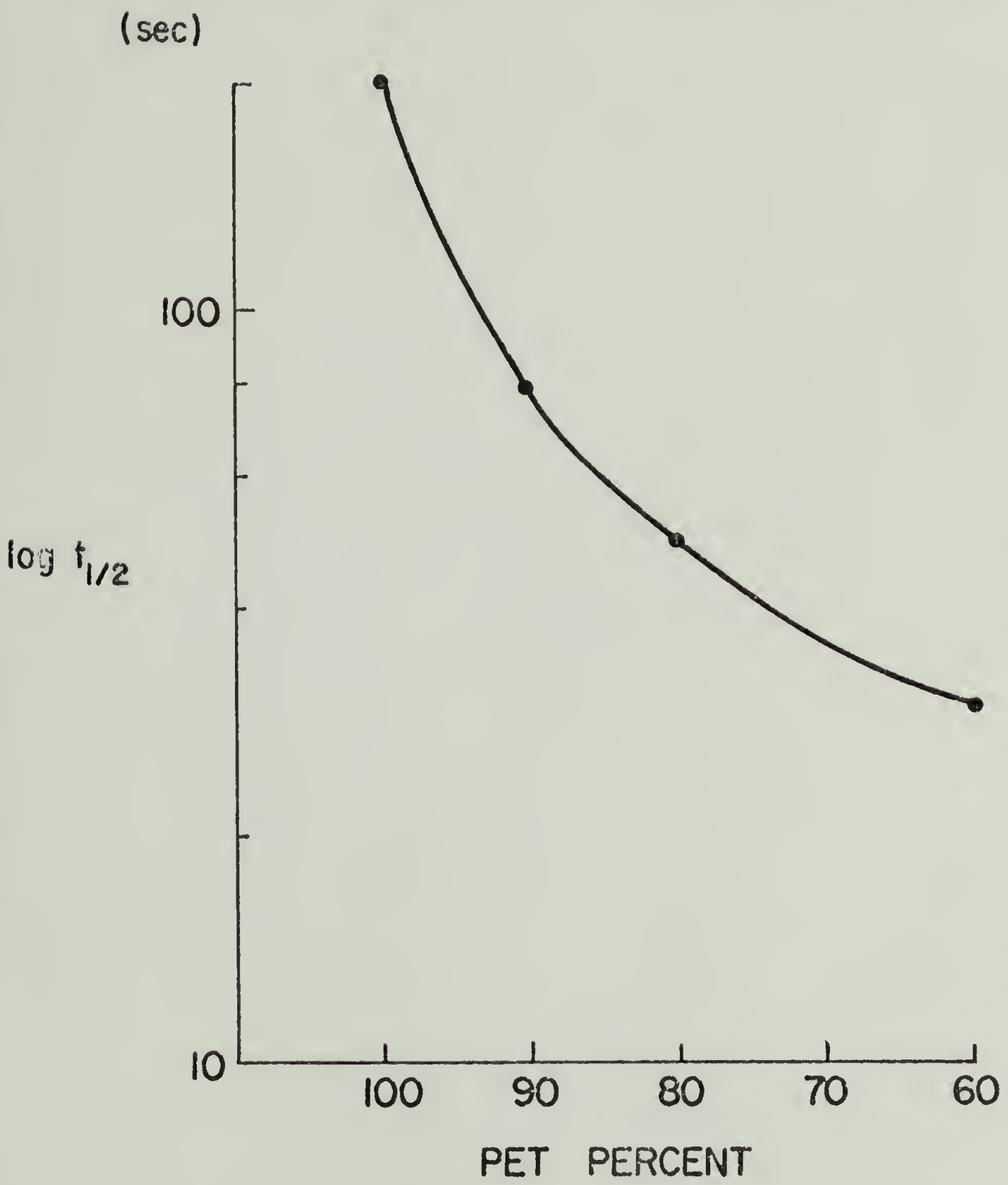
PET CRYSTALLIZATION HALF TIMES 130°C
(sec)
100
log $t_{1/2}$
10
100
90
80
70
60
PET PERCENT

Figure 35

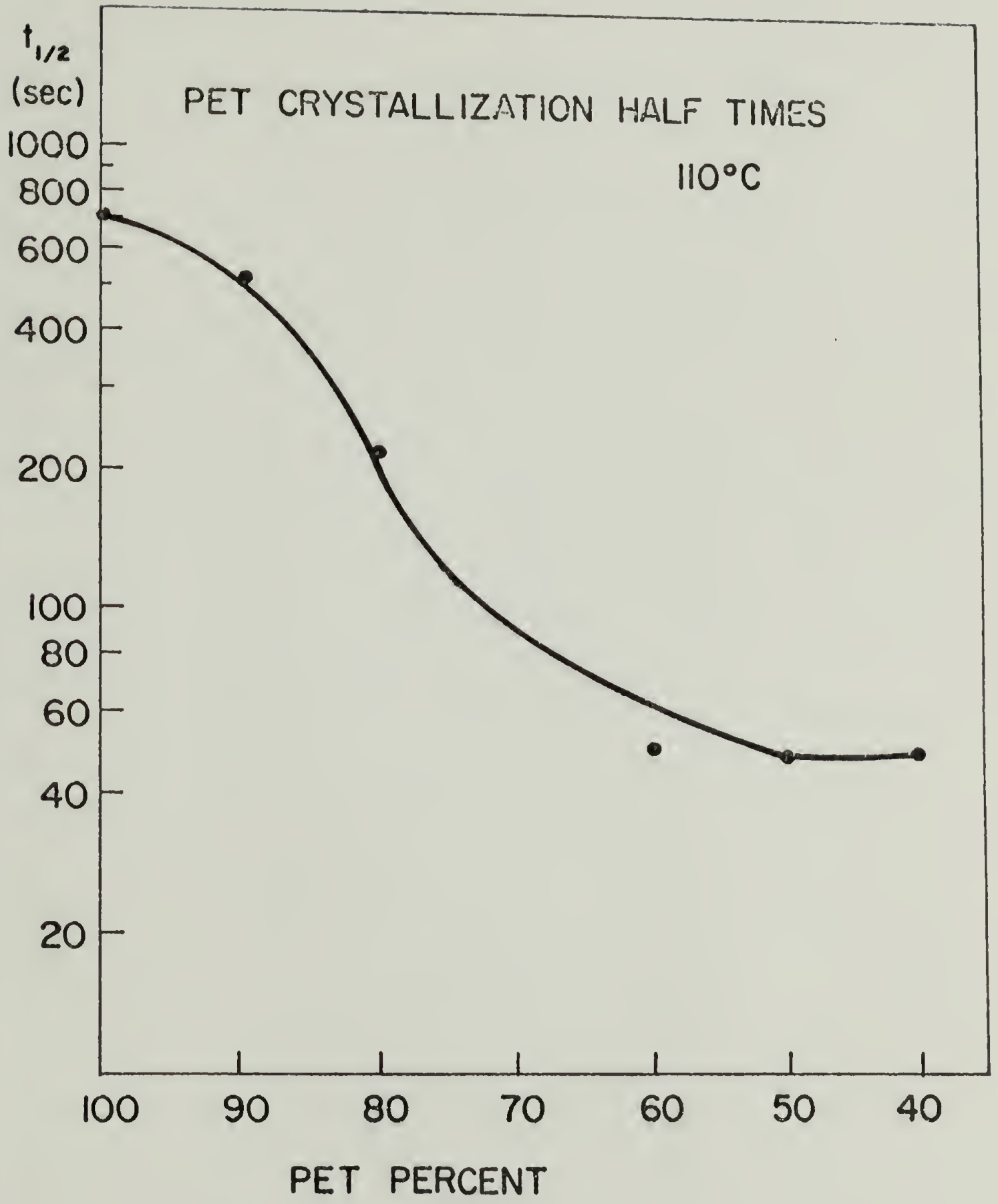
$t_{1/2}$
(sec)
PET CRYSTALLIZATION HALF TIMES
110°C
1000
800
600
400
200
100
80
60
40
20
100
90
80
70
60
50
40
PET PERCENT

Figure 36

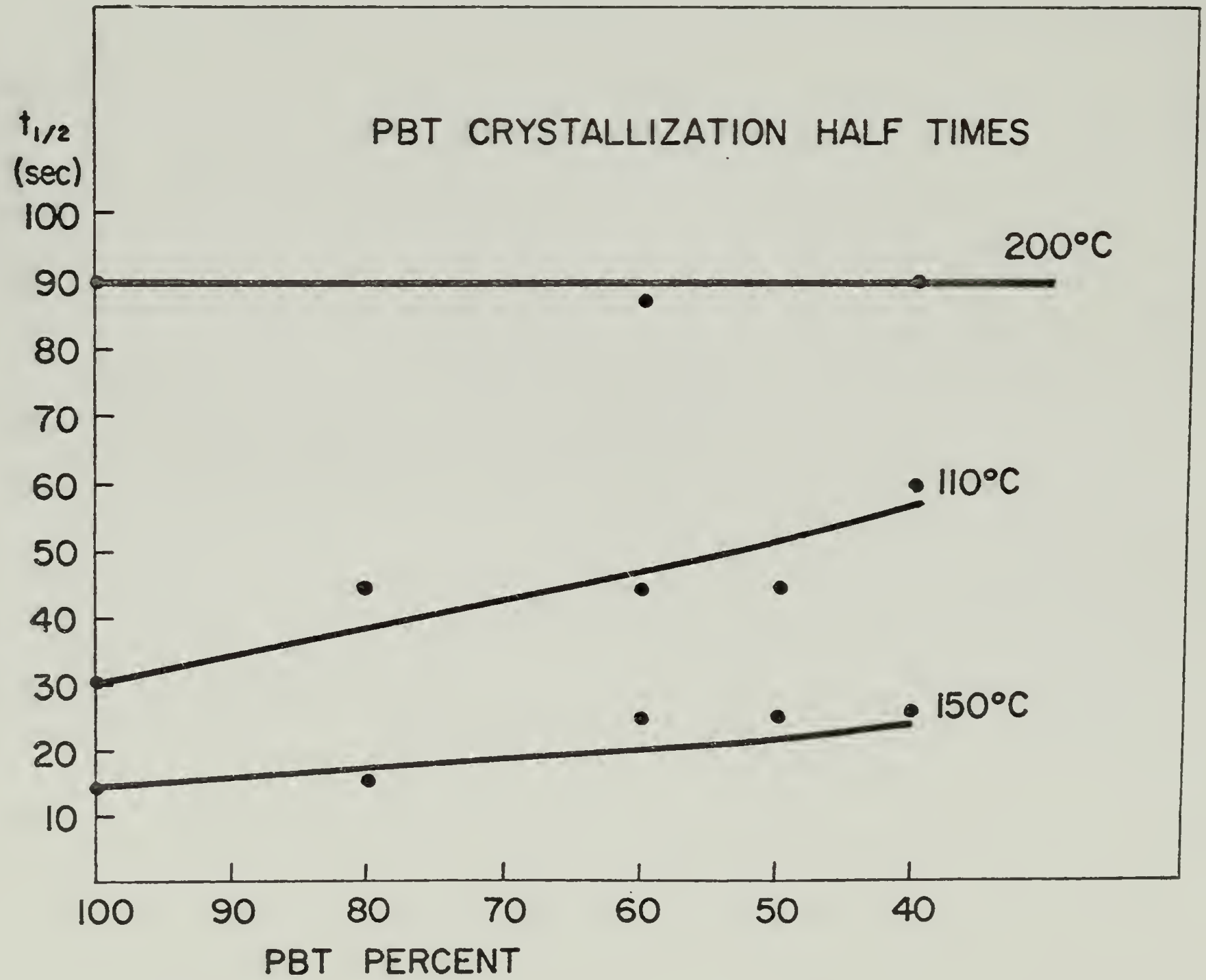
PBT CRYSTALLIZATION HALF TIMES
$t_{1/2}$ (sec)
100
90
80
70
60
50
40
30
20
10
200°C
110°C
150°C
100
90
80
70
60
50
40
PBT PERCENT

Figure 37

PBT CRYSTALLIZATION HALF TIMES 130 °C

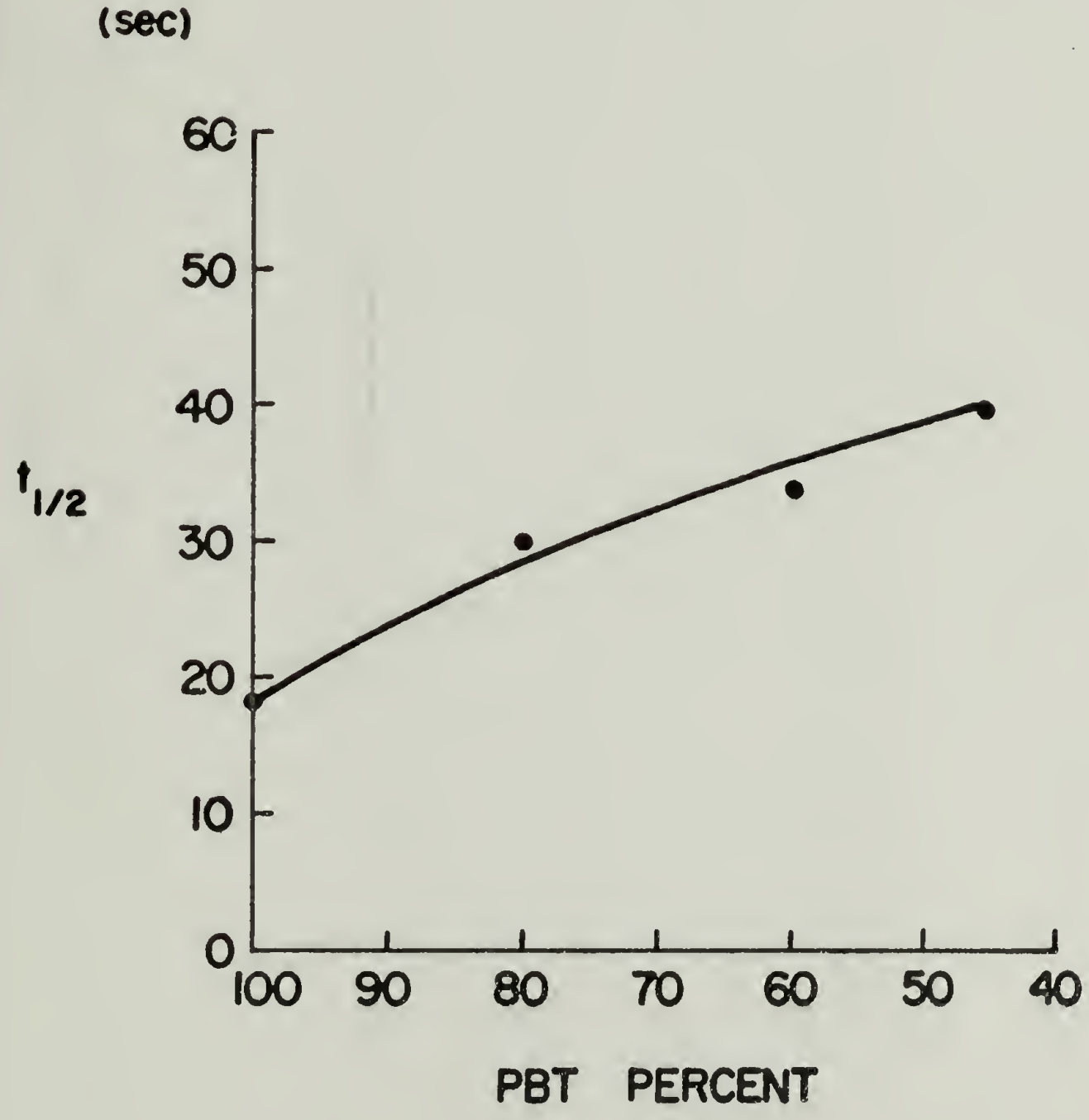

Figure 38

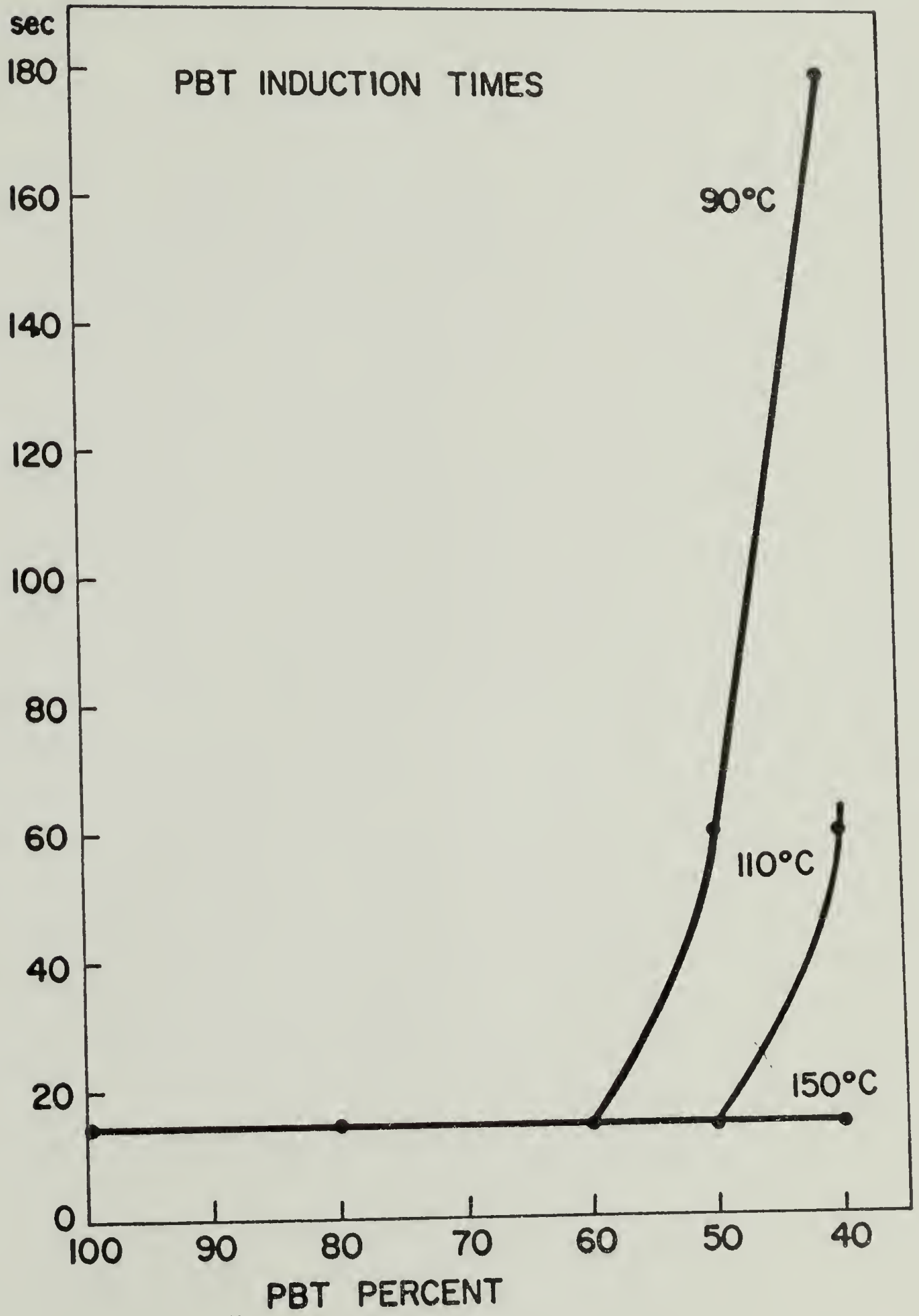
sec
PBT INDUCTION TIMES
180
160
140
120
100
80
60
40
20
0
90°C
110°C
150°C
100
90
80
70
60
50
40
PBT PERCENT

Figure 39

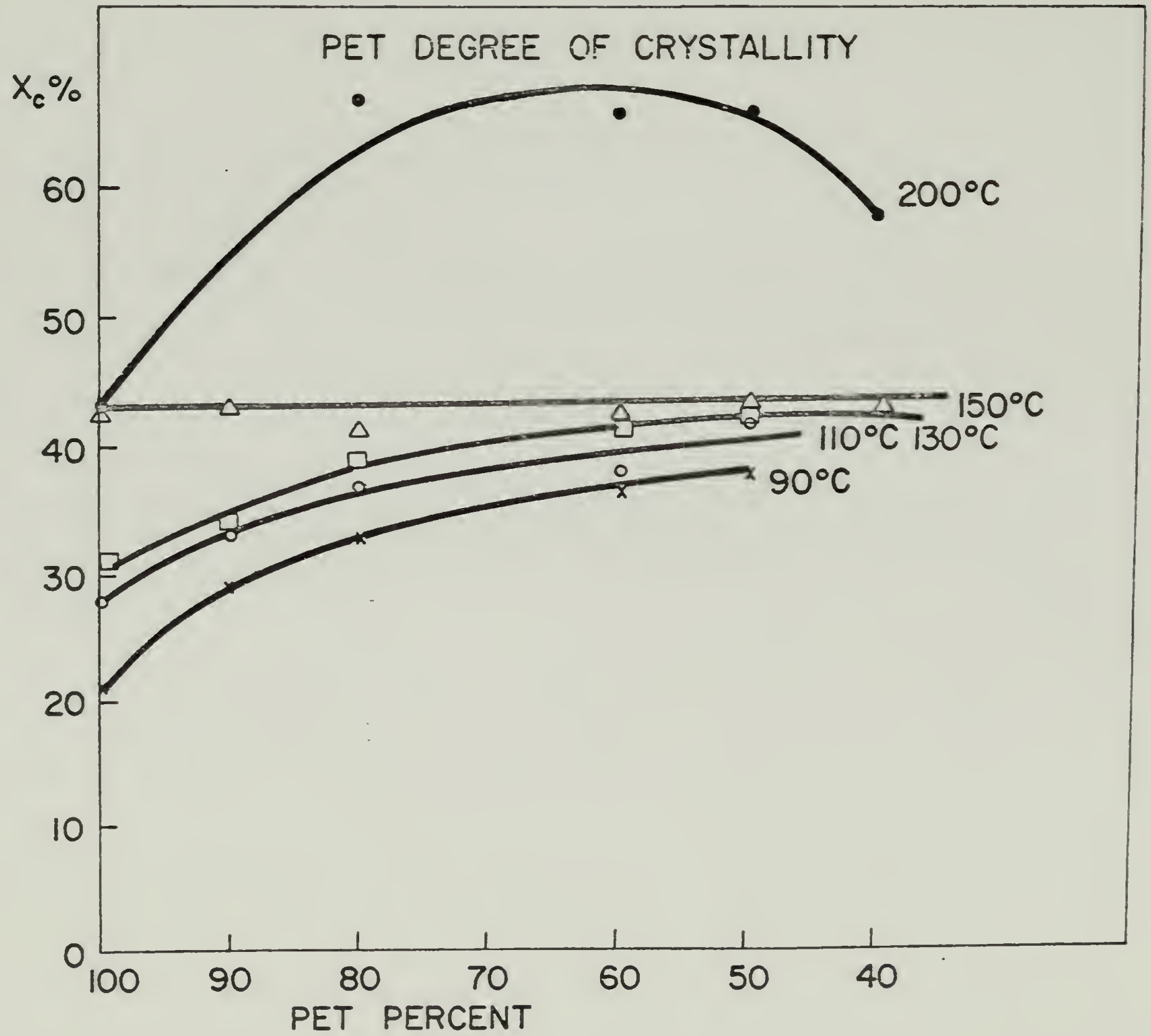
PET DEGREE OF CRYSTALLITY
X_c%
60
50
40
30
20
10
0
200°C
150°C
110°C 130°C
90°C
100
90
80
70
60
50
40
PET PERCENT

Figure 40

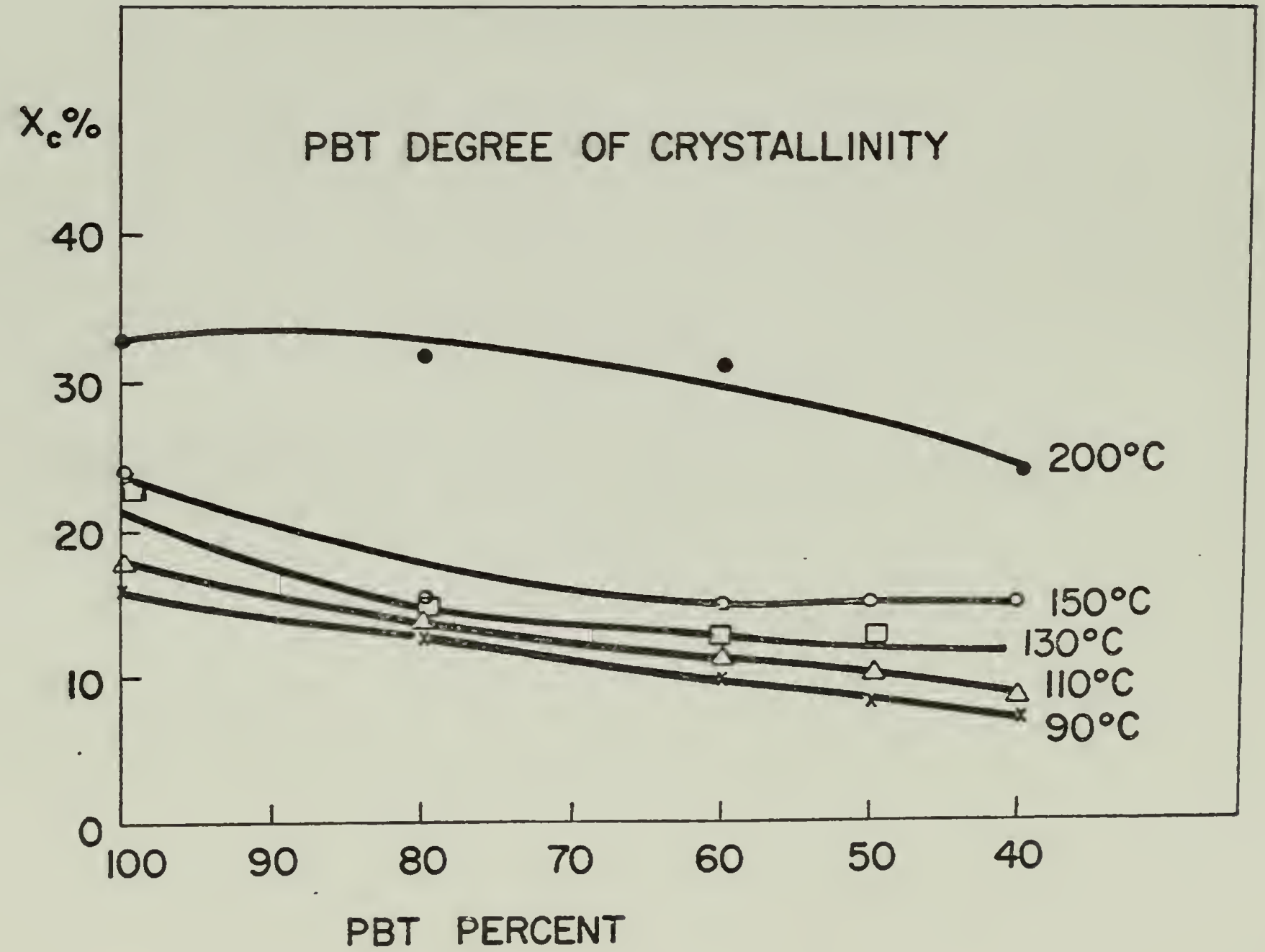
PBT DEGREE OF CRYSTALLINITY
X_c%
40
30
20
10
0
200°C
150°C
130°C
110°C
90°C
100
90
80
70
60
50
40
PBT PERCENT

Figure 41

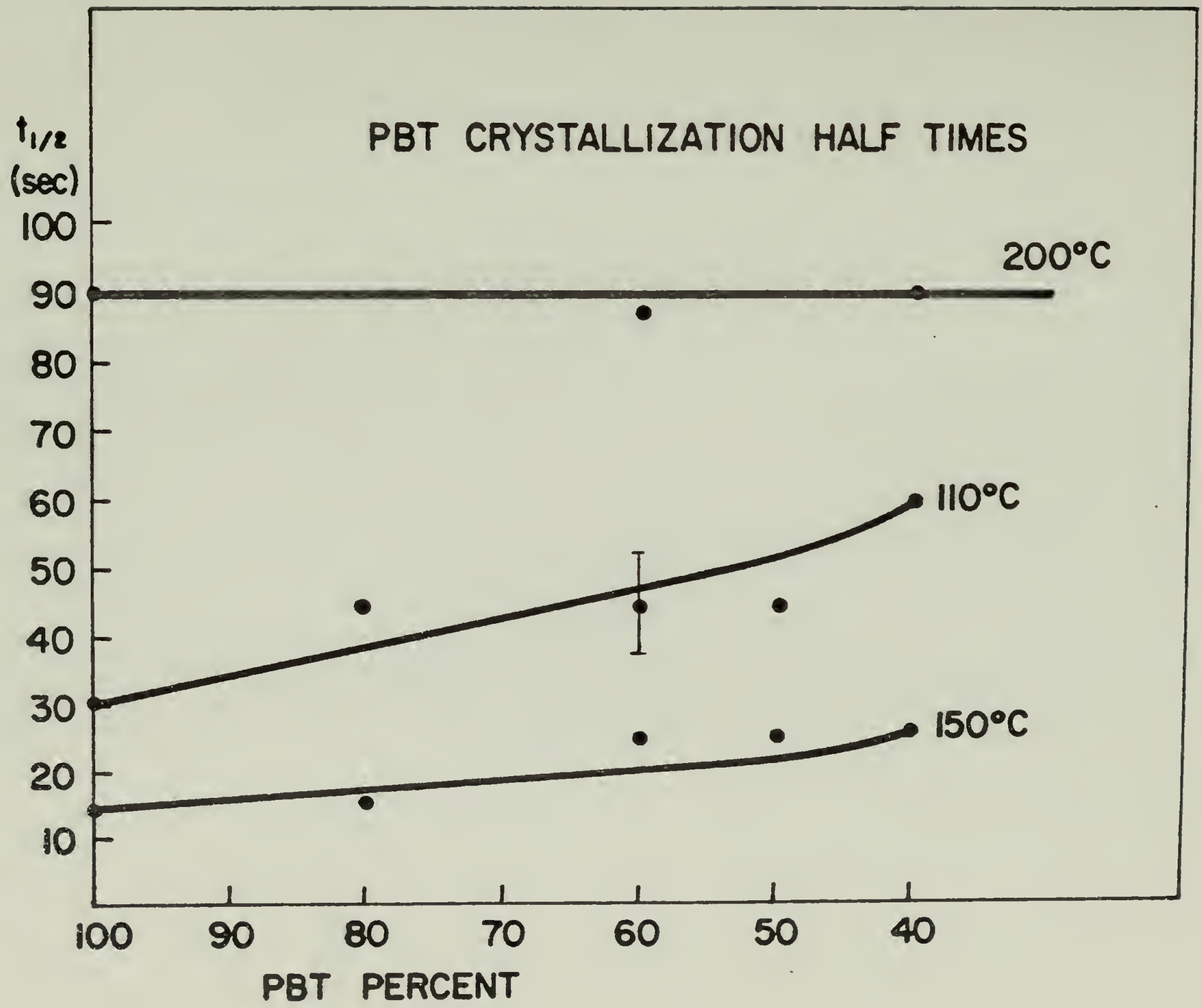
PBT CRYSTALLIZATION HALF TIMES
$t_{1/2}$ (sec)
100
90
80
70
60
50
40
30
20
10
200°C
110°C
150°C
100
90
80
70
60
50
40
PBT PERCENT

Figure 42

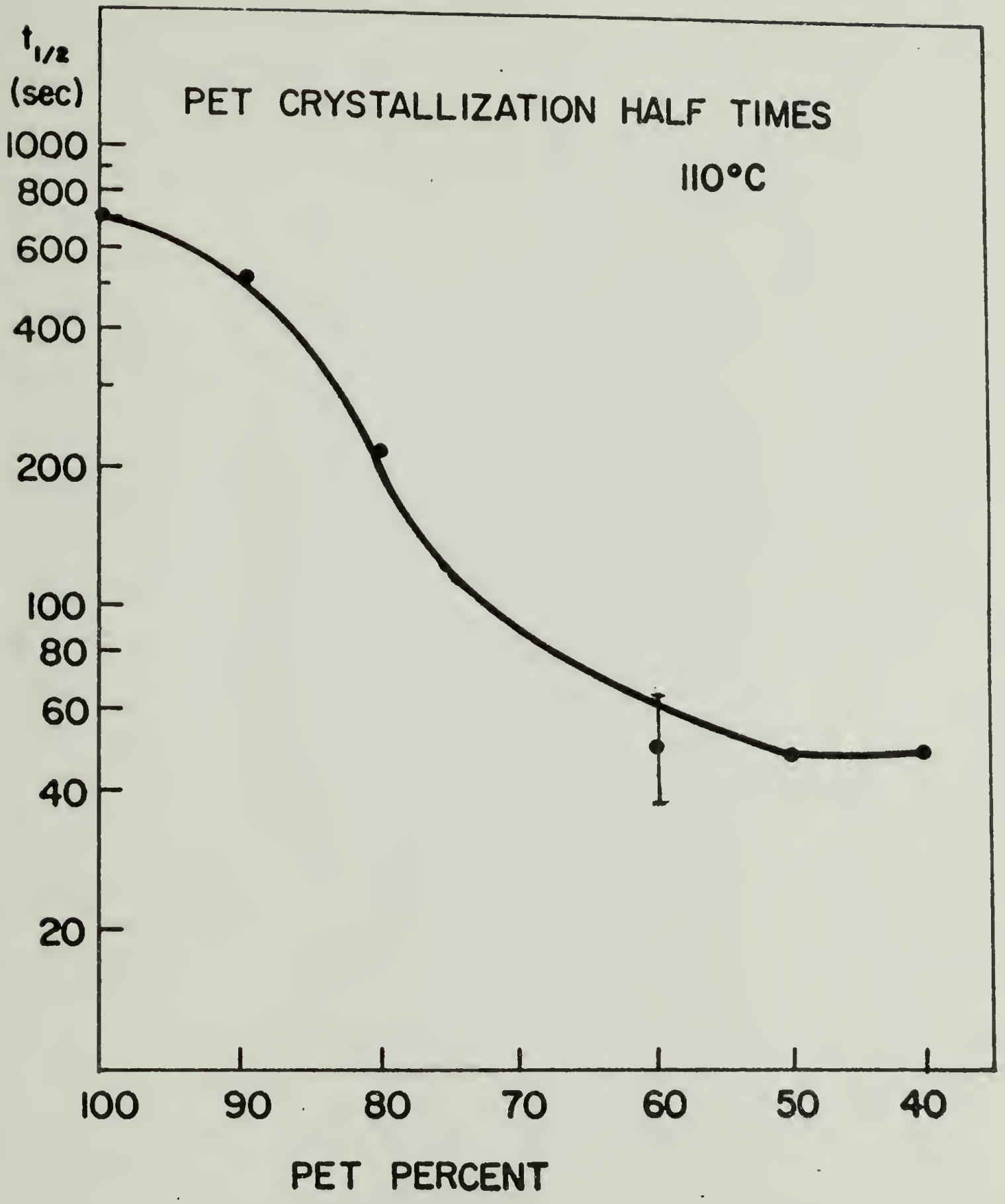
$t_{1/2}$ (sec)
PET CRYSTALLIZATION HALF TIMES
110°C
1000
800
600
400
200
100
80
60
40
20
100
90
80
70
60
50
40
PET PERCENT

Figure 43

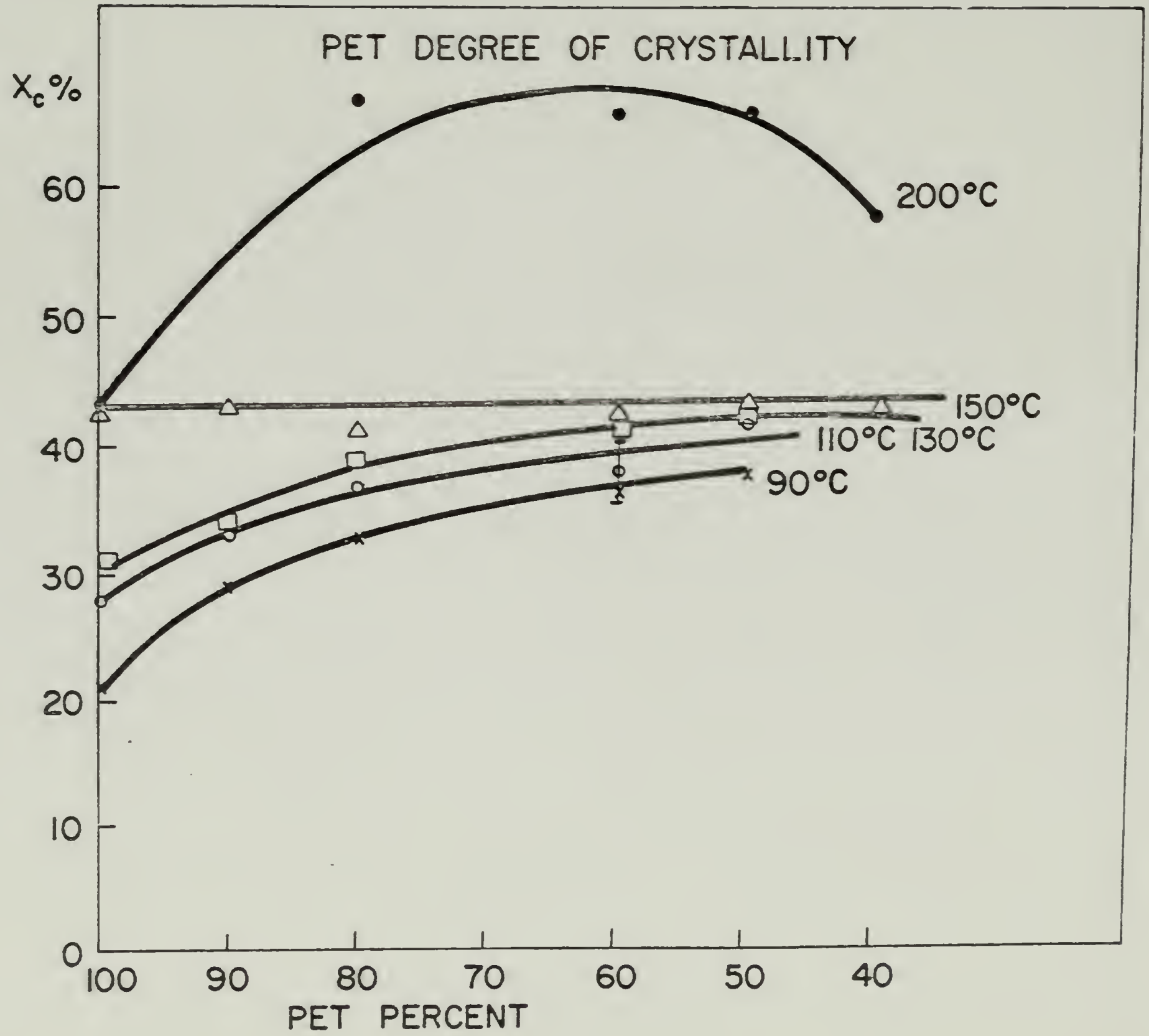
PET DEGREE OF CRYSTALLITY
X_c%
60
50
40
30
20
10
0
200°C
150°C
110°C
130°C
90°C
100
90
80
70
60
50
40
PET PERCENT

Figure 44

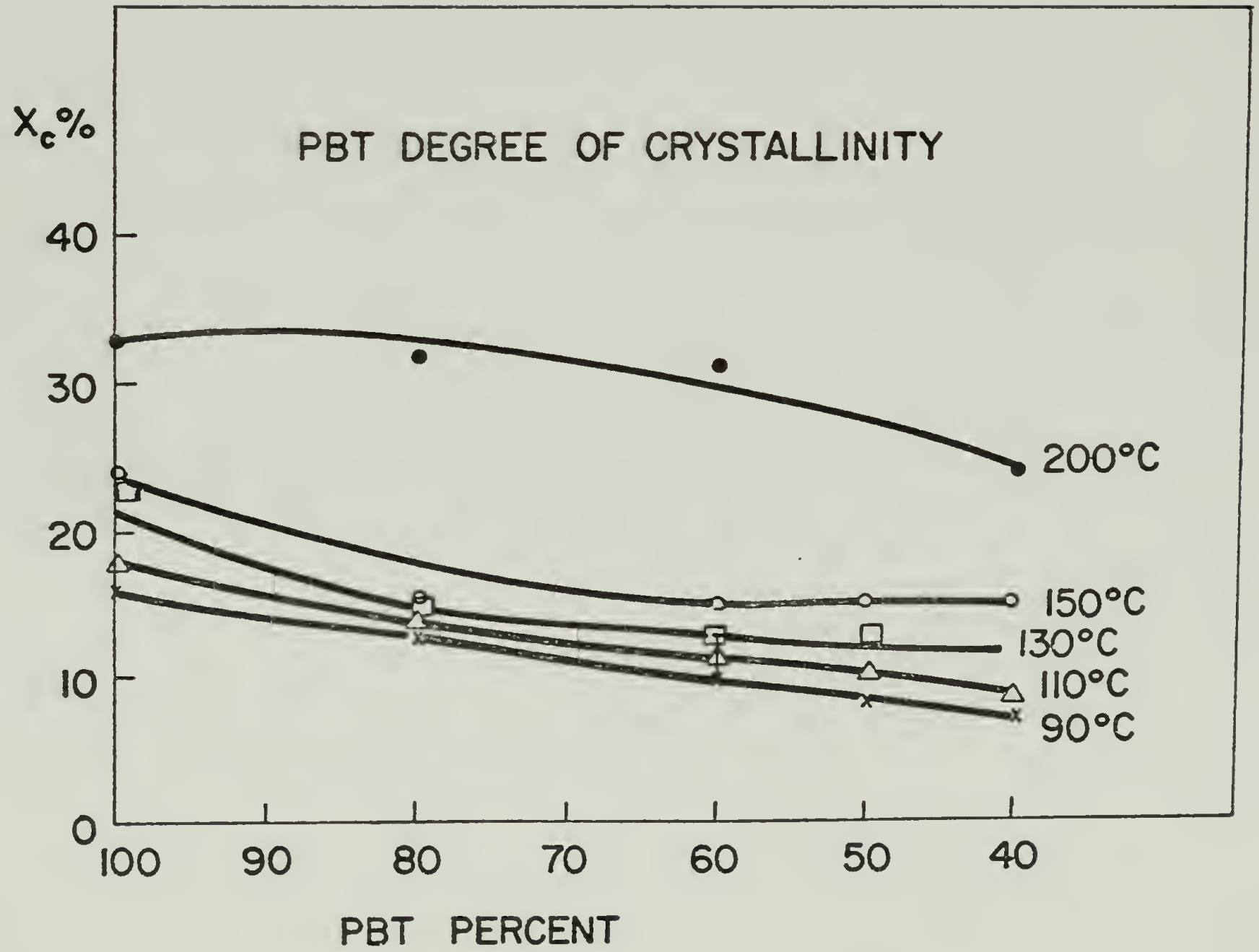
PBT DEGREE OF CRYSTALLINITY
X_c%
40
30
20
10
0
200°C
150°C
130°C
110°C
90°C
100
90
80
70
60
50
40
PBT PERCENT

Figure 45

THEORETICAL PLOT OF CRYSTALIZATION RATE VS. TEMPERATURE

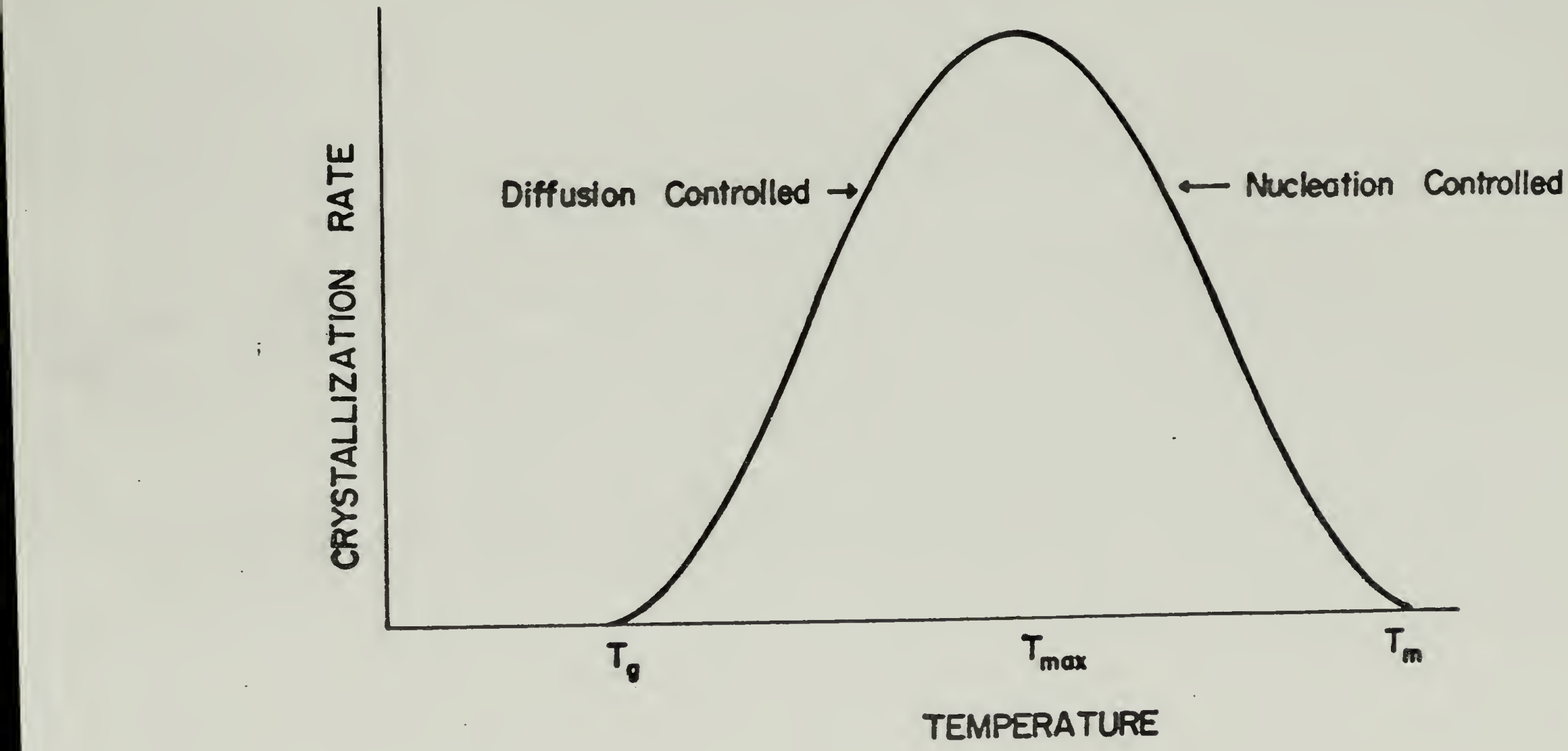

Figure 46

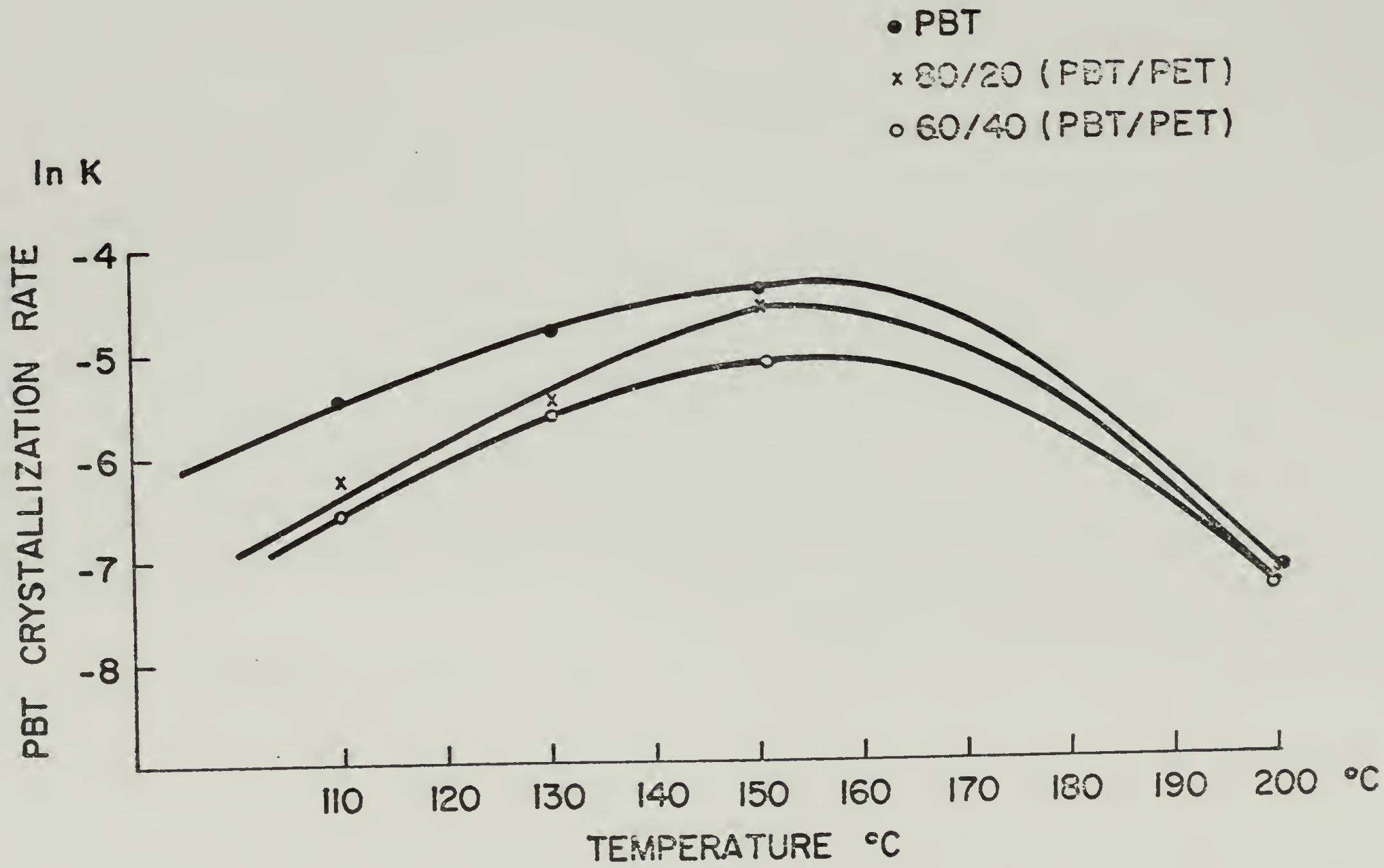
• PBT
x 80/20 (PBT/PET)
o 60/40 (PBT/PET)
ln K
PBT CRYSTALLIZATION RATE
-4
-5
-6
-7
-8
110
120
130
140
150
160
170
180
190
200 °C
TEMPERATURE °C

Figure 47

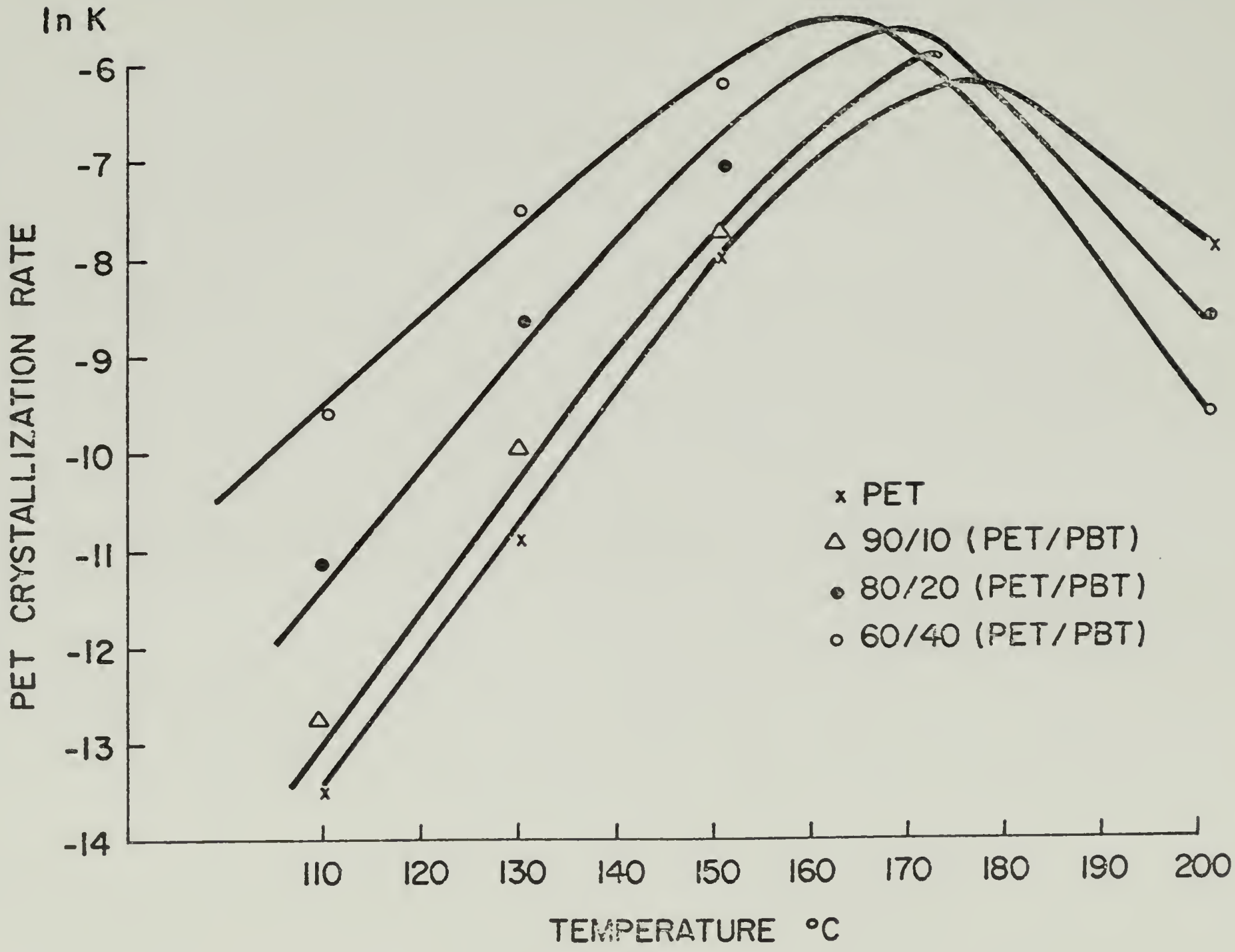
ln K
-6
-7
-8
-9
-10
-11
-12
-13
-14
PET CRYSTALLIZATION RATE
110
120
130
140
150
160
170
180
190
200
TEMPERATURE °C
x PET
△ 90/10 (PET/PBT)
• 80/20 (PET/PBT)
○ 60/40 (PET/PBT)

Figure 48

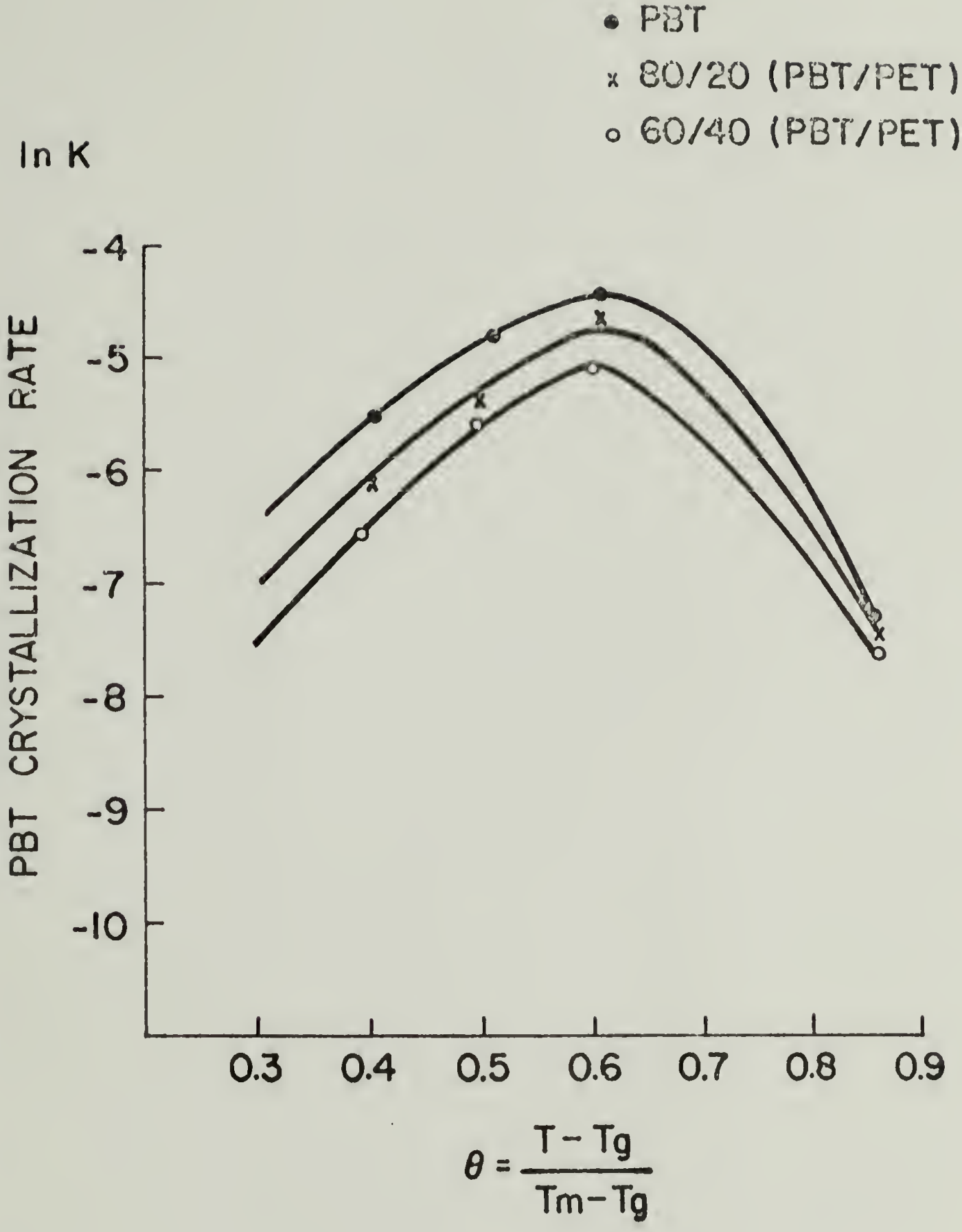
• PBT
x 80/20 (PBT/PET)
o 60/40 (PBT/PET)
ln K
PBT CRYSTALLIZATION RATE
-4
-5
-6
-7
-8
-9
-10
0.3
0.4
0.5
0.6
0.7
0.8
0.9
θ = (T − Tg) / (Tm − Tg)

Figure 49

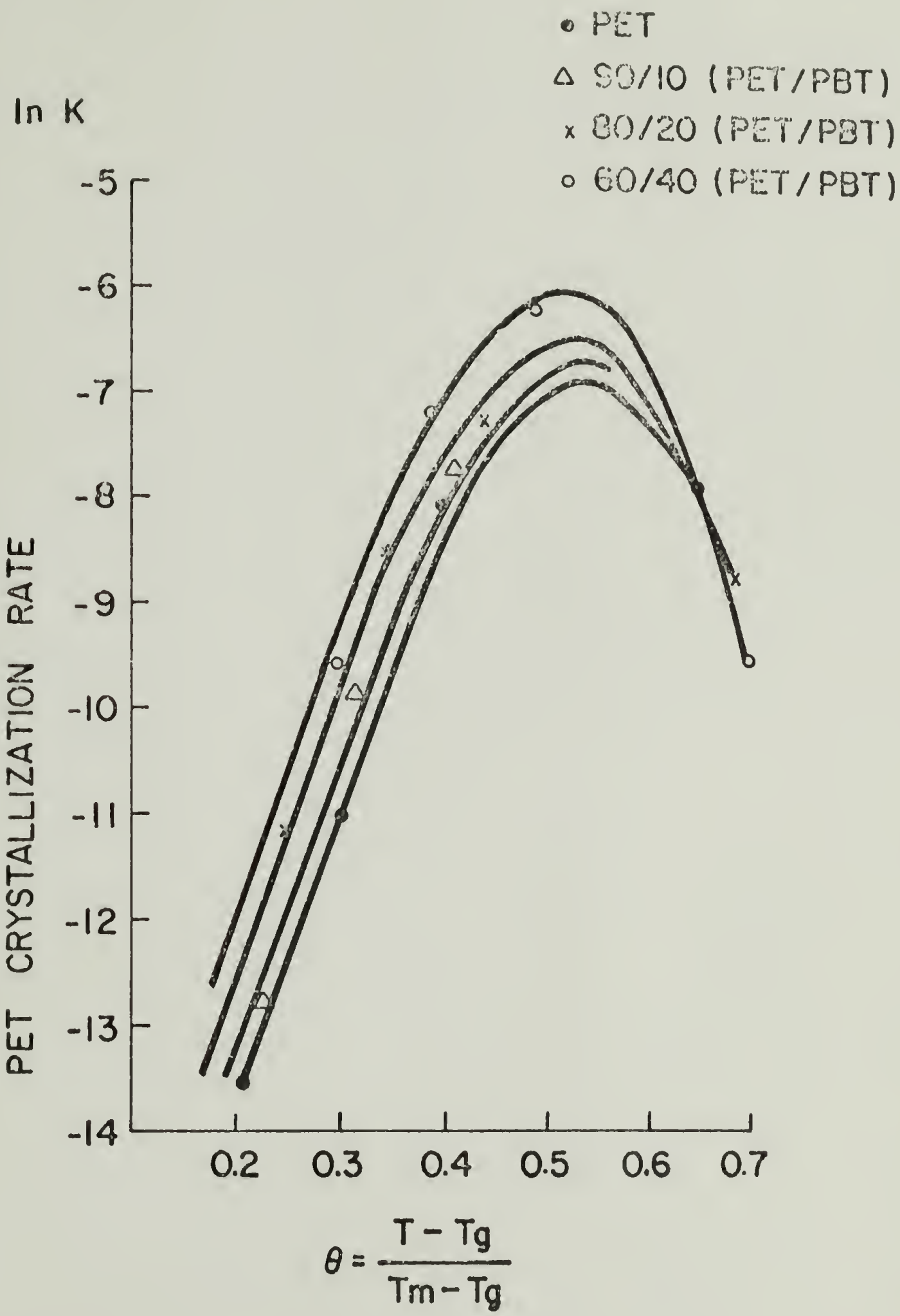
• PET
△ 90/10 (PET/PBT)
x 80/20 (PET/PBT)
○ 60/40 (PET/PBT)
ln K
PET CRYSTALLIZATION RATE
-5
-6
-7
-8
-9
-10
-11
-12
-13
-14
0.2
0.3
0.4
0.5
0.6
0.7
θ = (T − Tg) / (Tm − Tg)

Figure 50

THEORETICAL CURVES OF CRYSTALLIZATION RATE VS. CRYSTALLIZATION TEMPERATURE

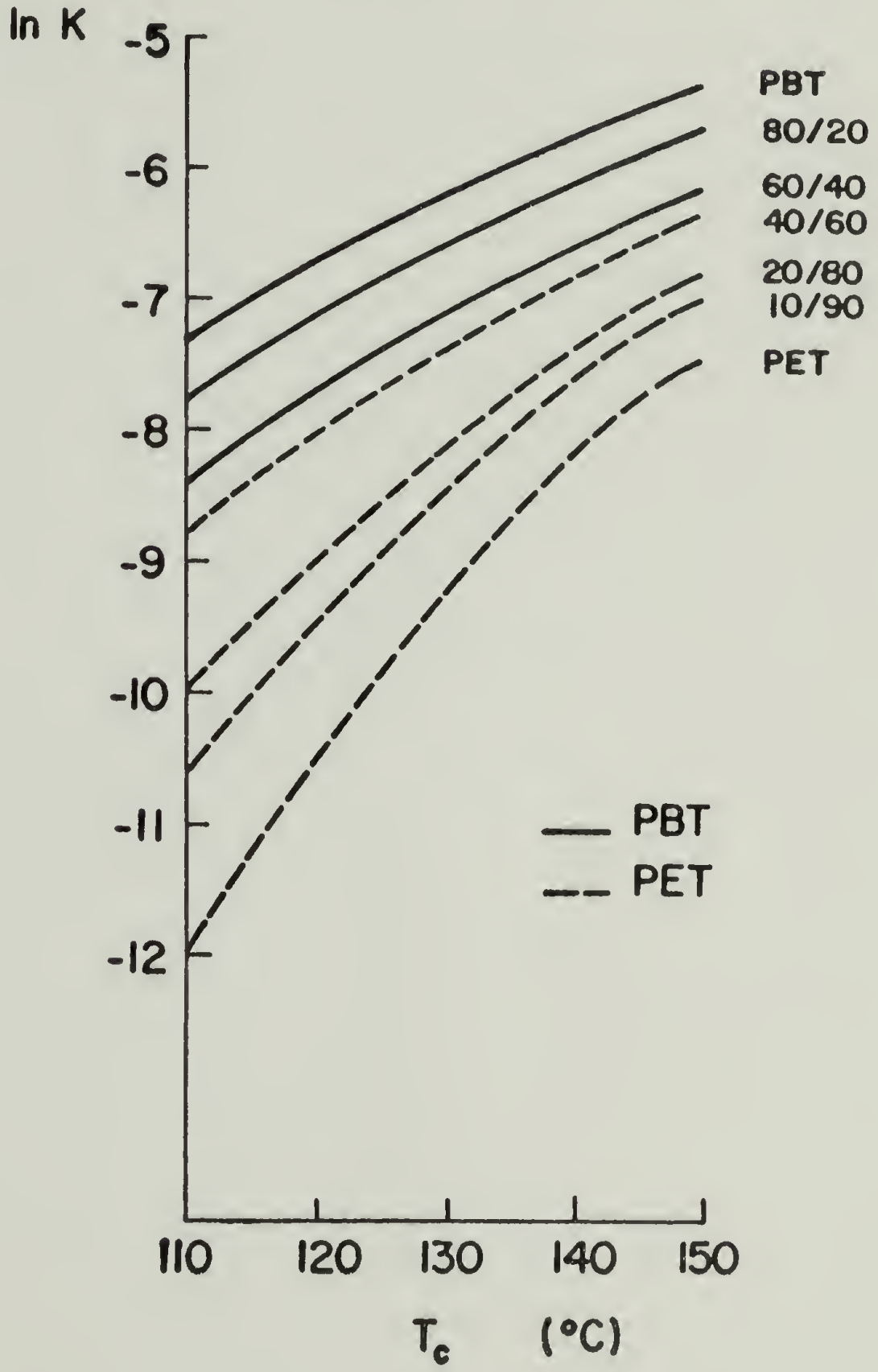

Figure 51

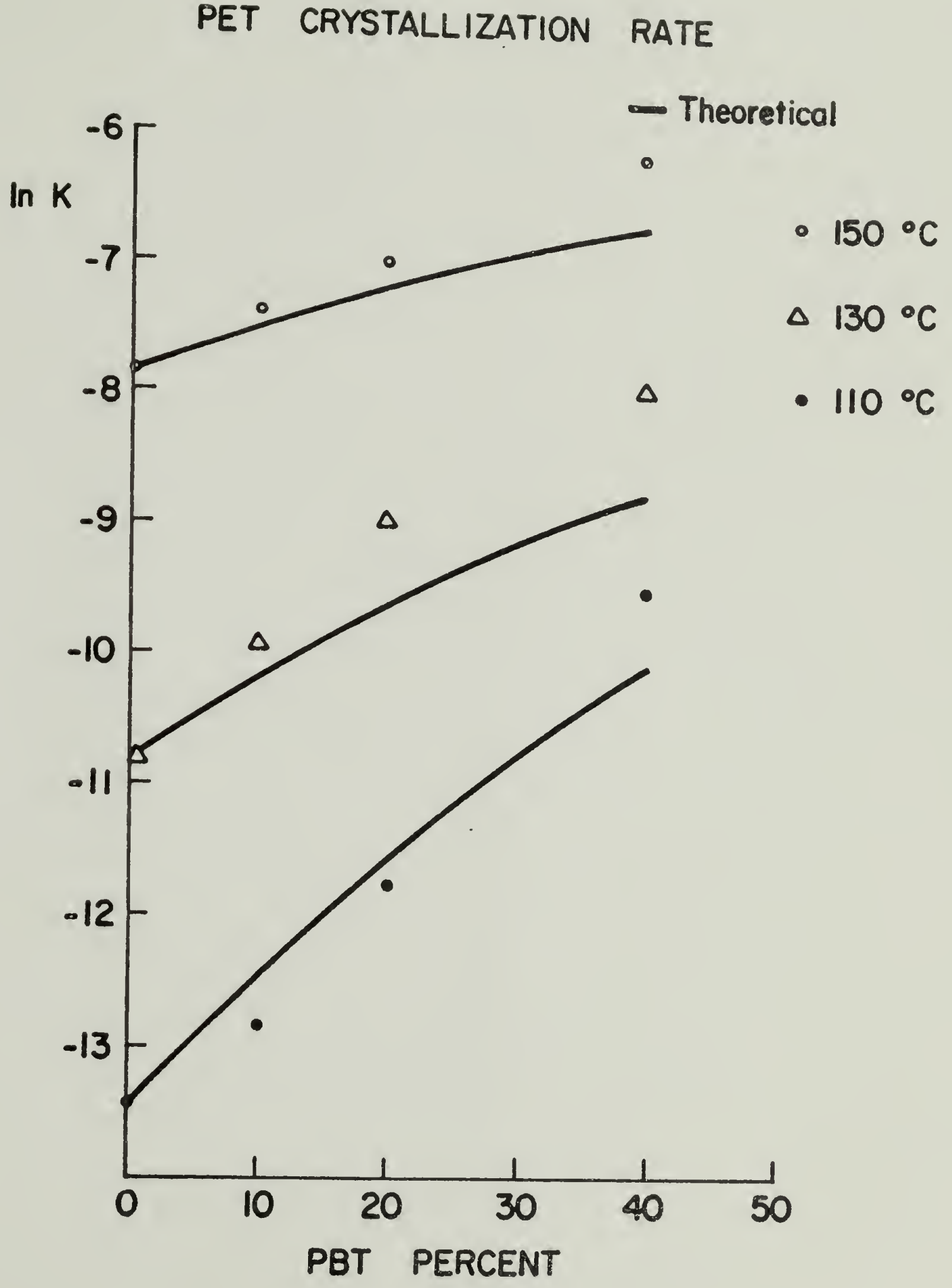
PET CRYSTALLIZATION RATE
Theoretical
ln K
-6
-7
-8
-9
-10
-11
-12
-13
150 °C
130 °C
110 °C
0
10
20
30
40
50
PBT PERCENT

Figure 52

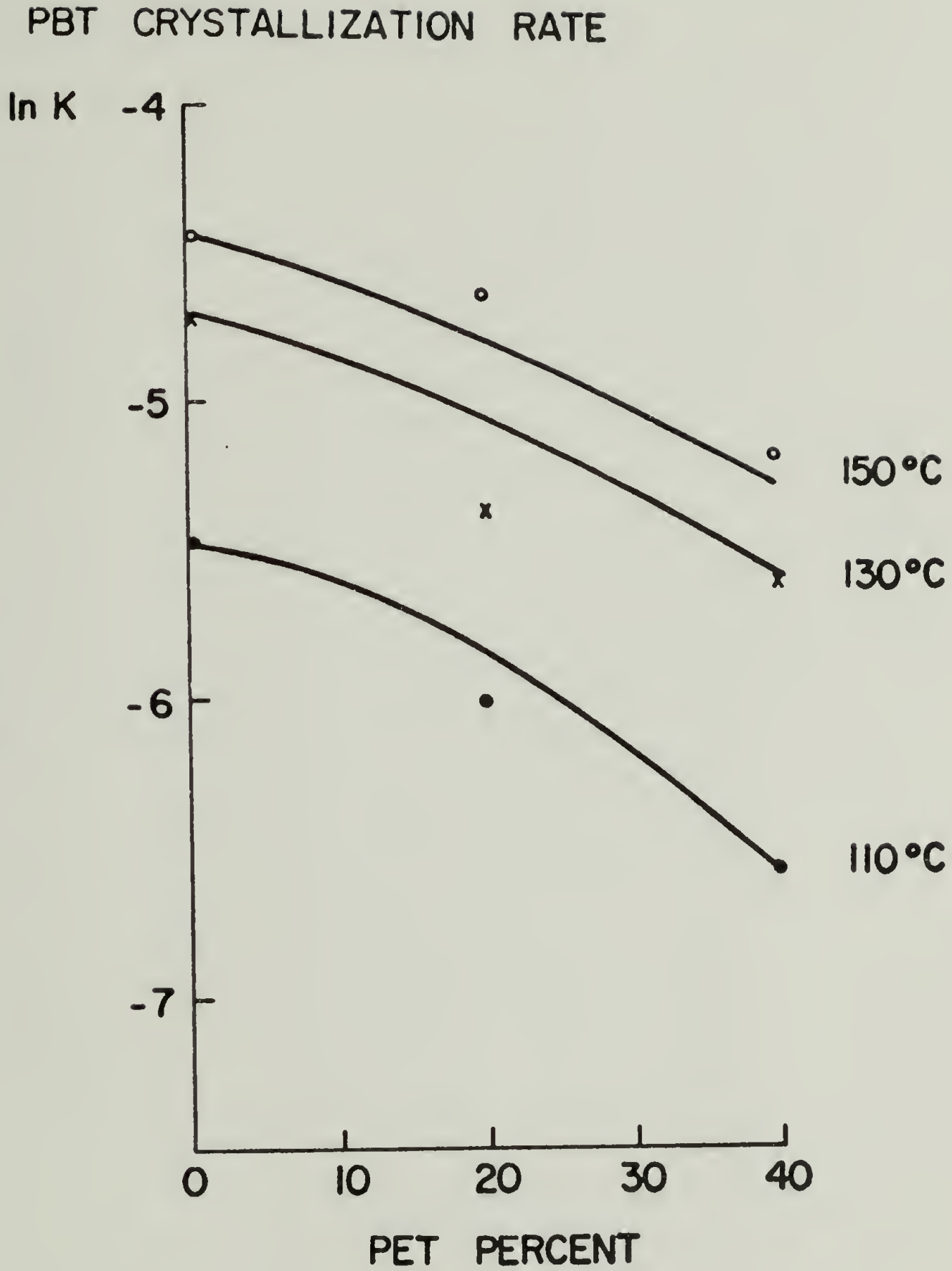
PBT CRYSTALLIZATION RATE
ln K
-4
-5
-6
-7
150°C
130°C
110°C
0
10
20
30
40
PET PERCENT

Figure 53

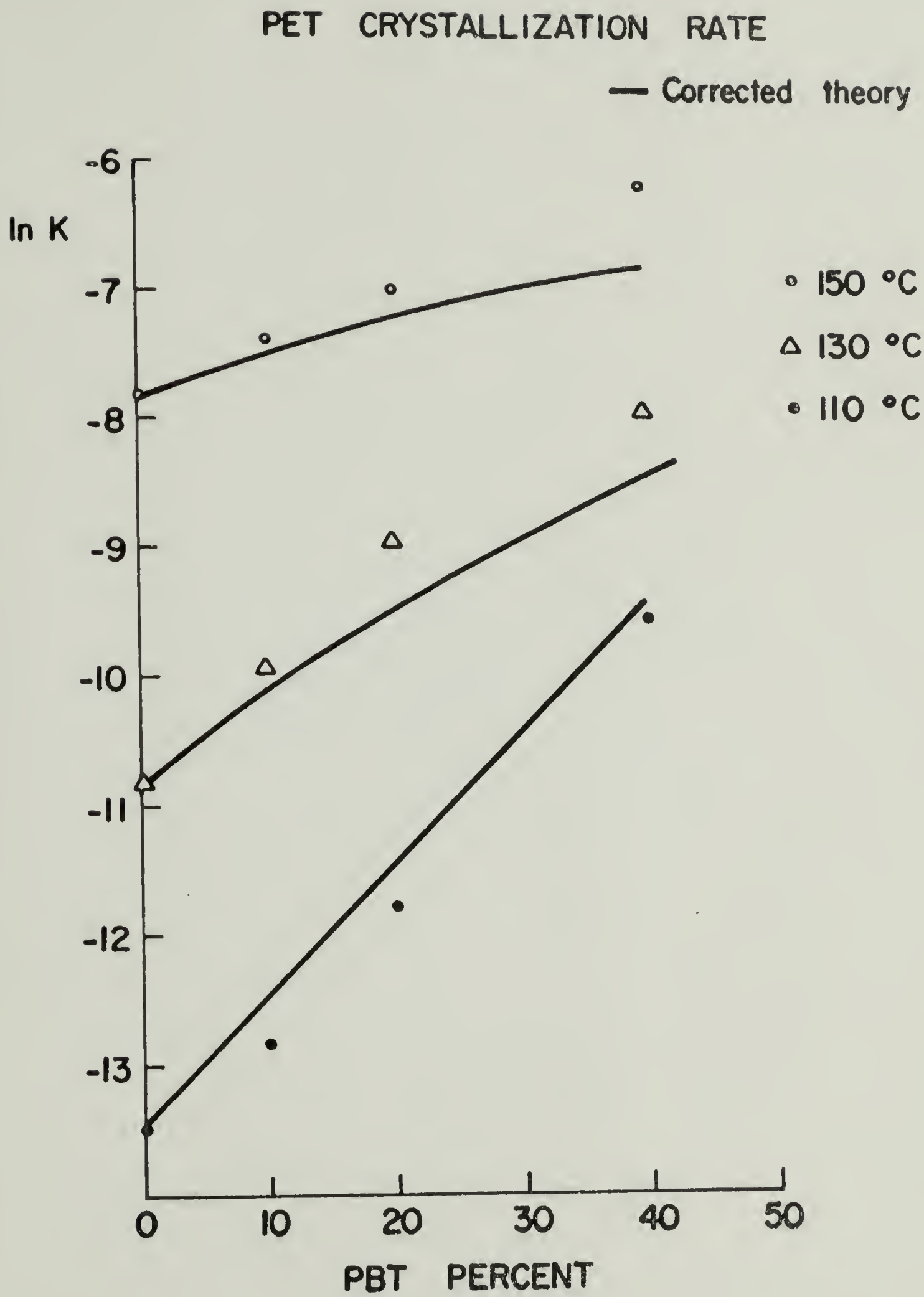
PET CRYSTALLIZATION RATE
— Corrected theory
ln K
-6
-7
-8
-9
-10
-11
-12
-13
0
10
20
30
40
50
PBT PERCENT
° 150 °C
△ 130 °C
• 110 °C

Figure 54

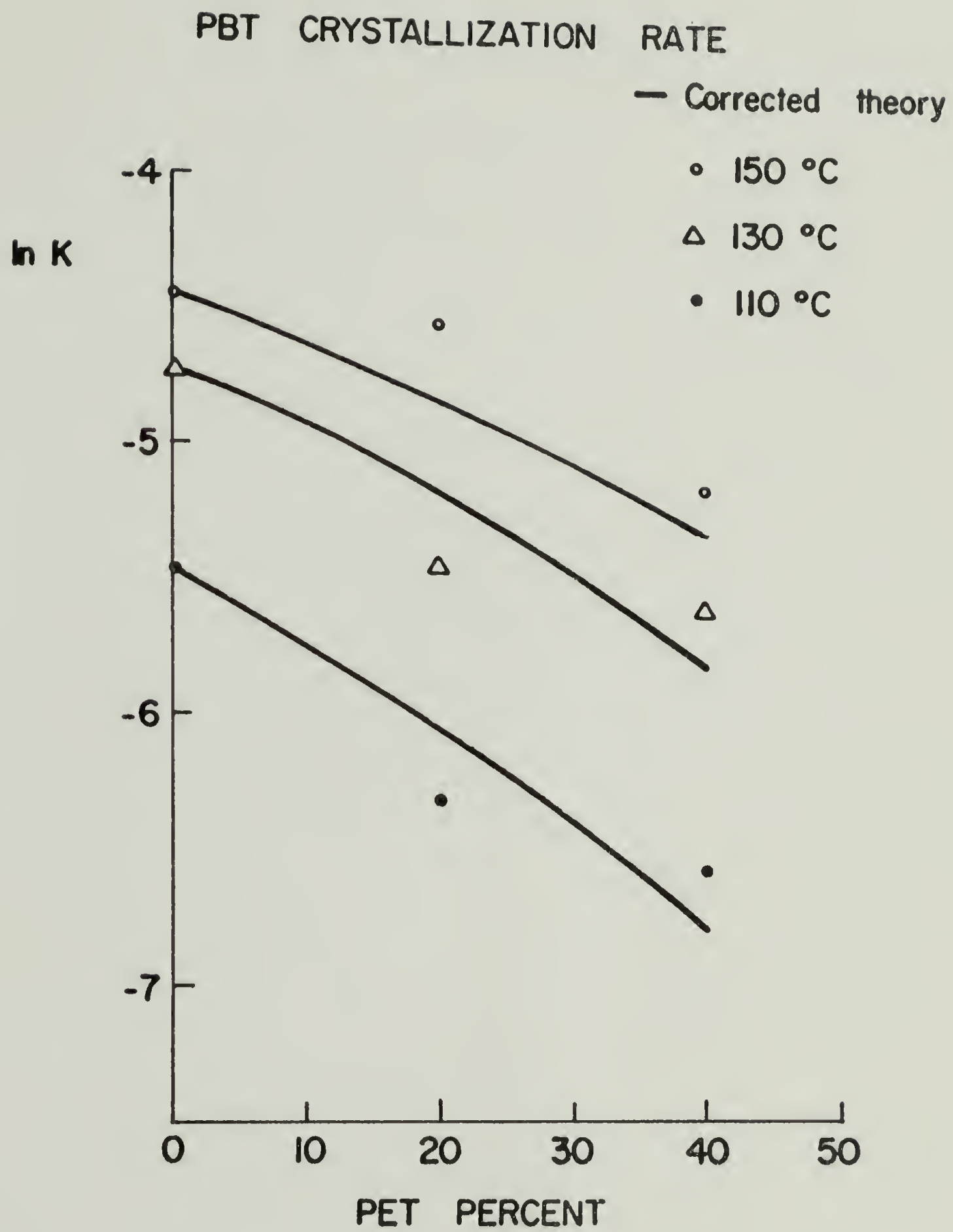
PBT CRYSTALLIZATION RATE
— Corrected theory
° 150 °C
△ 130 °C
• 110 °C
ln K
-4
-5
-6
-7
0
10
20
30
40
50
PET PERCENT

Figure 55

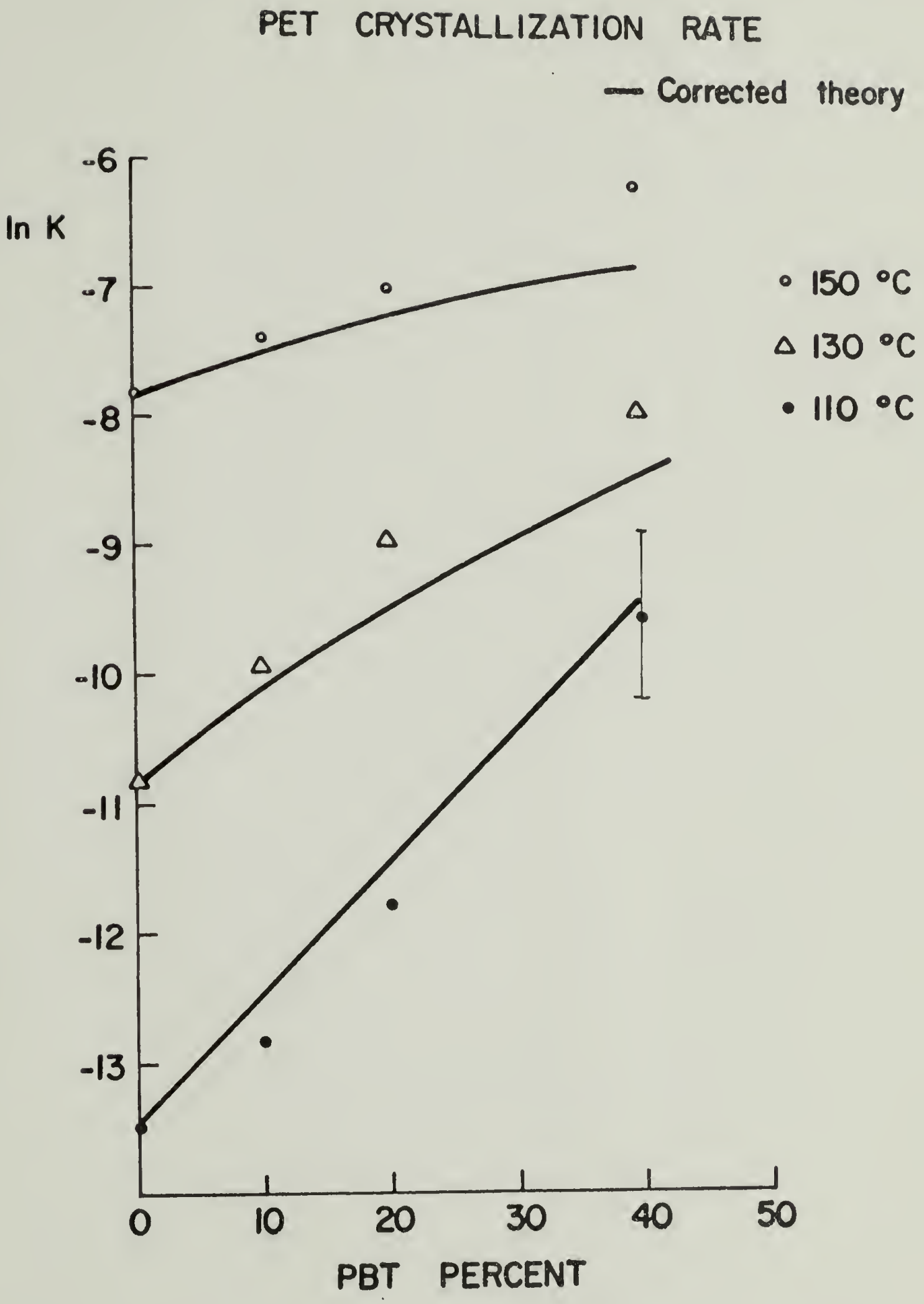
PET CRYSTALLIZATION RATE
— Corrected theory
ln K
-6
-7
-8
-9
-10
-11
-12
-13
0
10
20
30
40
50
PBT PERCENT
° 150 °C
△ 130 °C
• 110 °C

Figure 56

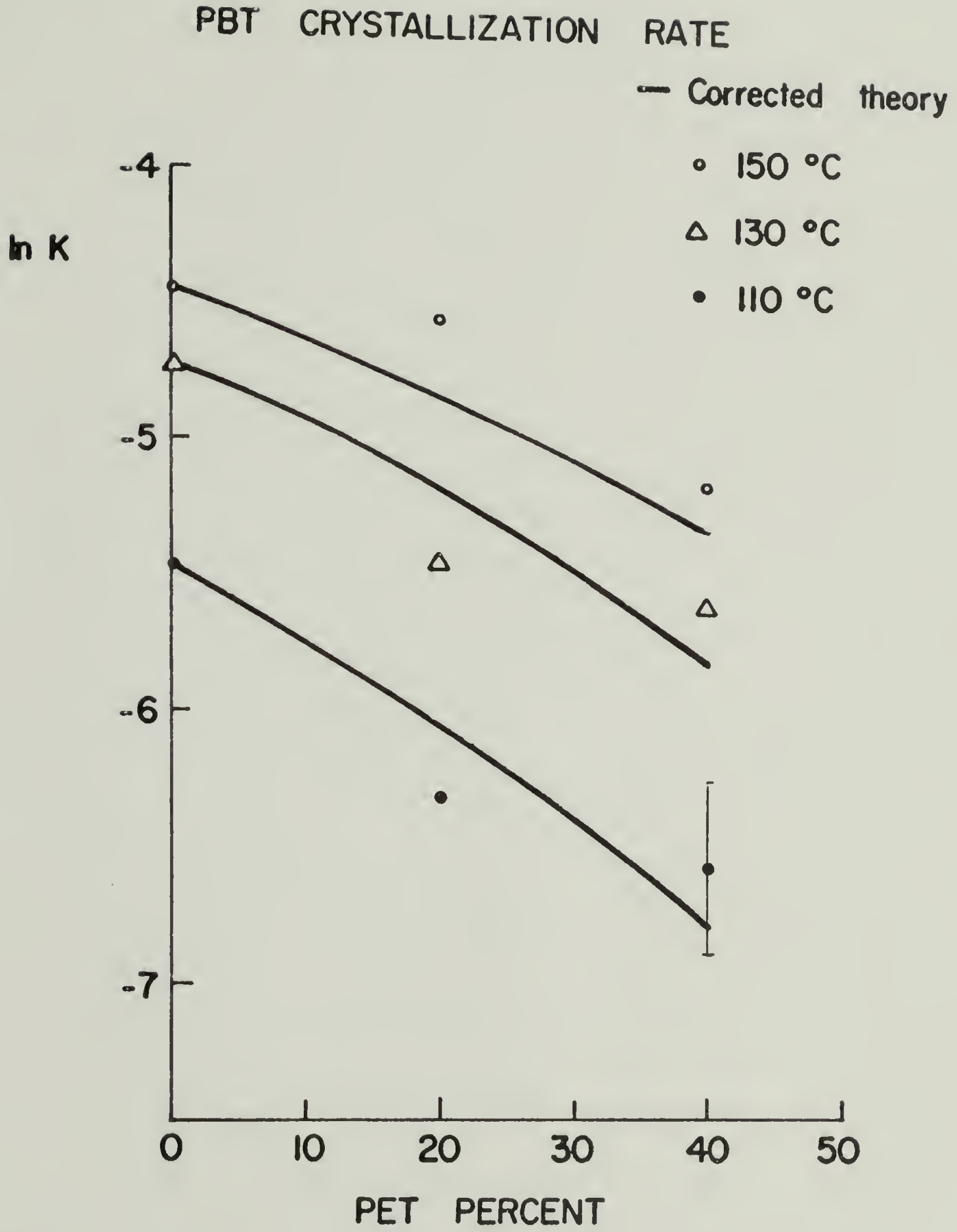
PBT CRYSTALLIZATION RATE
— Corrected theory
° 150 °C
△ 130 °C
• 110 °C
ln K
-4
-5
-6
-7
0
10
20
30
40
50
PET PERCENT

Figure 57

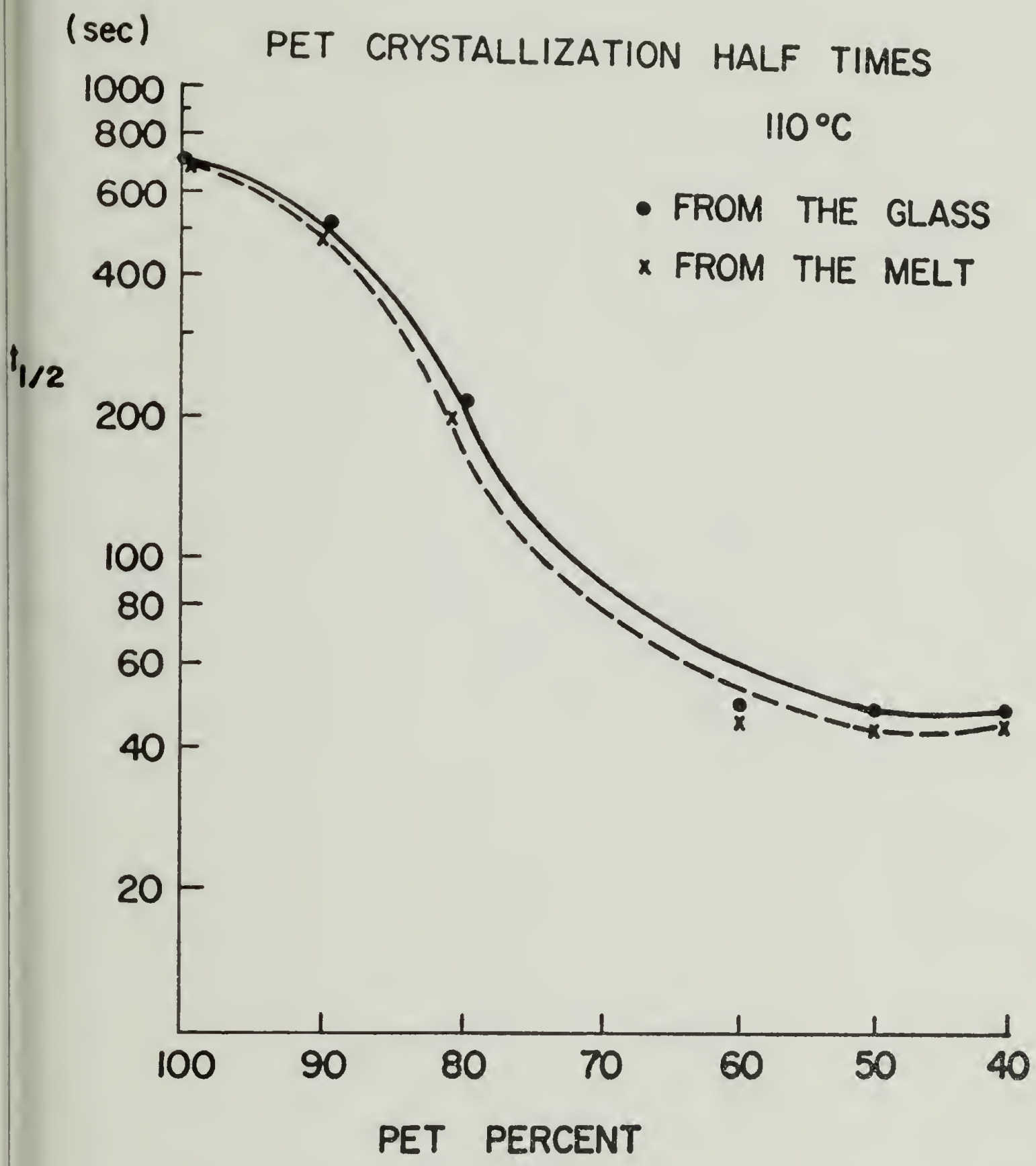
(sec)
PET CRYSTALLIZATION HALF TIMES
110 °C
• FROM THE GLASS
x FROM THE MELT
$t_{1/2}$
1000
800
600
400
200
100
80
60
40
20
100
90
80
70
60
50
40
PET PERCENT

Figure 58

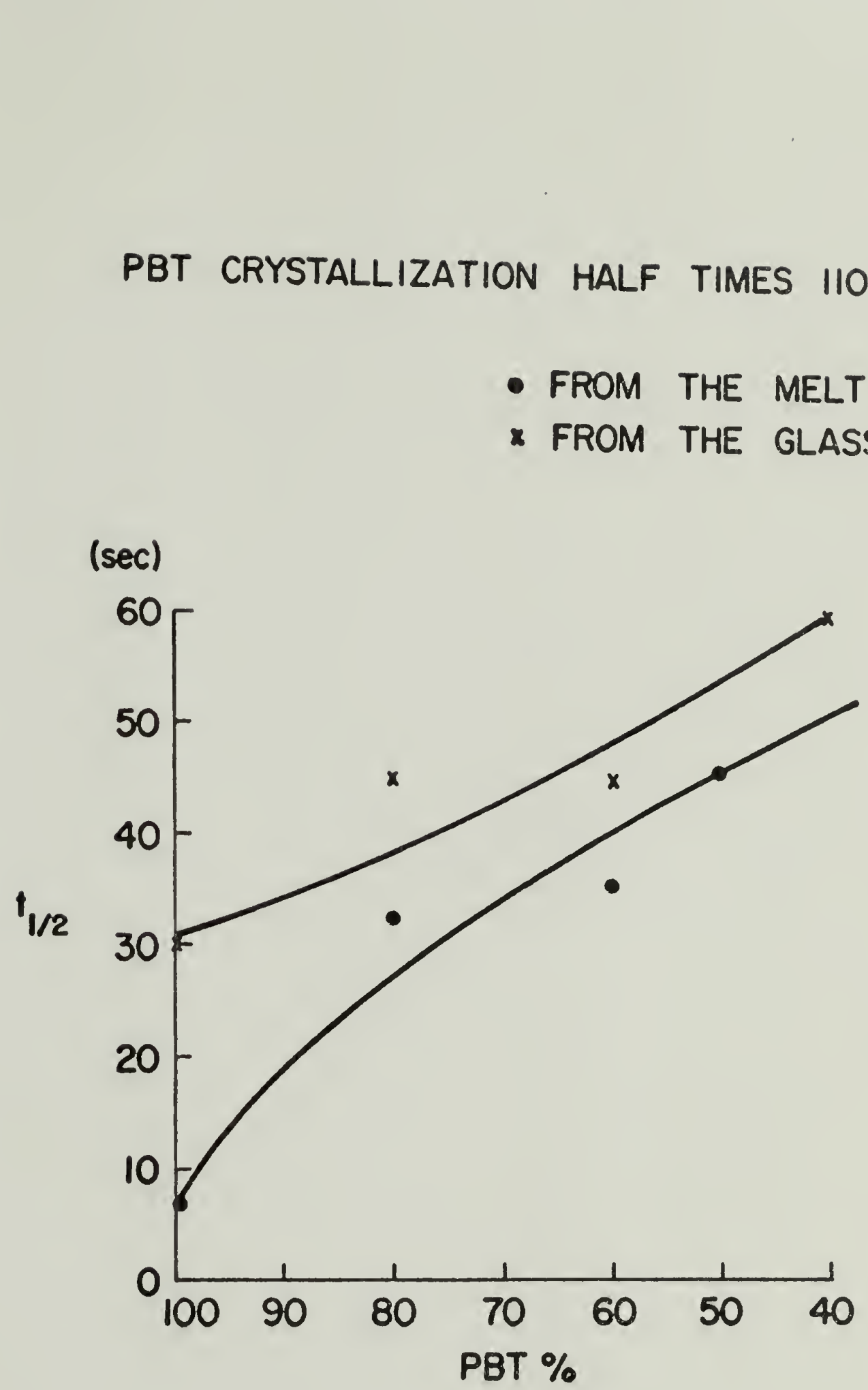
PBT CRYSTALLIZATION HALF TIMES 110 °C
• FROM THE MELT
x FROM THE GLASS
(sec)
60
50
40
30
20
10
0
$t_{1/2}$
100
90
80
70
60
50
40
PBT %

Figure 59

DEGREE OF CRYSTALLINITY OF THE PET PHASE

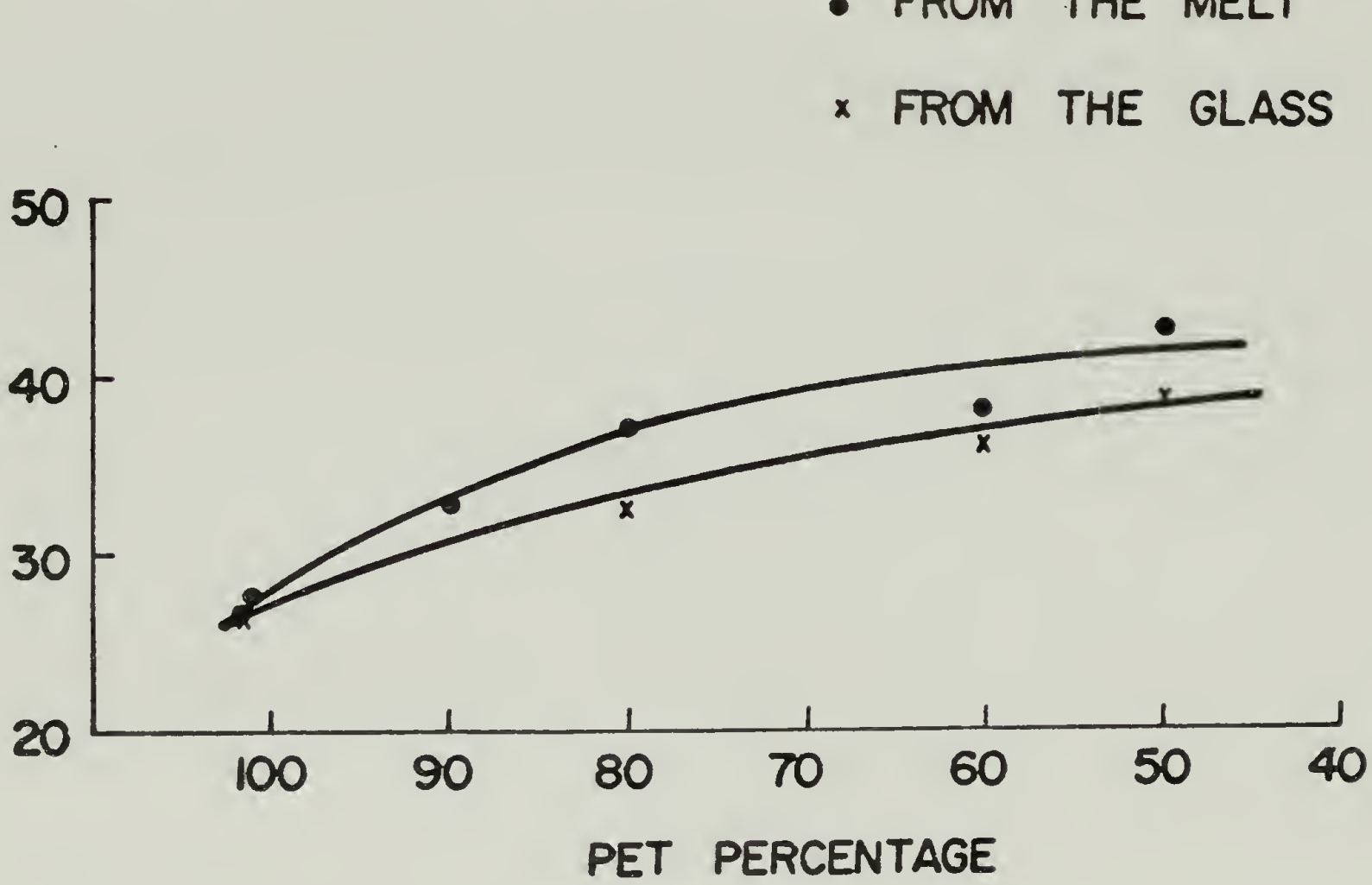

Figure 60

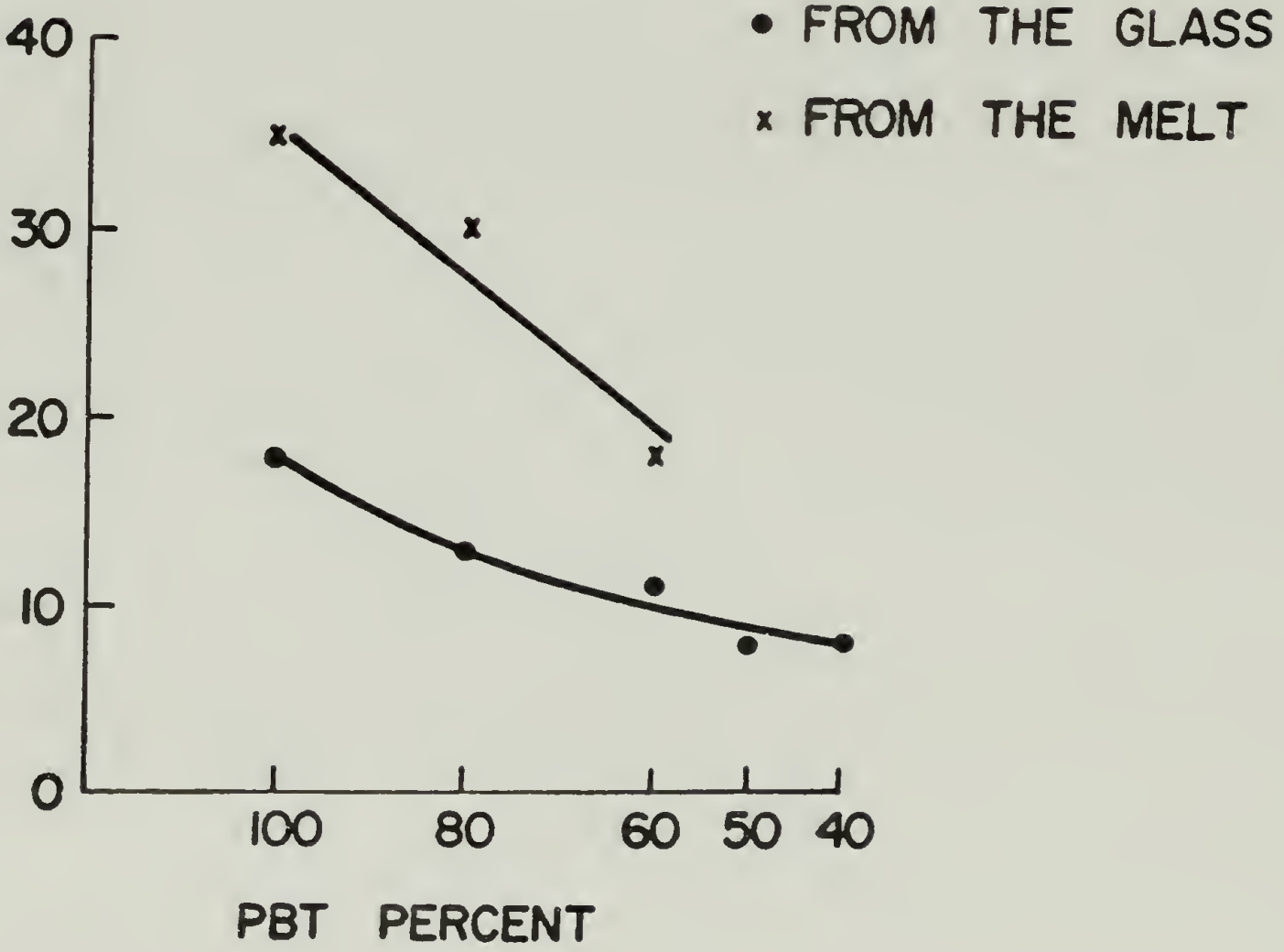
PBT CRYSTALLINITY AT 110 °C
• FROM THE GLASS
x FROM THE MELT
40
30
20
10
0
100
80
60
50
40
PBT PERCENT

Figure 61

INTRINSIC VISCOSITY VS. TIME IN THE MELT FOR THE 50/50 BLEND

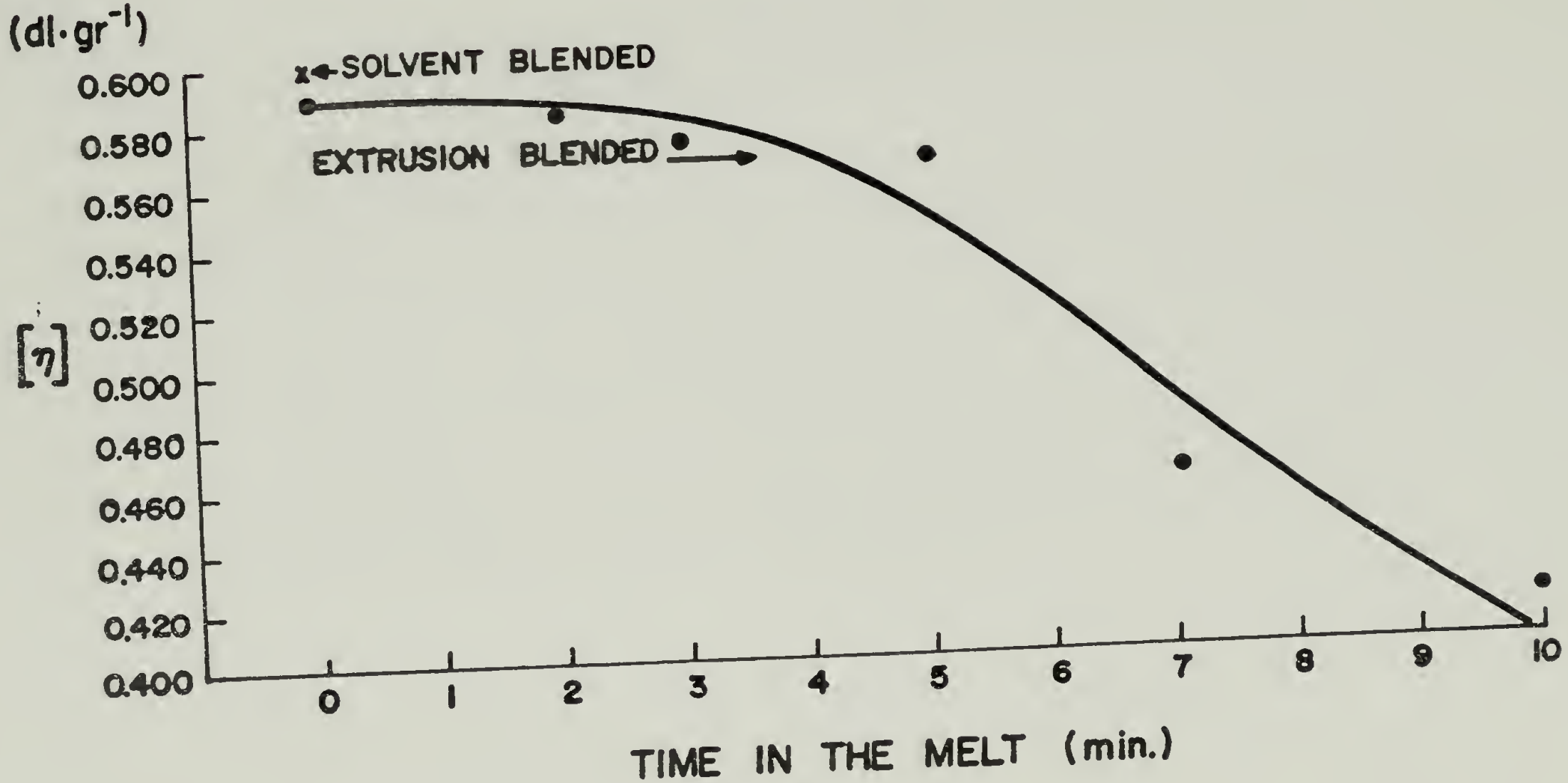

Figure 62

PBT CRYSTALLIZATION HALF TIMES VS. TIME IN THE MELT THE 50/50 BLEND

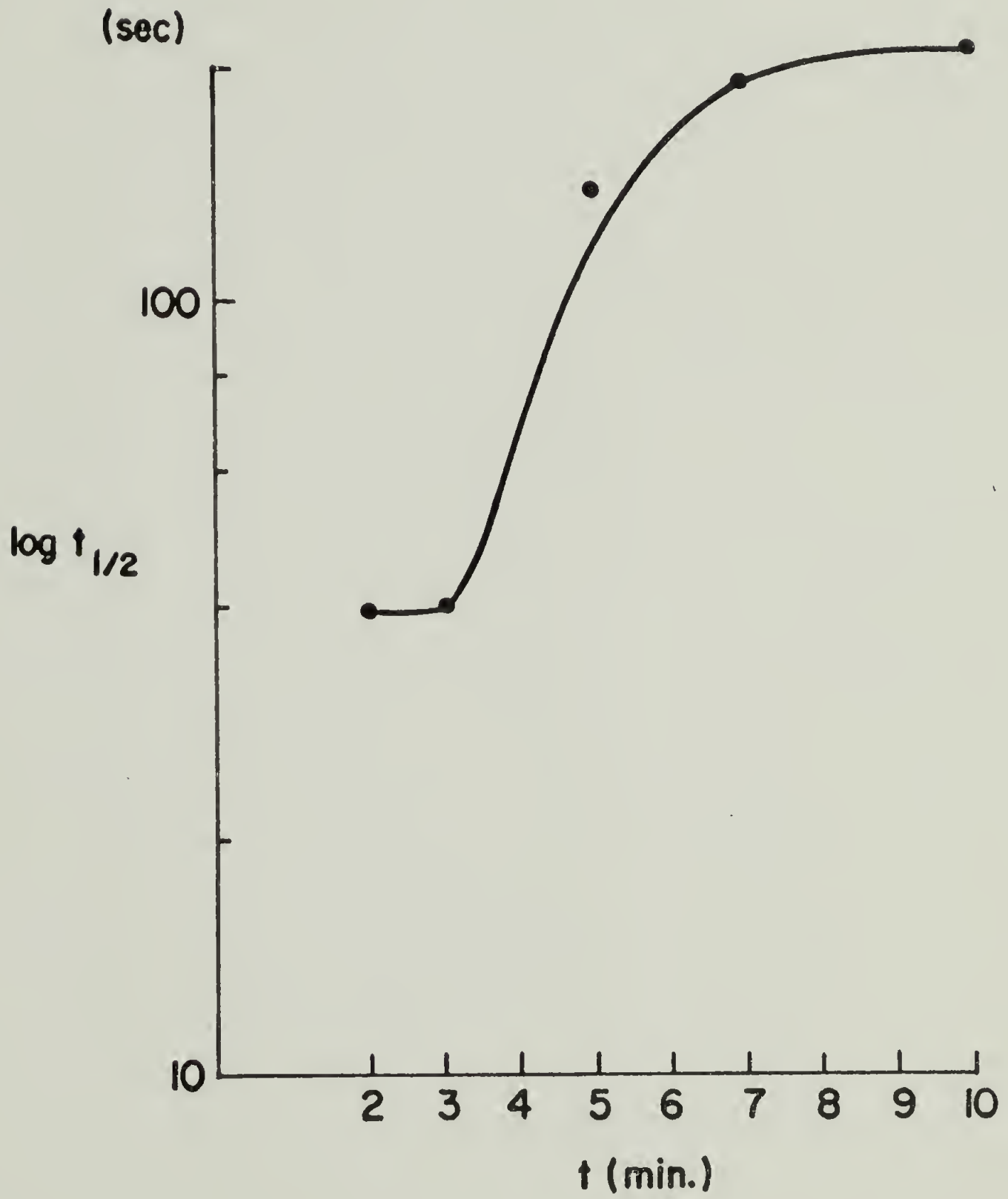

Figure 63

PET CRYSTALLIZATION HALF TIMES VS. TIME IN THE MELT IN THE 50/50 BLEND T_c = 90°C

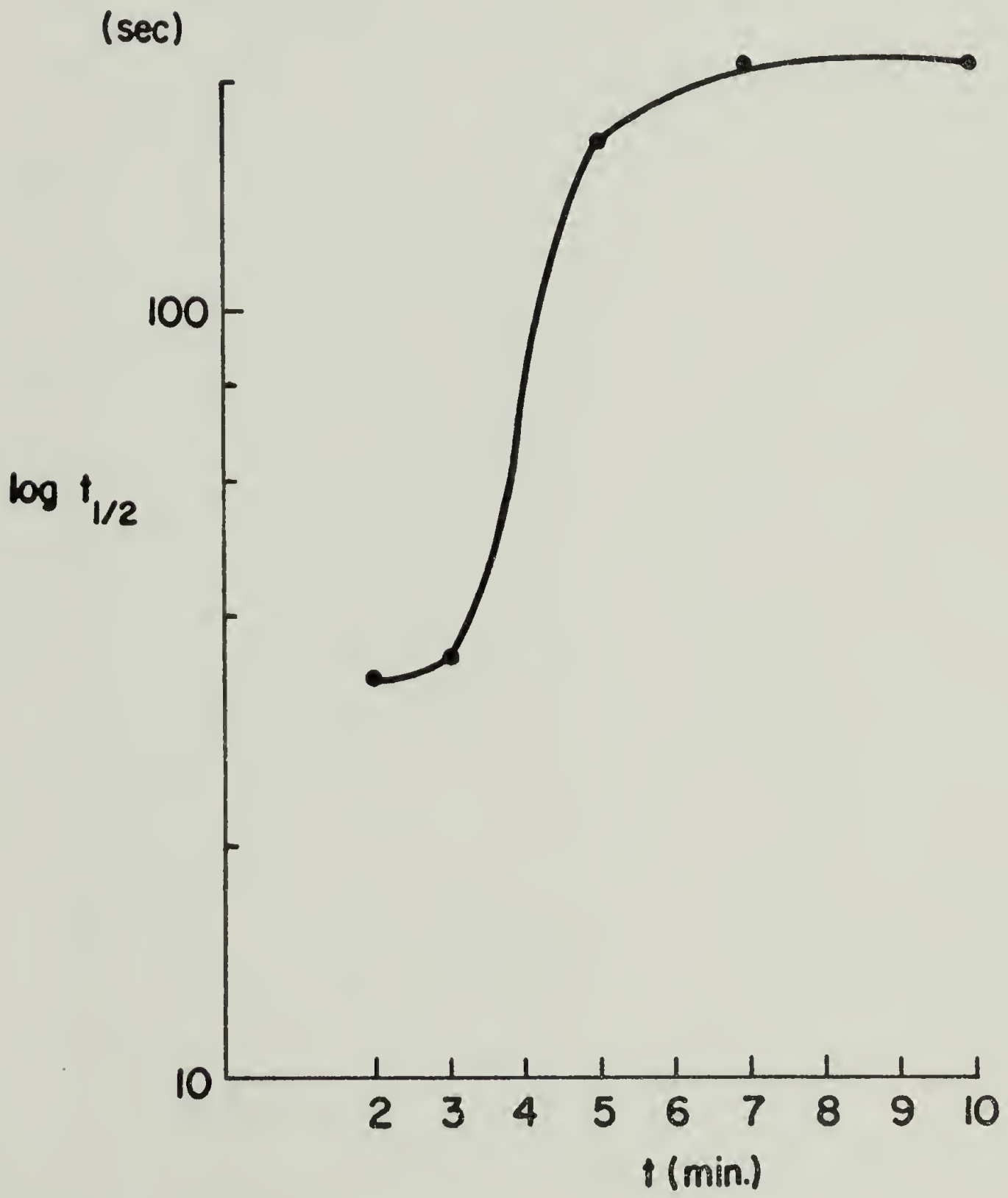

Figure 64

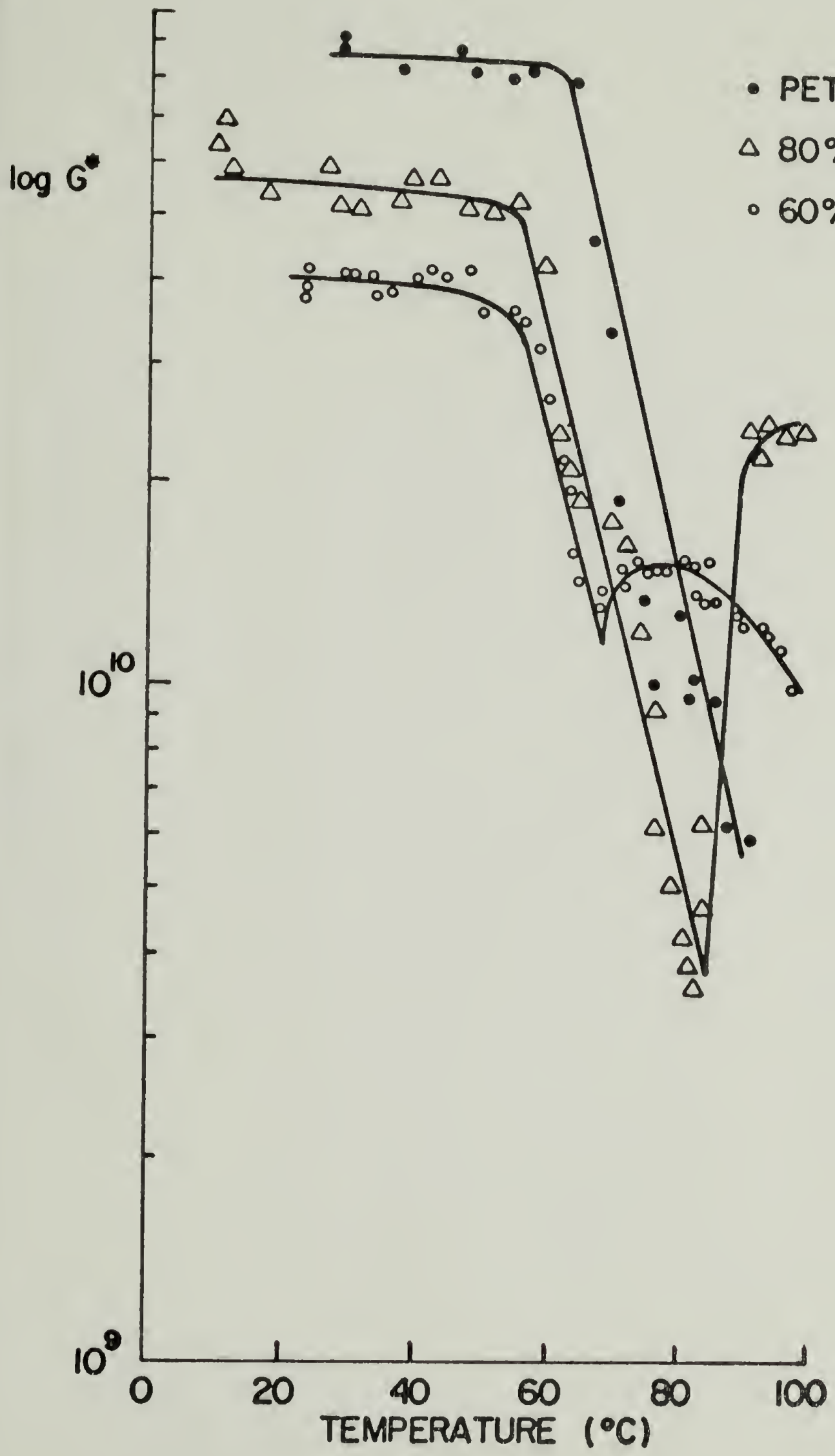

Figure 65

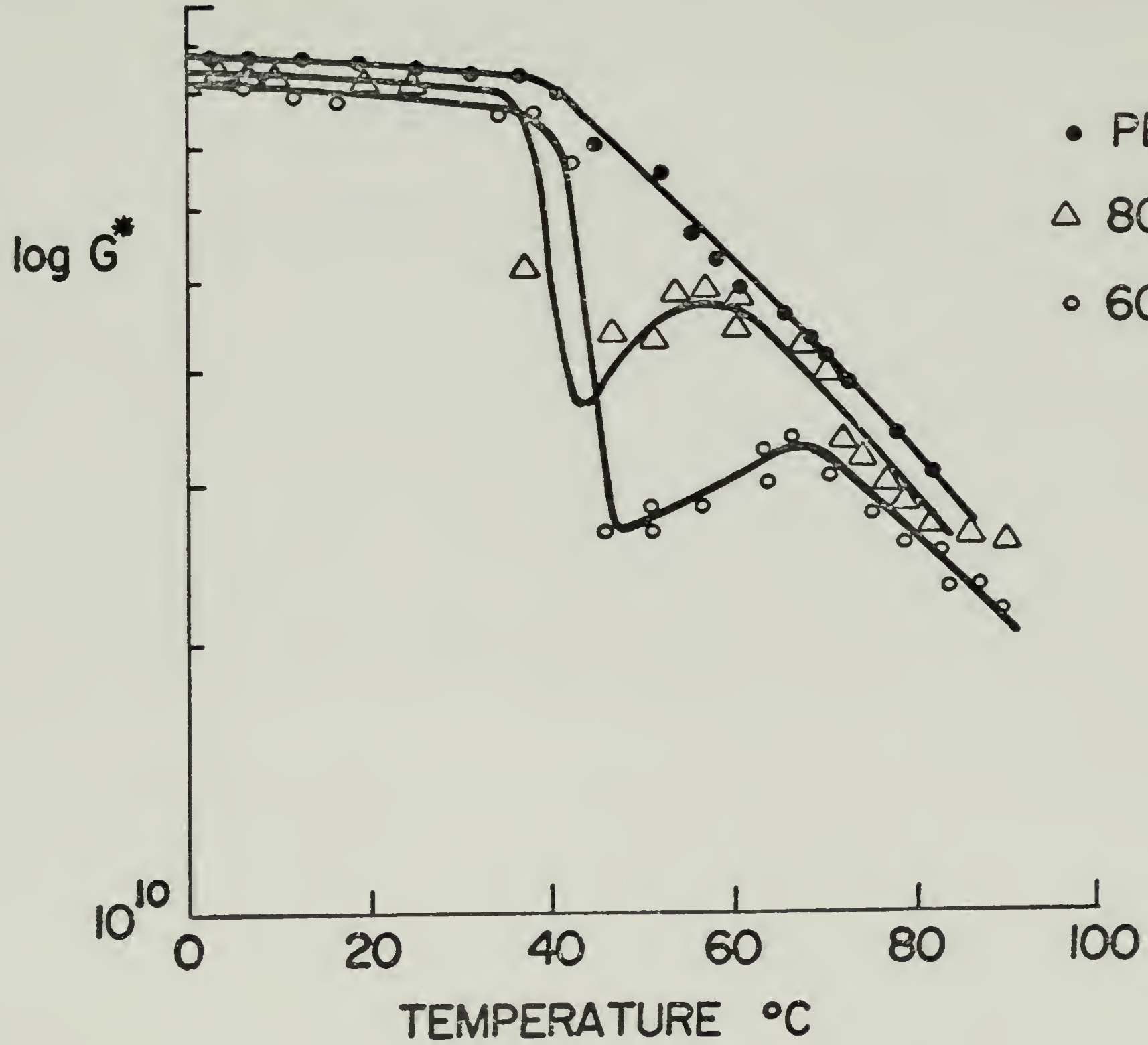

Figure 66

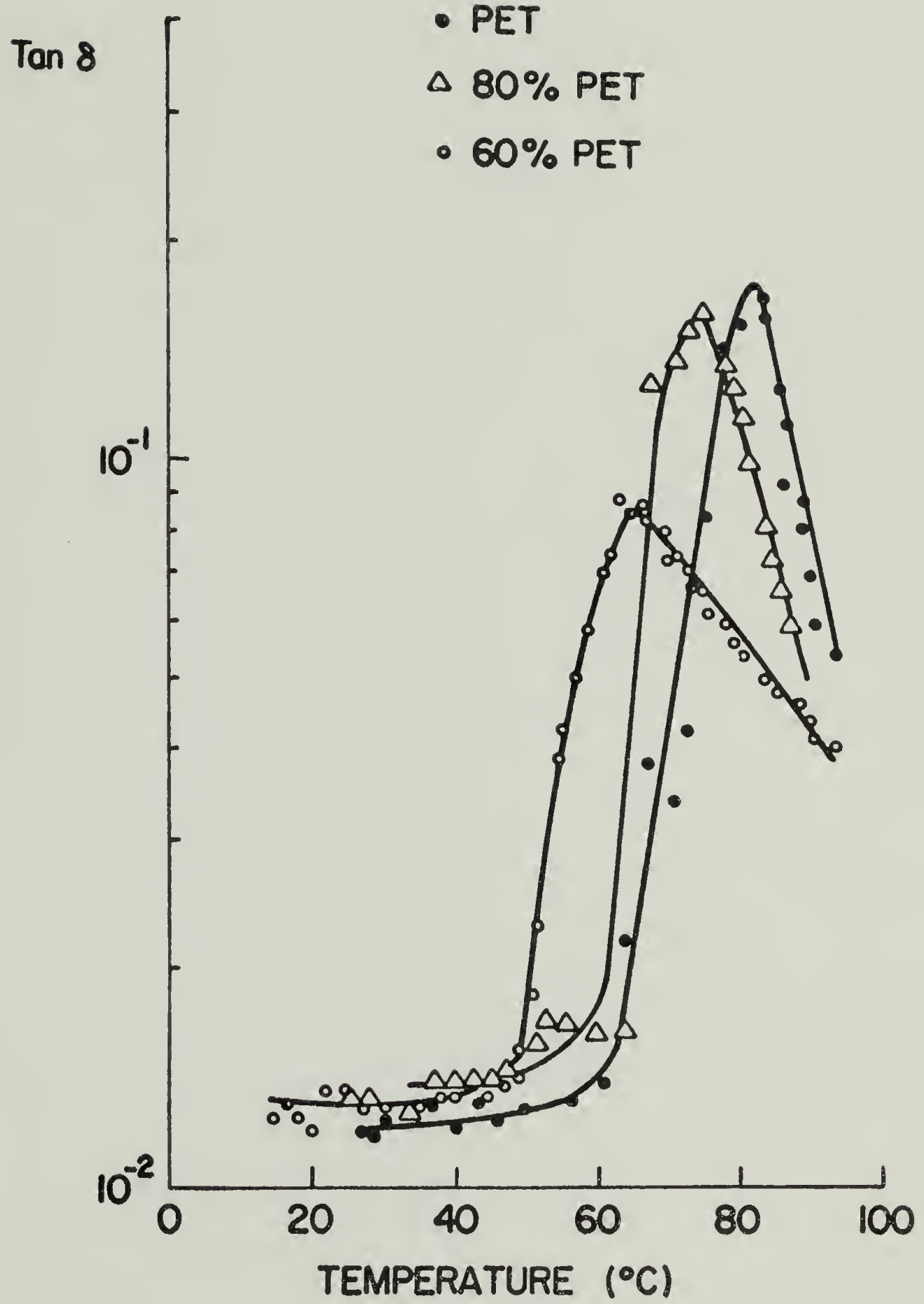

Figure 67

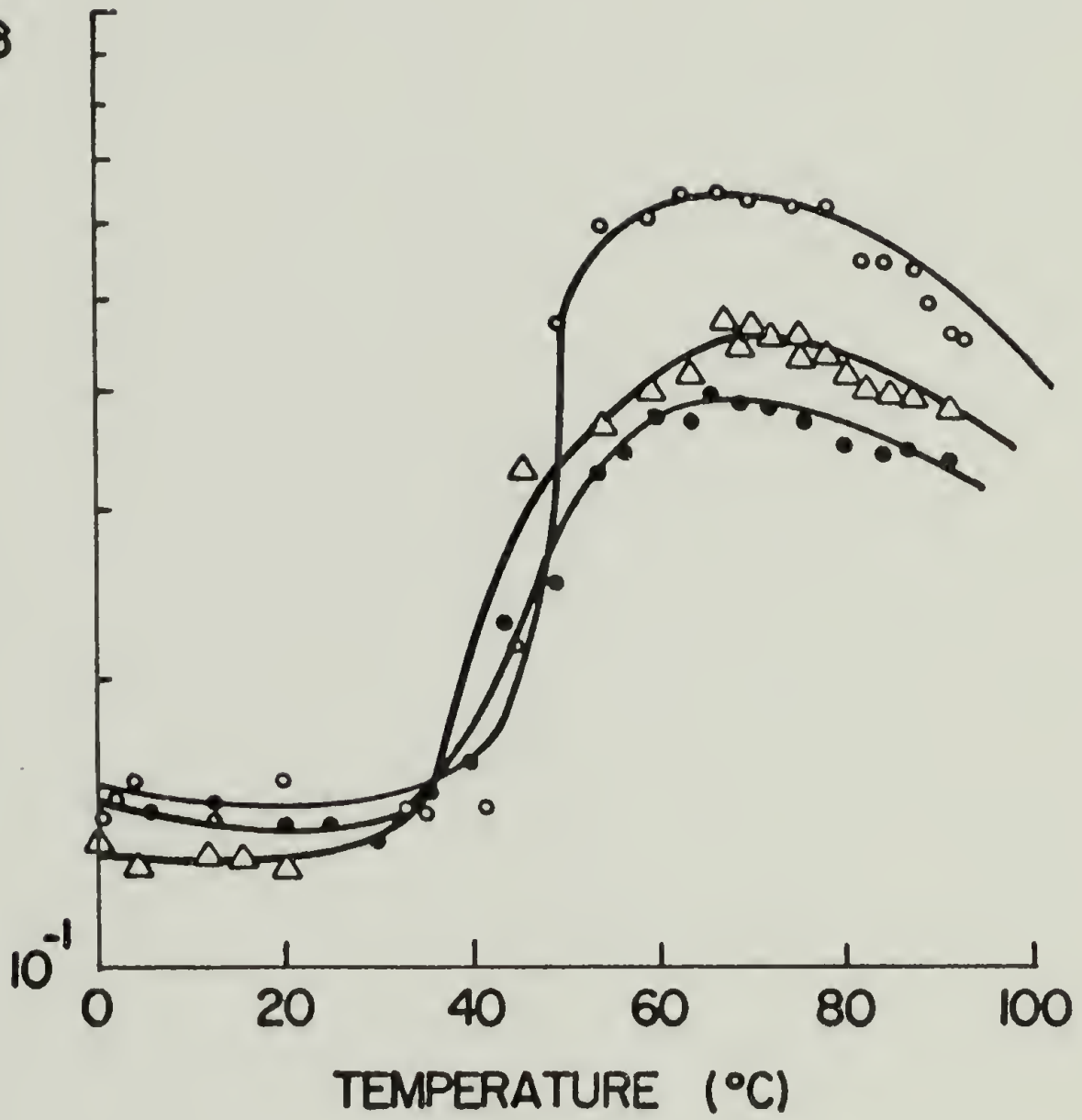

Figure 68

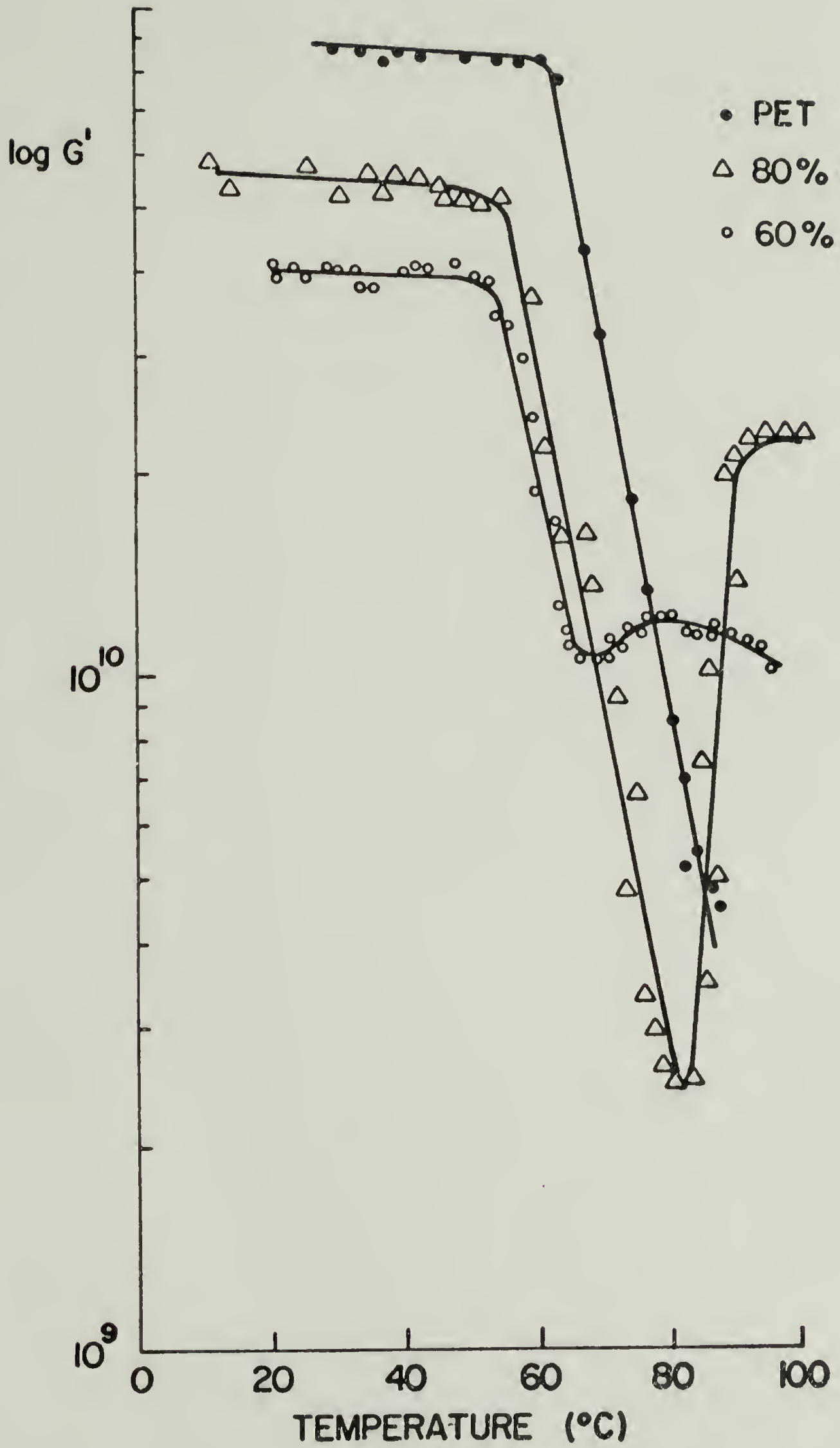

Figure 69

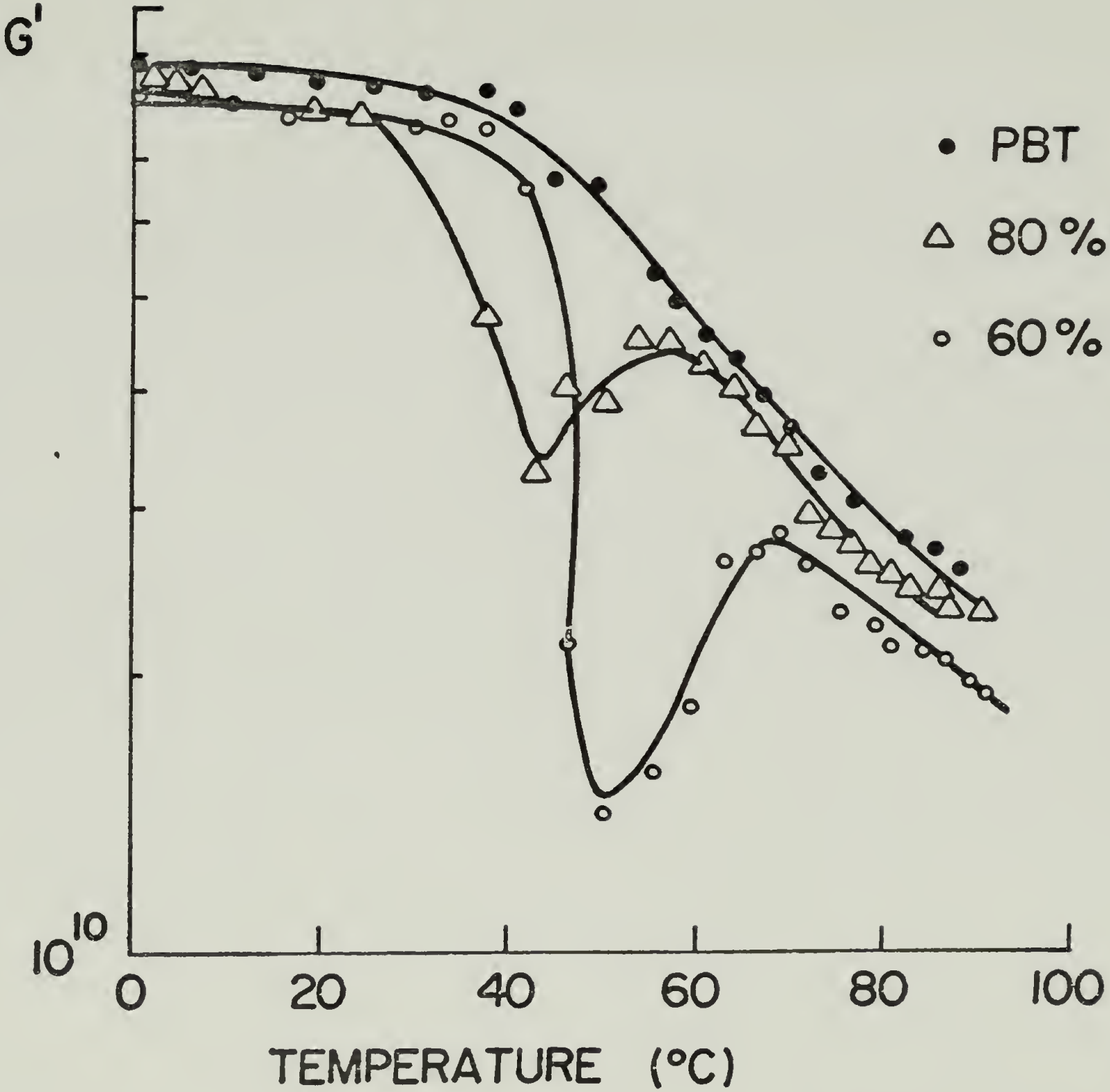

Figure 70

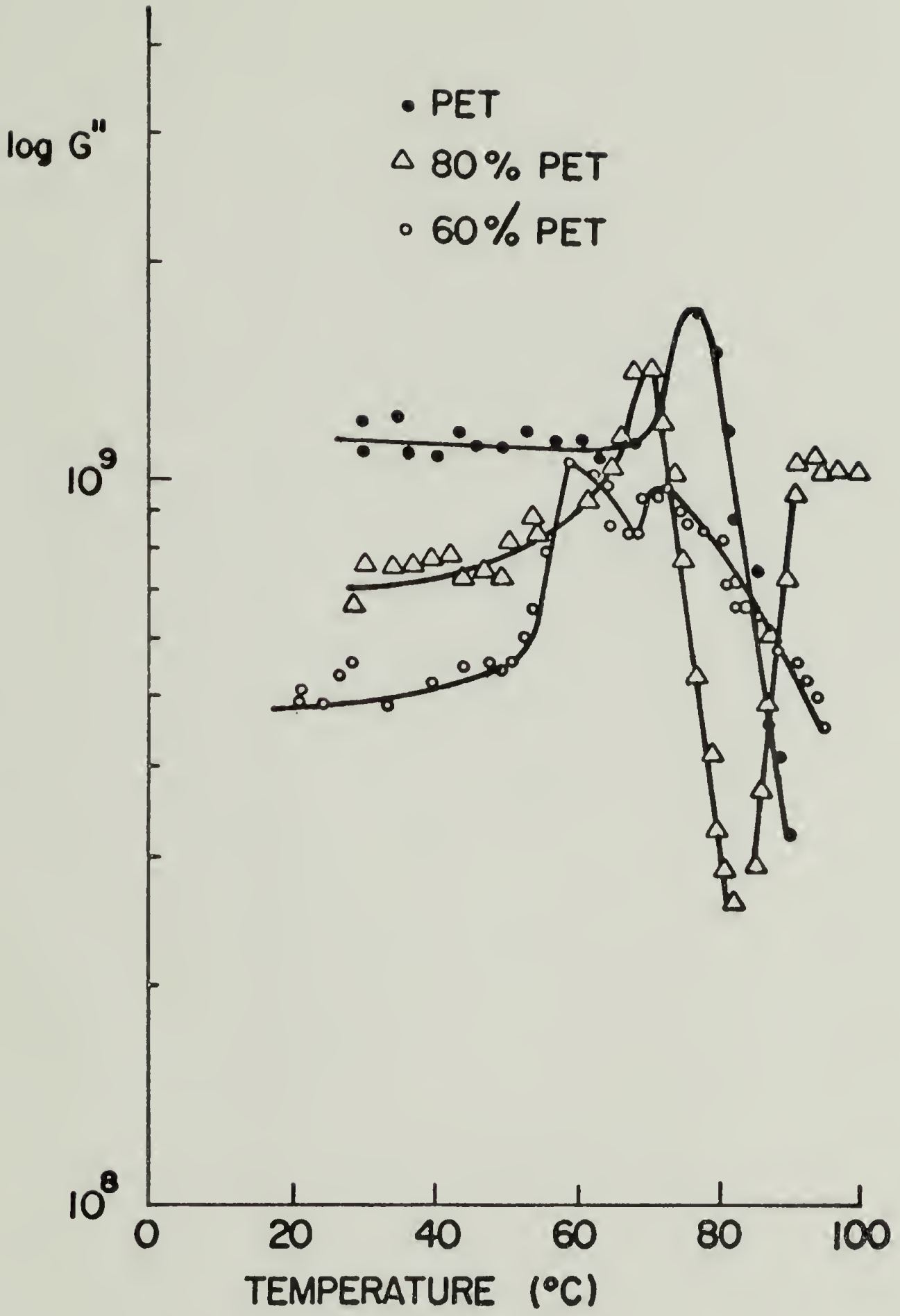

Figure 71

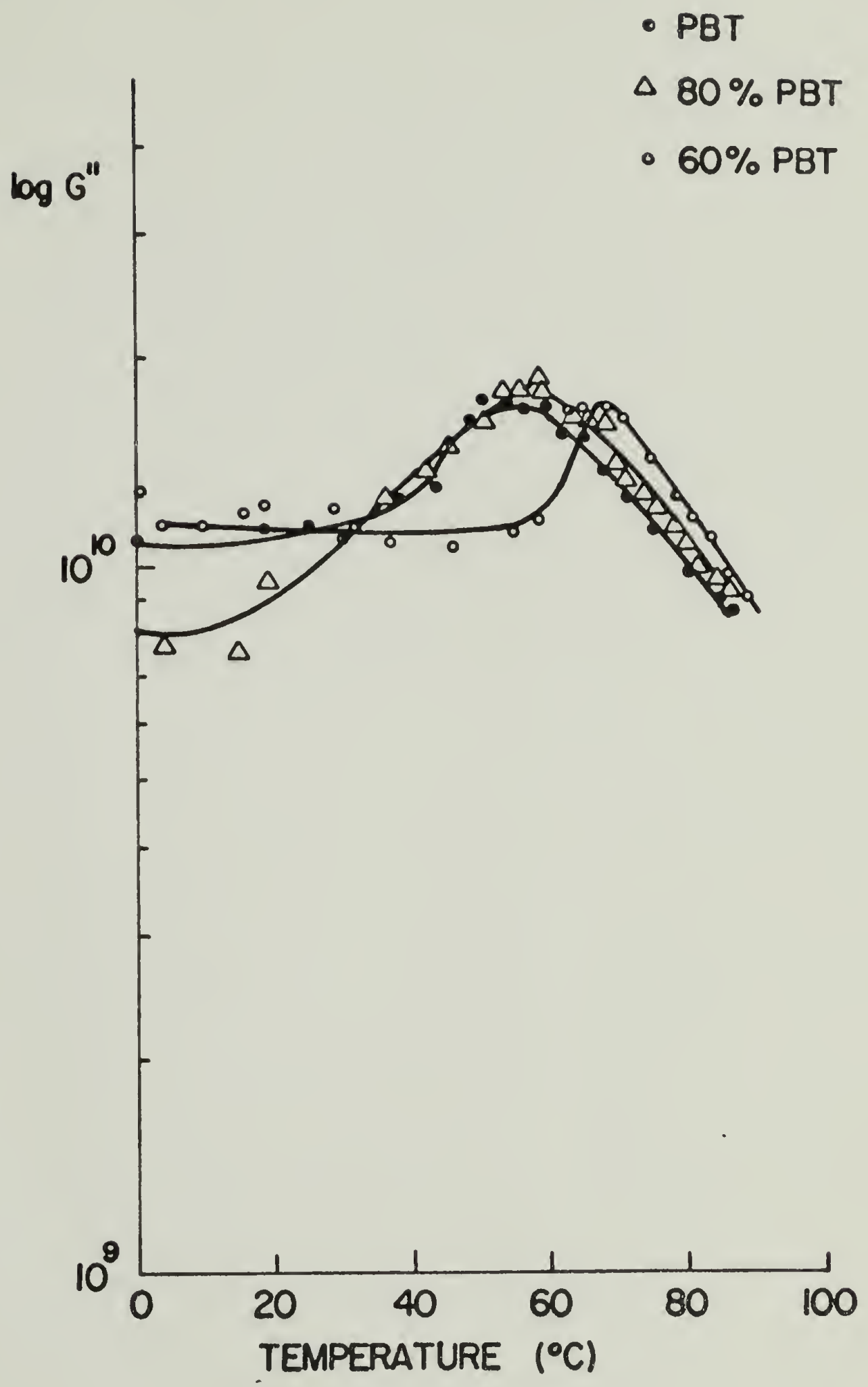

Figure 72

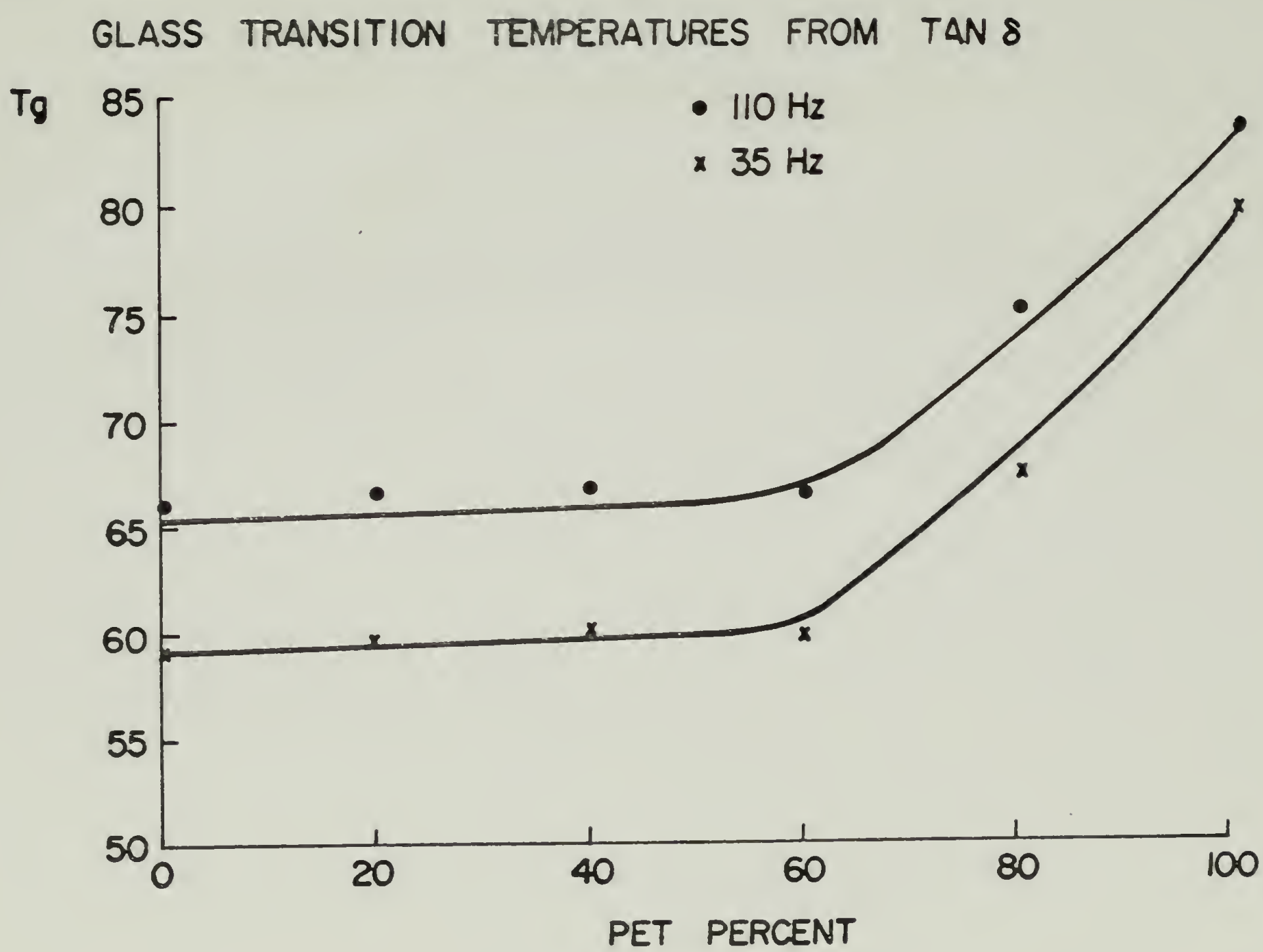
GLASS TRANSITION TEMPERATURES FROM TAN δ
Tg
85
80
75
70
65
60
55
50
• 110 Hz
x 35 Hz
0
20
40
60
80
100
PET PERCENT

Figure 73

GLASS TRANSITION TEMPERATURES FROM 6"

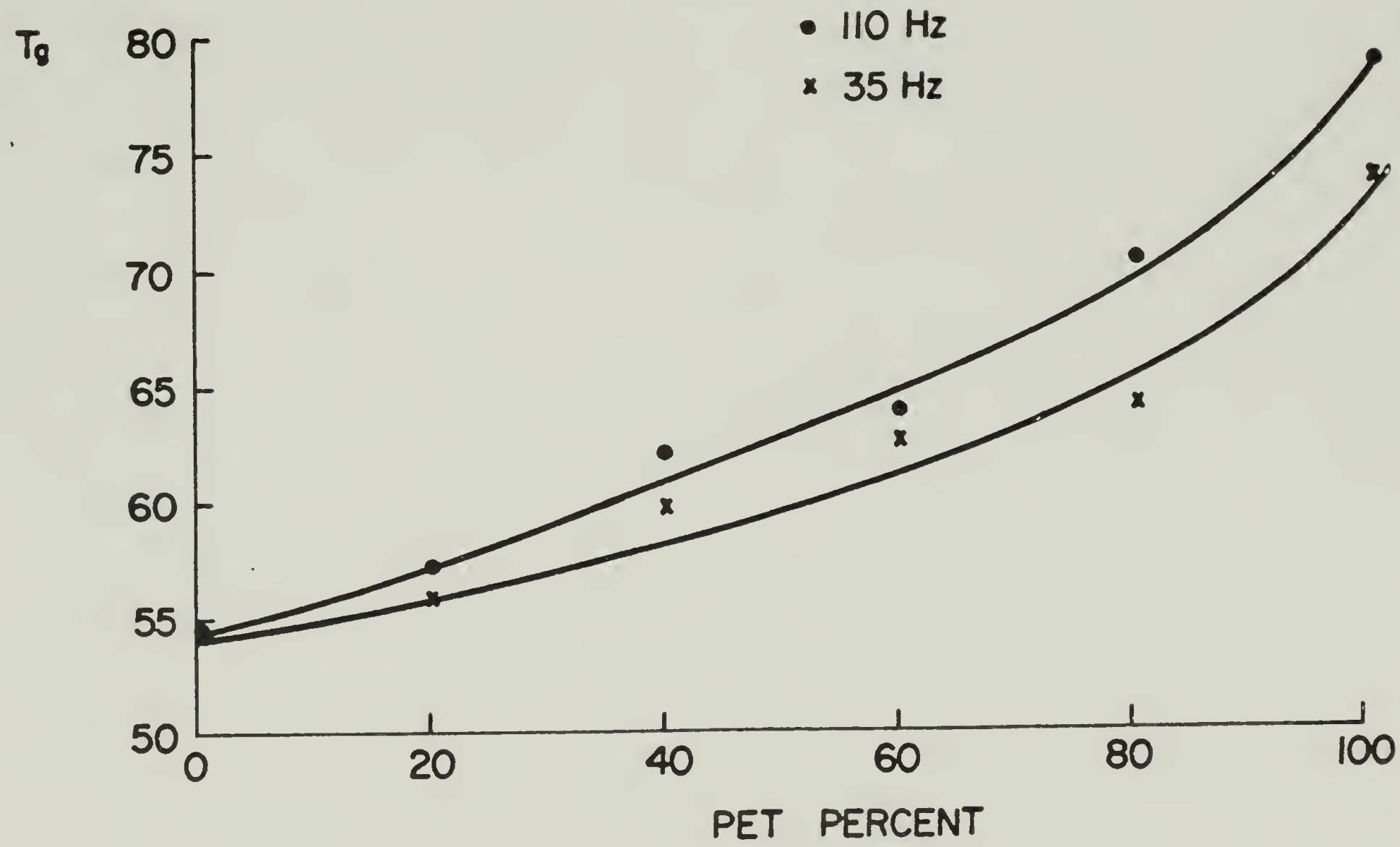

Figure 74